Master thesis report

Master thesis:

Maximum possible diameter of the Great Dubai Wheel

Final Report
16 February 2009

Name:	Wout Luites
Email:	wluites@gmail.com
Telephone number:	06-45370505
Student number:	1286854

TU Delft

a company of Royal Haskoning
CORSMIT
RAADGEVEND INGENIEURS

Student: Wout Luites
Balthasar van der Polweg 360
2628 AZ Delft
+31 (0) 6 45 370505
wluites@gmail.com
Student number: 1286854

Master thesis committee

Chairman prof.dipl.-ing. J.N.J.A. Vambersky
S2 1.36
Stevinweg 1
2628CN Delft
+31 (0)15 27 83 705
J.N.J.A.Vambersky@tudelft.nl

Committee member dr. ing. A.Romeijn
S2 2.55
Stevinweg 1
2628CN Delft
+31 (0)15 27 85 488
A.Romeijn@tudelft.nl

Committee member dr.ir. P.C.J. Hoogenboom
HG 6.48
Stevinweg 1
2628CN Delft
+31 (0)15 27 88 081
P.C.J.Hoogenboom@tudelft.nl

Committee member ir. D.P. Snijders
Corsmit Raadgevend Ingenieurs BV
Sir Winston Churchillaan 366B
2285 SJ Rijswijk (ZH)
+31 (0)70 39 49 305
d.snijders@corsmit.nl

Committee member ir. L.J.M. Houben
S2 2.27
Stevinweg 1
2628CN Delft
+31 (0)15 27 84 917
L.J.M.Houben@tudelft.nl

Preface

This report is the result of a Master thesis at Delft University of Technology, faculty of Civil Engineering and Geosciences, department Structural Engineering. The subject of the Master Thesis is the Great Dubai Wheel. This subject triggers many questions not only from an engineering point of view, but for me, with an interest in structural engineering and special structures, one question stood out: *"Why only a diameter of 185m when already a Ferris wheel in Beijing is planned of 208m?"* This Master thesis will study this question and focus on the maximum possible diameter of the Great Dubai Wheel.

For their help and guidance during this Master thesis and interest in the subject I would like to thank my Master thesis committee. Special thanks must go to dr. A. Romeijn for his weekly guidance and enthusiasm. Furthermore I would like to thank Corsmit for supplying all of the necessary facilities to do the research, and I would like to thank the Master thesis committee but especially Dennis Snijders of Corsmit for the insight that it wasn't the intention to calculate the Great Dubai Wheel as not feasible, but to take on the challenge to make a feasible design.

Finally I would like to thank my girlfriend, family and friends for their support during this Master thesis.

Wout Luites
Delft, February 2009

Summary

In December 2007 Royal Haskoning has won an international design competition organized by the Great Wheel Corporation in which they ask for a concept master plan for a unique hotel. The design of Royal Haskoning featured a 185m tall Ferris wheel in which the hotel was situated. The main difference between a classic Ferris wheel and the design of Royal Haskoning is that the design of Royal Haskoning hasn't got spokes. More and more Ferris wheels are build all over the world as landmarks, up until the design of Royal Haskoning the focus was on building taller and taller, in Beijing a Ferris wheel of 208m is currently being realized. This raised the question why is the Great Dubai wheel only planned at 185m, and even more importantly: *"What is the maximum possible diameter of the Great Dubai Wheel?"*

In this Master thesis the maximum possible diameter of the Great Dubai Wheel has been investigated. To be able to state the maximum diameter of the Great Dubai Wheel the Master thesis can be broken down in three parts.

[1] Limitations of the current design;

[2] Possible improvements to the design;

[3] Maximum possible diameter of the improved design;

In the first part the limitations of the current design have been analyzed. This made clear that the proposed design wasn't feasible; the main problem was the lack of effectiveness of the used material. In the second part of the Master thesis some proposed solutions have been investigated, and in the third and final part of the Master thesis the improved design has been analyzed and the maximum diameter of the Great Dubai Wheel has been stated.

Throughout the project parametric design has been used as a very useful tool. Because the intention of the project was to find the maximum possible diameter of the Great Dubai Wheel, the structural model had to be changed continuously. Via a spreadsheet the complete input-file for the structural analysis program was written, this made it possible to quickly change the model and to determine if the proposed solutions were actually effective or not, and also to easily derive the maximum diameter of the Great Dubai Wheel.

The conclusion is that the improved design of the Great Dubai Wheel has got a maximum possible diameter of about 210m.

Index

1. Introduction

To get a firm insight in the structure of the Great Dubai Wheel it is important to know how the forces act in the structure. This is even more emphasized by the objective of this Master thesis, to find the maximum possible diameter of the Great Dubai Wheel.

The report and research is roughly divided into three main parts. In the first part, chapter 4 until 10, the limitations of the Great Dubai Wheel are researched. To get a firm insight of the structure of the Great Dubai Wheel, the performed analysis is increased in complexity of the model when going further into the analysis. The analysis will go from a simple ring-model into a full 3D-frame model of the Great Dubai Wheel.
The second part of the Master thesis (chapter 11) focuses on possible improvements to the Great Dubai Wheel to reduce the stresses and stress ranges. The solutions are all compared to the original model to check what the improvement is.
The last part of the Master thesis (chapter 12 and 13) will implement the biggest improvements from the second part into the design, and the maximum diameter of the improved design will be determined. Also the conclusions and recommendations for further research is stated in this part.

This Master thesis is only possible if the project demands and restrictions are known. But because the maximum diameter is searched for, the project restrictions should not be as strict that there is no room for improvement. It therefore chosen to first review the original design from a prior study [13], and from that base knowledge go deeper into the Great Dubai Wheel and come with solutions which are beneficial for the main bearing structure.

1.1. Definitions

This paragraph will set definitions for the entire report.

1.1.1. Steel properties

Yield stress (f_y)	=	355 N/mm^2
Young's Modulus (E)	=	2.1 *10^5 N/mm^2
Poisson's ration (v)	=	0.3

1.1.2. Global axis

Throughout this report the following axes definitions have been used.

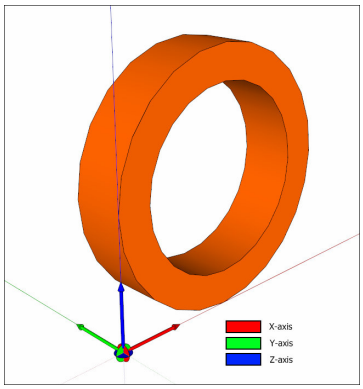

Figure 1.1: Global axis

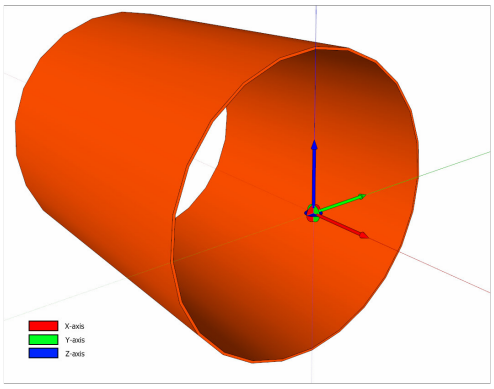

Figure 1.2: Local axis (element axis)

1.1.3. Wheel and supporting structure

When in this report the Great Dubai Wheel is mentioned,

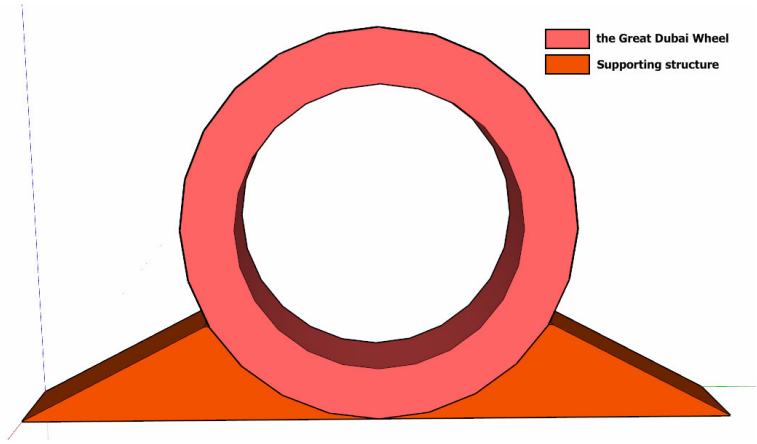

Figure 1.3: Wheel and supporting structure

1.1.4. Different elements in the Great Dubai Wheel

The Great Dubai Wheel consists of different types of elements, in figure 1.4 and figure 1.5 the elements are named, these names are used throughout the entire Master thesis.

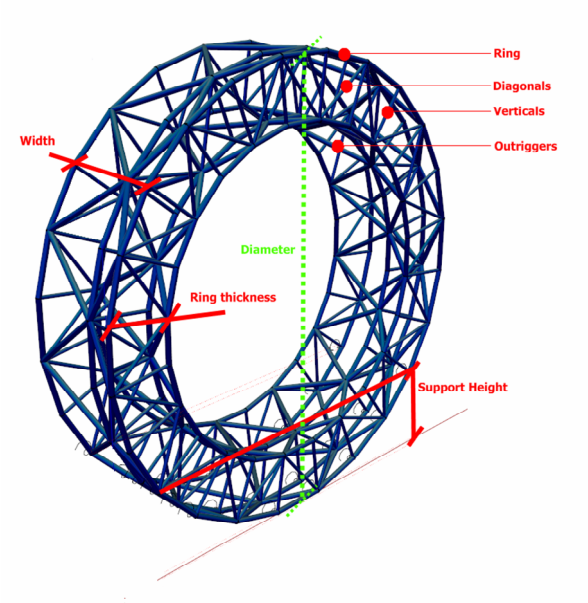

Figure 1.4: Different elements and parameters

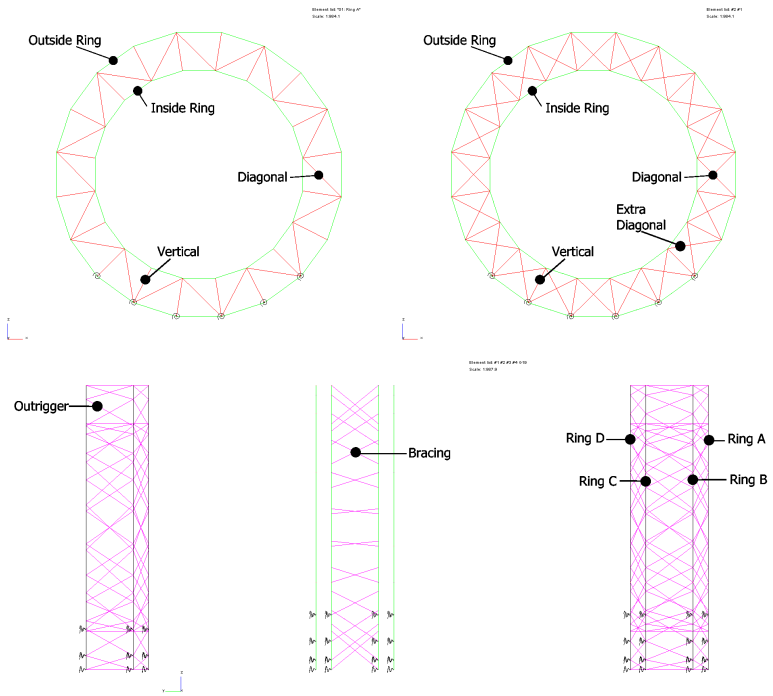

Figure 1.5: Different elements

2. Literature study

In this literature study it is meant to make clear what a Ferris wheel exactly is. What problems are expected to occur in a structure which is free to rotate? What parameters are of importance? And how some challenges in the Great Dubai Wheel are dealt with.

2.1. Ferris wheel in general

To get a first and good insight in this Master thesis it is important to know what a Ferris wheel exactly is and for this Master thesis it is specifically important to know why it is important to have the biggest Ferris wheel in the world, and what are the specific structural aspects of a Ferris wheel.

2.1.1. What is a Ferris wheel?

A Ferris wheel is a ride meant to give the possibility to the people to have a panoramic view over a city or some specific area. The name Ferris wheel comes from the inventor "George Washington Gale Ferris, Jr. (1859-1896)". He built the first Ferris wheel in 1893 in Chicago as a landmark for the "World's Colombian Exposition". This first Ferris wheel stood 81m high, and was demolished in 1906. The Ferris wheel was meant to give the people a nice view over the city of Chicago and the "World's Colombian Exposition", but also to have a sort of landmark (status symbol) which was intended to be put in the same spectrum as the Eiffel tower in Paris.

To show that the first Ferris wheel indeed was a innovative structure, the axis of the Ferris wheel was at that time with 70 tons the largest steel forging ever fabricated. The function of the Ferris wheel as a landmark became more important with the fabrication of the London Eye in 2000.

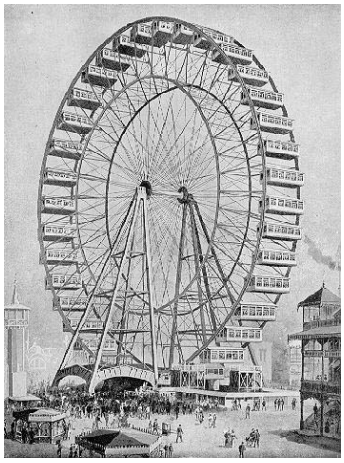

Figure 2.1: First Ferris wheel

Figure 2.2: Das Wiener Riesenrad

The oldest Ferris wheel which is still in operation today is the "Wiener Riesenrad" in Vienna, Austria. This Ferris wheel is 64.75m tall, and has a diameter of 60.96m. The "Wiener Riesenrad" contains 15 capsules. When the wheel was first build it contained 30 capsules but in the Second World War the wheel burned down, and it was chosen to rebuild the "Wiener Riesenrad" with only 15 capsules.

2.1.2. Classic Ferris wheel concept

The classic concept of a Ferris wheel is a rim which is connected to an axel by spokes like a very big bicycle wheel in which the capsules are connected to the rim, see figure 2.3 and figure 2.4. The capsules are kept level due to their self weight.

Figure 2.3: Bicycle wheel

Figure 2.4: Classic Ferris wheel concept (London Eye)

By prestressing the spokes it is possible to lower the stress ranges which otherwise would have occurred and this way minimizing the expected damage due to fatigue in the rim. This concept of prestressing was already applied in the original Ferris wheel.
Modern Ferris wheels distinguish themselves as being light steel structures. Comfort of the passenger will suffer sometimes because of this, as prestressed light steel structures don't have enough damping in their own system. Some sort of additional damping is therefore applied to all the modern Ferris wheels in one way or another.

2.1.3. Why the biggest?

Why is it important to have the biggest Ferris wheel? In fact why is it important to have the biggest one of anything? This question is a question that anyone can and possibly has to answer for themselves. Some might say that there is no need for again a bigger/taller something and other ones might say that going bigger/taller is the only way to keep ahead of the competitors.
When Dubai is taken into consideration, it is a city/country in which buildings are growing taller and taller every year. Plans of a skyscraper of more than 1000m tall are already in the final stages of approval. And when looking at the Ferris wheel specifically: in Beijing a Ferris wheel of 208m is already being built and because Dubai wants to have everything just a little bit bigger as the competitors, Dubai wants to go bigger, that is why it is a little bit odd that the first design only mentioned a height of 185m.
But it still is the question if by building bigger the landmark state of the object also grows. When looking at the Ferris wheel still the first modern Ferris wheel, the "London Eye" (figure 2.5) with a diameter of 135m has the biggest landmark status and it is at the moment not the biggest Ferris wheel, the "Singapore flyer" is 165m. If other cities achieve

the same landmark symbol by building a higher Ferris wheel like the Great Beijing Wheel (208m figure 2.6) is certainly not a given constant.

Figure 2.5: London Eye river view

Figure 2.6: Great Beijing Wheel (ready end of 2009)

Because of this question whether the status really depends on size alone, a radical new concept has been proposed for the "Great Dubai Wheel", which is a Ferris wheel without spokes. A nice detail in this is that the original "design" of the "London Eye" also didn't have any spokes (figure 2.7).

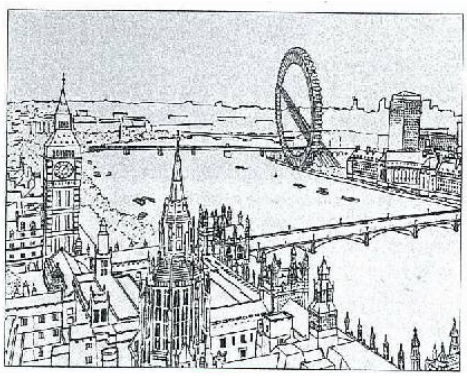

Figure 2.7: London Eye original design [10]

2.1.4. Ferris wheel without spokes

There is not one Ferris wheel without spokes anywhere in the world. At least not one Ferris wheel without any spokes in which the entire structure is rotating. In Tokyo, Japan a so called Ferris wheel named "the Big-O" (see figure 2.8) is constructed. But whether this is a Ferris wheel or a very slow roller coaster is still under debate. The concept is a stationary ring on which the capsules drive on a rail.

Figure 2.8: Big-O, Tokyo [8]

The main difference is shown in figure 2.9. In the left wheel the entire structure is rotating, and on the right only the capsules are rotating and the ring is stationary.

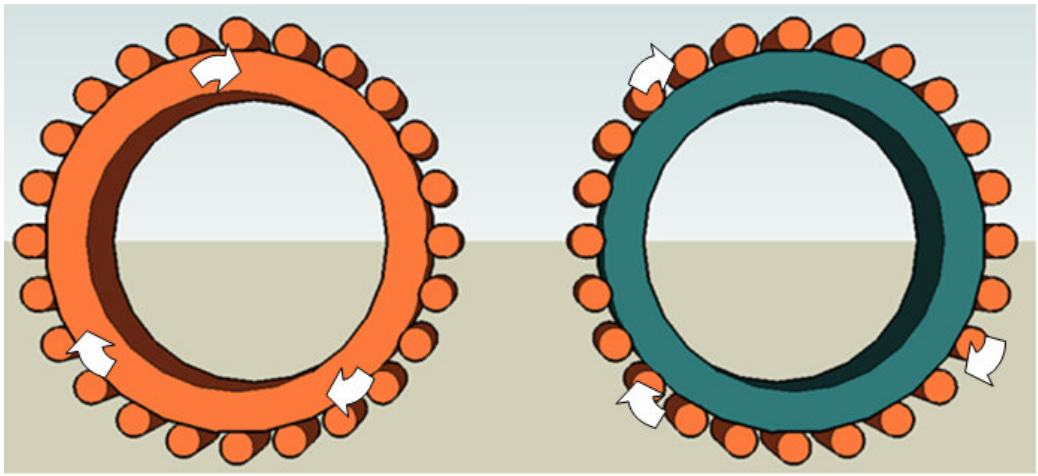

Figure 2.9: What's rotating?

The main difference on a structural point of view is that the normal Ferris wheel is complexly dynamic loaded, and the right one is almost completely statically loaded.

2.2. Classic Ferris wheel parameters

In order to understand the fundamental differences between the two introduced concepts of Ferris wheels in the previous chapter, the parameters of a classic Ferris wheel concept are investigated. This is especially done for the kind of loading, the weight of the structure, geometrical properties etc. For this analysis the "London Eye" is reviewed.

2.2.1. London Eye

Name	The British Airways London Eye Project also known as the Millennium Wheel
Location	London, Great Britain
Year	2000
Client	The London Eye Company
Main sponsor	British Airways
Main contractor	Hollandia
Duration of a rotation	½ hour
Weight	1100 tonnes

Table 2.1: London Eye general info

Figure 2.10: London Eye

Diameter	135m
Number of capsules	32
Height rim	6m
Width rim	9m
Size capsules	8m * 4m

Table 2.2: London Eye geometrical properties

Steelgrade	S355
Sections	Ø457x16mm Ø244.5x8mm
Number of cables	64 normal cables Ø70mm 16 rotation cables Ø70mm

Table 2.3: London Eye mechanical properties

- In total 32 capsules with a capacity of 25 persons each are placed on the wheel. The total capacity per rotation is 800 persons. Per day a total of 19200 customers can enjoy a ride in the London Eye.
- Because the London Eye is a prestressed welded steel structure not a lot of damping can be expected from it. So the dynamic amplification factor due to wind loading is severe. To still be able to ensure the passengers comfort, the wheel is equipped with 64 tuned mass dampers. These dampers make sure that the customers don't suffer from nausea.
- The original design of the London Eye consisted of 32 spokes but the wheel failed on fatigue, so the number of spokes was increased to 80. All the cables are prestressed so the cables will always stay under tension.
- Fatigue was an important issue in the design. Because of this the London Eye needed to be constructed as flat as possible (building tolerances were severe only a out of plane tolerance of 20mm of the total structure was allowed).
- The wheel is designed for a period of 50 years. During these 50 years the wheel will be opened 12 hours a day and a full rotation takes 30 minutes. The total number of rotations then becomes 438.000.

When interpreting the available literature about the "London Eye" it becomes clear that the entire structure is heavily fatigue sensitive. This was solved by more than doubling the spokes. Also the building tolerances were very small.

The ratio of self weight to variable weight of the "London Eye" is:
1 person weighs about 100kg → 1 person is 1kN.
About 800 customers can enjoy the "London Eye" at one time → 800kN.
Self weight of the structure is 1100 ton. → 11000kN;
Ratio variable load → permanent load

$$\frac{800}{11000} * 100\% = 7.3\%$$

3. Outside the Box

This Master thesis is about finding the maximum possible diameter of the "Great Dubai Wheel" and some problems are known from a prior study by Bolleboom [13]. In an early stage some possible solutions are "shouted", which are mentioned in this chapter. This was done in an early stage because in an early stage the lack of knowledge of the structure will help to find solutions which in a later stage will seem feasible but would not have been thought of at that stage.

3.1. Shouting to the box

Helicopters which keep the wheel upright 24/7;	
Building which supports the wheel;	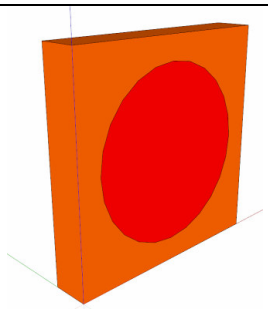
Why rigid joints?;	Why not use hinges?
Supporting structure ellipse instead of circular;	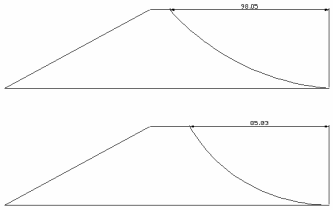
Other E-modulus;	
Other material;	For instance timber, titanium, aluminium, concrete.
Add an extra ring for taking the wind forces;	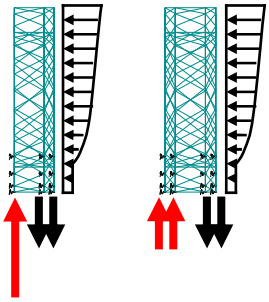
Make the ring stationary	see figure 2.9;
Other stiffness foundation;	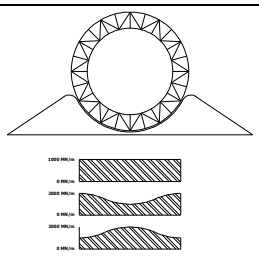
Diagonals skip a segment;	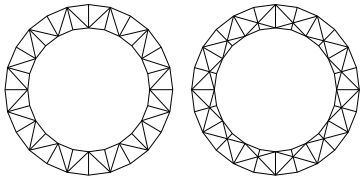
Cables for the diagonal elements;	

3.2. Girder types

- In the original design the girder is a modified Warren truss. Another possibility is a fully closed box girder;

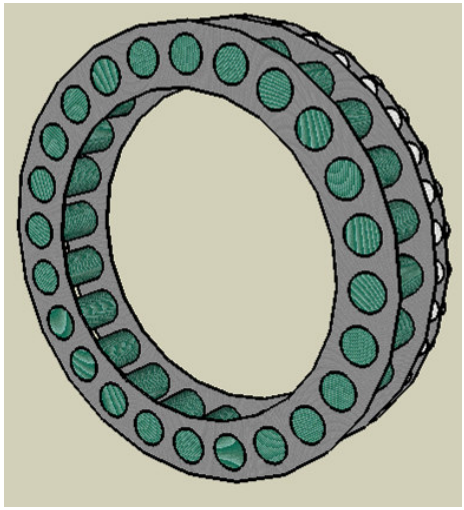

Figure 3.1: Box girder

  - Fully closed ring, made out of 3 box girder rings or I shaped rings. These types of girders are much less sensitive to fatigue behaviour. Also the support conditions can be optimized by supporting the ring over its full length. This way the peak moments and normal forces are reduced. The self weight of the structure will be increased by this type of girder. With this type of girder the full inertia bending moment can be used instead of the 40-60% that can be used in a truss girder. The self weight will be higher for this type of girder because more material is needed to fill the whole sides.

- Crosses instead of single diagonals, see figure 3.2;

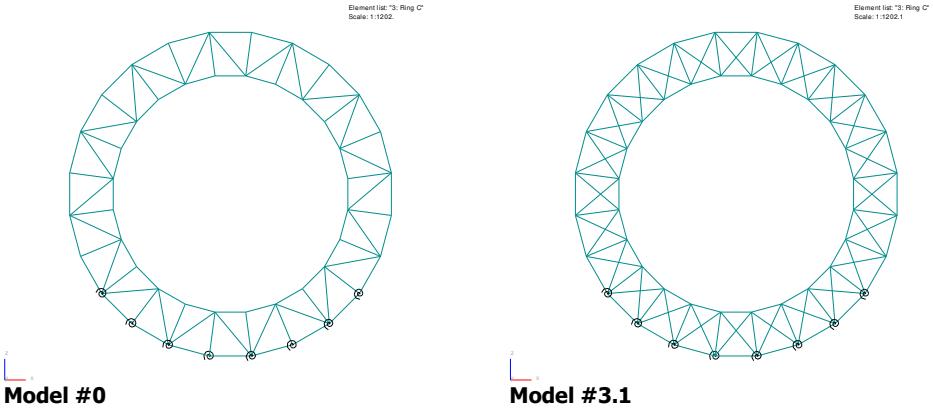

Model #0 **Model #3.1**

Figure 3.2: Modified Warren truss and cross truss

- Increasing the ring thickness;

- Reduce wind loading by rotating the entire structure;
  - Put the entire structure on some sort of rotating disc (sort of weather-vane figure 3.3).

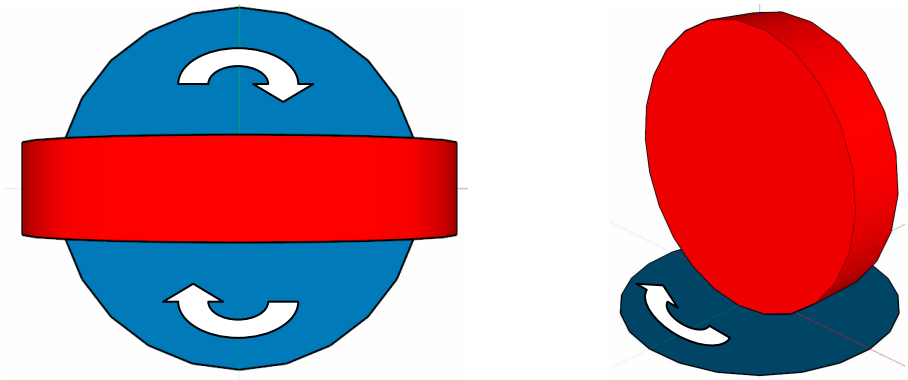

Figure 3.3: Weather-vane

- Different # of section;
  - Segmentation 24 -> 36 or 40 for instance;
- Other sections instead of CHS;

3.3. Prestressing the Great Dubai Wheel in one way or another

Classic Ferris wheels are prestressed by the spokes, this in order to reduce the moments in the structure. Ways in order to prestress the Great Dubai Wheel are:

- Triangular prestressing;
- Circular prestressing;
- Prestressing in the verticals;

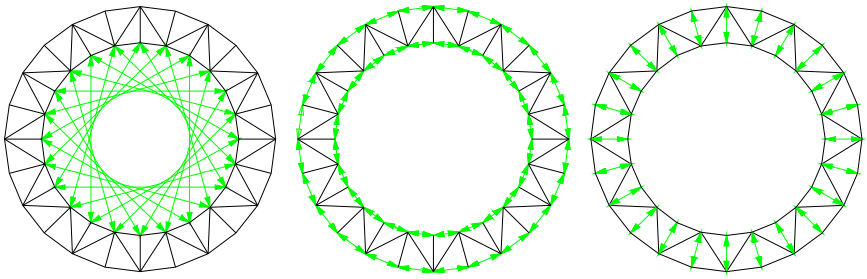

Figure 3.4: Ways to prestress

Normal forces in the structure will grow due to prestressing but probably the moments will be reduced. So it may be possible that the maximum stresses in the structure will get bigger due to prestressing, but the stress range will get smaller.

4. 2D-ring model

The wheel can be seen as a 2D-truss, as seen in figure 4.1. For a simply supported (Warren) truss it is possible to simplify the mechanical model to a simply supported prismatic beam. The normal forces in the upper and lower chord are then easily derived from simple moment equilibrium.

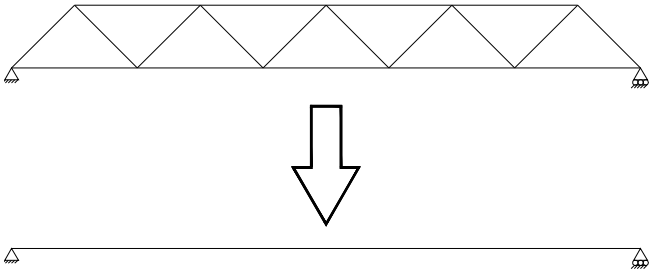

Figure 4.1: Truss modelled into a beam

Also the deflection can be derived by the "vergeet-me-nietjes", but because the real girder is a truss girder not all the properties can be easily derived. For instance the inertia bending moment will not be the sum of the inertia bending moment of the sections plus the Steiner part. This is because also shear deformation will be present. The decrease of the EI is easily derived by modelling the truss girder in OASYS-GSA put a point load in the middle node, and with the deflection in the output, together with the vergeet-me-nietjes the EI is calculated. See paragraph 4.1.3.

This leads to the following simplification of the model.

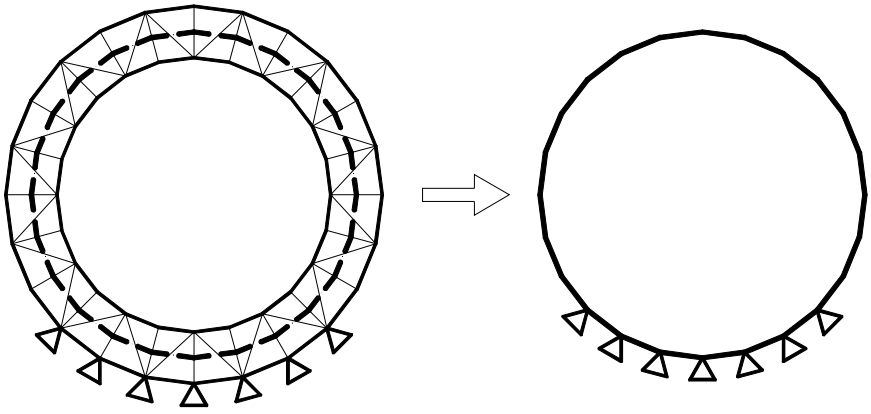

Figure 4.2: Simplification of the 2D-truss model

The dashed ring in the middle will be modelled and analyzed. This means that the diameter of the analyzed model is $\frac{185+135}{2} = 160m^1$.

4.1. Parameters

Of course some parameters have to be known before the analyses can be done. This first part of the Master thesis is about finding the maximum diameter by the current parameters. The parameters are chosen the same as in a prior study to the wheel [13].

- Ring thickness is 25m;
- Width of wheel is 40m[1];
- Support stiffness (k=1000 MN/m[1]) per support;
- Capsules;
  - # of main capsules is 24;
  - SW of capsules (SW_{cap}= 3600 kN);

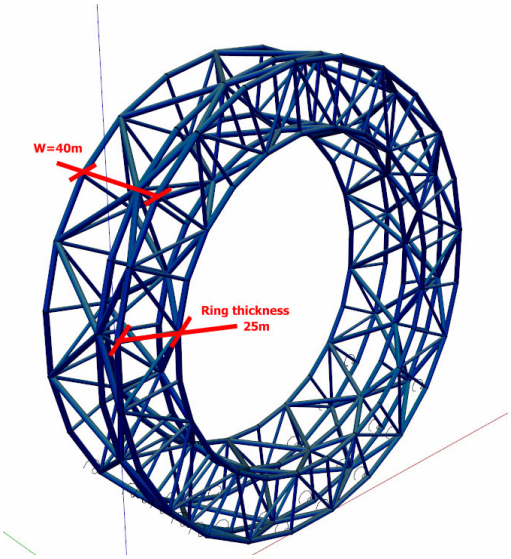

Figure 4.3: Parameters 2D-ring model

4.1.1. Supports

In a prior study [13] the supports are modelled as springs with k = 1000MN/m[1]. Because there are three rings that are modelled as one the spring coefficient will be 3000MN/m[1].

The supports are modelled so that the supports act perpendicular to the structure. The spring stiffness of k=1000MN/m[1] is approximately equal to a support which consists of ten standard prefab foundation poles.

4.1.2. Sections

In a prior study [13] two sections are used. These sections are also used for this preliminary work. Because a 2D-ring model is used the cross sections are recalculated to be able to model in a correct way.

The two sections that are used in the prior research:

- Circular hollow section 2220/40 (d=2220mm, t=40mm).

Area	A=	273947	[mm^2]
$I_{yy} = I_{zz}$	=	$1.628*10^{11}$	[mm^4]
$W_y=W_z$	=	$1.467*10^8$	[mm^3]
Weight per m^1	G=	21.094	[kN/m^1]

Table 4.1: Section 2220 - 40

- Circular hollow section 1440/40 (d=1440mm, t=40mm).

Area	A=	175929	[mm^2]
$I_{yy} = I_{zz}$	=	$4.314*10^{10}$	[mm^4]
$W_y=W_z$	=	$0.599*10^8$	[mm^3]
Weight per m^1	G=	13.547	[kN/m^1]

Table 4.2: Section 1440 - 40

Because the structure is made of trusses, shear deformation can not be neglected. A reduction of the Steiner part is taken into account. This reduction can be in the range of 60%. How much this reduction exactly is determined by comparing the results of two models (simplified beam model and a frame model). In this case the reduction of the Steiner part is 50%, which is considerable.

The cross section of one ring is displayed on the right.

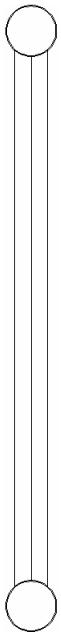

The moment of inertia with Steiner's rule becomes.

$$I_{yy} = 2*I_{own} + \sum A*a^2$$

$$I_{yy} = 2*1.628*10^{11} + 2*273947*\left(\frac{25000}{2}\right)^2$$

$$I_{yy} = 8.577*10^{13} \quad mm^4$$

$$A = 2*A_{2220/40}$$

$$A = 2*273947 = 0.548*10^6 \quad mm^2$$

Because this is only for one ring the area and moment of inertia are multiplied by three.

$$I_{yy} = 3*8.577*10^{13} = 2.573*10^{14} \quad mm^4$$

$$A = 3*547894 = 1.64*10^6 \quad mm^2$$

4.1.3. Reduction EI

Because the wheel does not only deform due to bending, but also due to shear deformation the inertia bending moment is reduced to take this into account. The reduction factor is determined, by taking the deformation from the OASYS-GSA model and calculating the appropriate inertia bending moment (I). The hand calculation is given in figure 4.4.

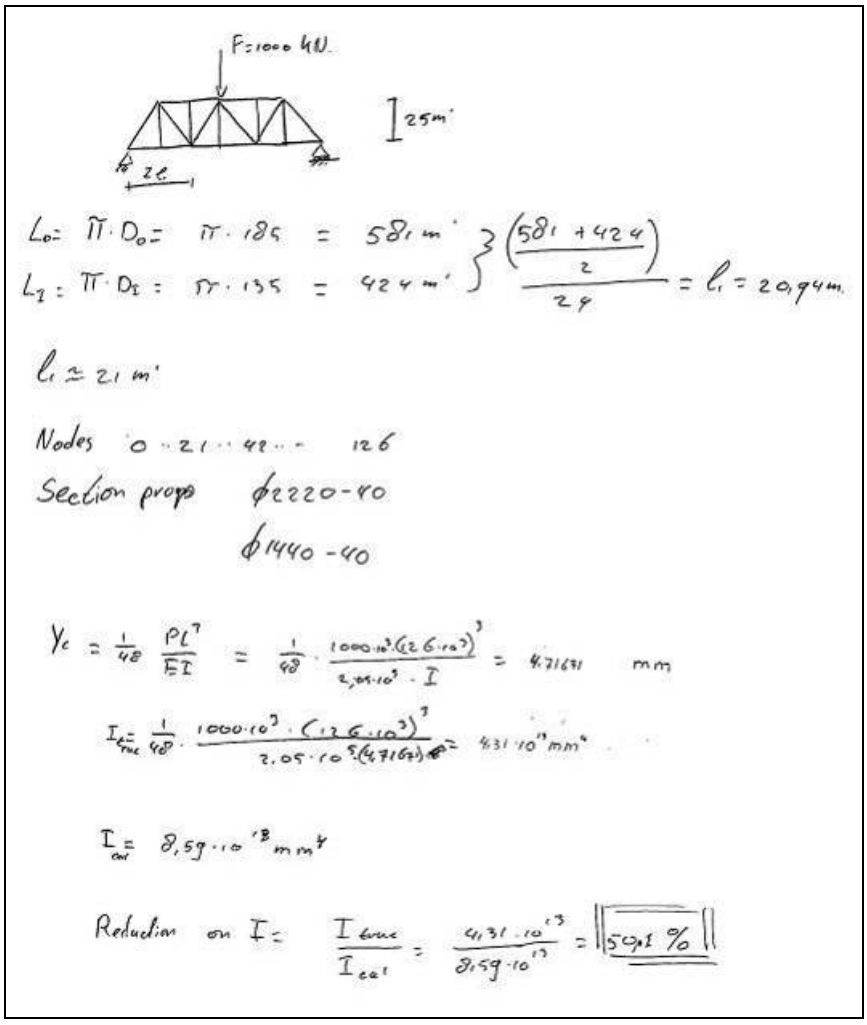

Figure 4.4: Hand calculation reduction I

In addition to this deformation there is the contribution caused by joint flexibility of all members. Normally this contribution is neglected but for this type of structure this will result in larger displacements. The displacement of the model with rigid joints is 4.7mm and with hinges is 4.8mm. The calculation in figure 4.4 is not greatly affected by this.

4.2. Loading

The loading consist of several elements. At first only the self weight of the structure and the capsules in considered. The purpose of these first steps is to get a feeling for the structure. What aspects play an important role when trying to maximize the diameter?

- Self weight

The self weight of the structure is calculated by taking the total length of the section needed and multiply it by its weight per meter and this for both sections:

Total length CHS 2220/40

#	Description	L	Unit
24	Diagonal between the outer rings big	38.511	[m^1]
24	Diagonal between the inner rings big	34.792	[m^1]
24	Diagonal between the outer rings small	26.136	[m^1]
24	Diagonal between the inner rings small	20.261	[m^1]
72	Outer ring	24.147	[m^1]
72	Inner ring	17.621	[m^1]

Table 4.3: Length CHS 2220

Total length of section CHS 2220/40 is 5880 m^1.
The total dead load of section CHS 2220/40 (A= 0.274m^2, γ=7700 kN/m^3) is 124.0 *10^3 kN.

Total length CHS 1440/40

#	Description	L	Unit
72	Diagonals in the rings	32.411	[m^1]
72	Verticals	25.000	[m^1]

Table 4.4: Length CHS 1440

Total length of section CHS 1440/40 is 4134 m^1.
The total dead load of section CHS 2220/40 (A= 0.176m^2, γ=7700 kN/m^3) is 55.98 *10^3 kN.

Total dead load becomes: 180.0 *10^3 kN. (This is not exactly equal to the dead load of the prior study [13] 230.2*10^3 kN; this is because the wheel is divided into 24 segments instead of 36 of the prior study). This load is inserted into the model as nodal forces.

Load per node will become $F_{eg} = \frac{180.0*10^3}{24} = 7500kN$.

- Capsules

Each capsule weighs 3600kN. There is a total of 24 capsules. So the total load from the capsules is 86.4 *10^3 kN.

The weight of a capsule is taken from the prior study [13]:

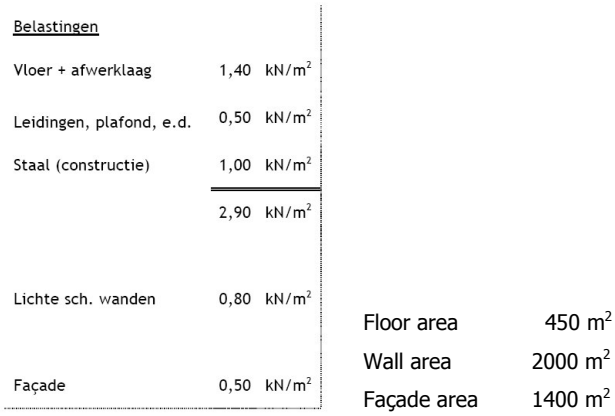

Belastingen		
Vloer + afwerklaag	1,40	kN/m²
Leidingen, plafond, e.d.	0,50	kN/m²
Staal (constructie)	1,00	kN/m²
	2,90	kN/m²
Lichte sch. wanden	0,80	kN/m²
Façade	0,50	kN/m²

Floor area	450 m²
Wall area	2000 m²
Façade area	1400 m²

Figure 4.5: Capsule weight [13]

- Other loads

Because the prior study [13] pointed out that the self weight of the structure is the critical load on the structure, other loads like wind loads or snow loads, are for this preliminary indicative calculations not taken into account.

4.3. Support

Interesting is to look at how the structure reacts when the supporting structure is raised. The prior study [13] shows that it is preferable to raise the height of the supporting structure as much as possible. The thing to show with the simplified model is how the moment and normal forces distribution as well as the deflections react by raising the supporting structure. This gives insight in how much can be optimized in a later stage of the design by raising the supporting structure, when the diameter is changed.

The following procedure is followed. Seven models are constructed in OASYS-GSA see figure 4.6. The first model only has one support and the last model has supports over half its height. By looking at the changing member forces a conclusion is drawn of the most optimal solution. The demand of the architect is that the height of the supporting structure does not exceed ¼ * the diameter. This demand could be possibly released when the design for whatever reason isn't feasible and can be made feasible by raising the height of the supporting structure.

It is expected that the higher the supports are placed the more preferably the situation becomes. How big the advantage of increasing the height of the supporting structure is, is investigated in this chapter.

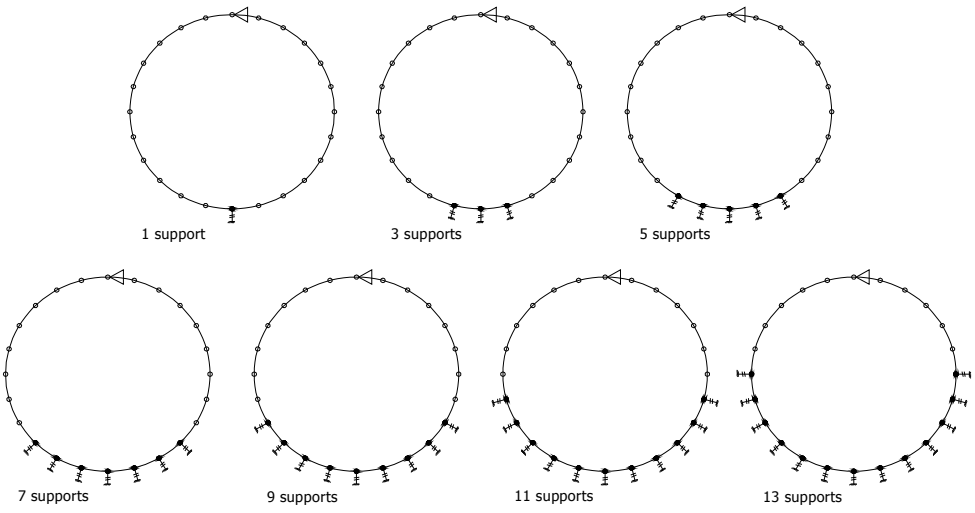

Figure 4.6: Support conditions considered

The support in x-direction at the top is to make the models stable. The reaction forces in these supports are 0, but when not present singularity occurs.

For stability issues the models with 1, 3 5 and possibly 7 supports in place, are not feasible, the reaction forces and displacements are too large. But the analysis will also contain the analysis of the models with less than 7 supports to get a feeling for the influence of the increase of the number of supports. The following support conditions are checked:

# of supports	Highest support [m]
1	0.000
3	2.726
5	10.718
7	23.431
9	40.000
11	59.294
13	80.000

Table 4.5: Support conditions checked

4.4. OASYS-GSA model

The Great Dubai Wheel consists of three rings. For this ring model these three rings are modelled as one ring. This is done by assuming that the coupling between the rings is a stiff connection. In reality this is not true, but the nature of this analysis is only indicative and meant to come with conclusions about the sensitivity of height of the supporting structure on load distributions and deformations, as mentioned in chapter 4. For the load distribution special attention is paid on fluctuating axial forces and bending moments. This because of fatigue as discussed in chapter 9.

The OASYS-GSA ring model consists of 24 elements. It is chosen to use 24 segments because in the Great Dubai Wheel 24 main capsules are used and therefore 24 segments. The supports are modelled as springs perpendicular to the structure. A spring stiffness of k=1000MN/m is used. This is roughly the stiffness of a foundation of ten prefab concrete foundation poles.

4.4.1. Check the model

To check the model a hand calculation is made. A concentrated load is placed on the structure at the top node. The structure will deform because of this. In the top part two points of inflection appear. In these points the moments are zero. It is then possible to model this point as a simple support. The distance l1 between the two points of inflection is estimated at 2/3 * D

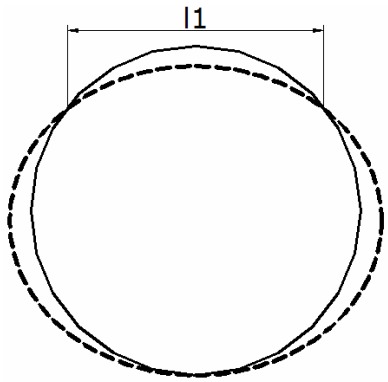

Figure 4.7: Points of inflection

The maximum moment is calculated as the model shown in figure 4.8 is analyzed.

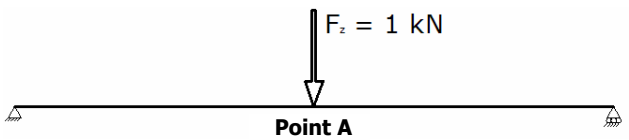

Figure 4.8: Very simple model

With elementary mechanics it is shown that:

$$\sum F|_V = F_z + R_l + R_r = 0$$
$$R_l = R_r = -\tfrac{1}{2} * F_z$$

$$\sum M|_A = -\tfrac{1}{2} * F_z * \tfrac{1}{2}(l_1) + M_A = 0$$
$$M_A = \tfrac{1}{2} * 1000 * \tfrac{1}{2}\left(\tfrac{2}{3} * 160\right) = 26.6kNm$$

The output of OASYS-GSA gives a moment of 25.3kNm; it seems that the estimated distance between the two points of inflection is estimated too high. When the distance from OASYS-GSA is used, the hand calculation also results in a moment of 25.3kNm.

Another check for the model is to look at the sum of the reaction forces and if it is as predicted. This is done for all the models.

4.5. Results OASYS-GSA model

4.5.1. Moments

The Great Dubai Wheel is a Ferris wheel therefore the whole structure rotates. This means that every node of the structure will be in all positions over a period of 6 hours. Figure 4.9 shows what this means for the moment distribution in a node of the structure. Node position 1 is at the point located furthest to the right and moved counter clockwise along the wheel. The wheel rotates every 6 hours and 24 points are looked at, so the moment at every 15 min is known. The model with 9 supports is considered (supports until ¼ times the diameter).

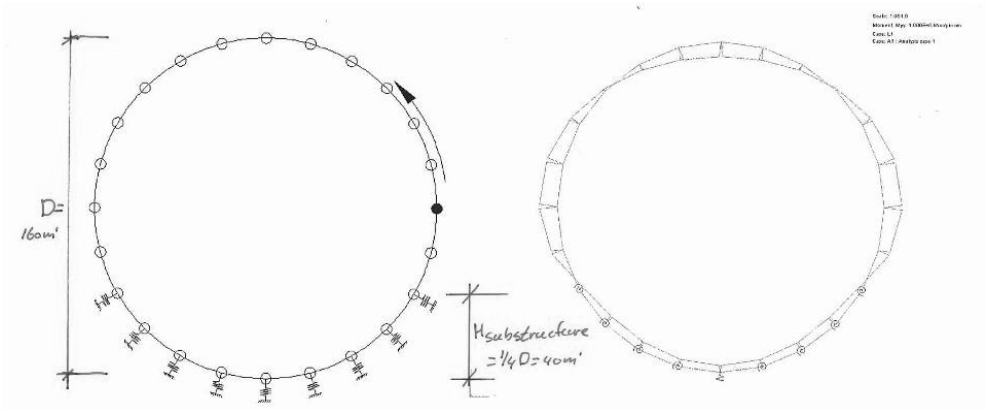

Figure 4.9: Start point rotation and moment line

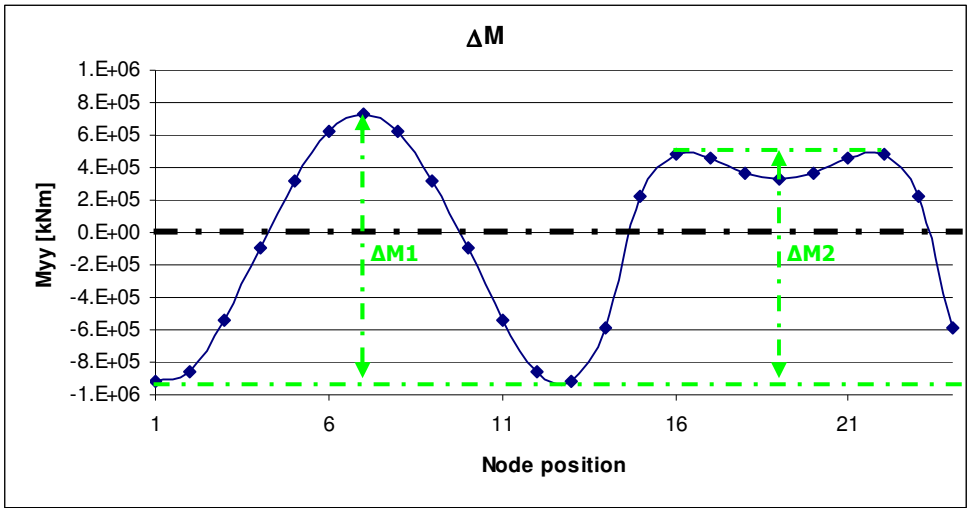

Figure 4.10: Graph of Myy with 9 Supports, ΔM1 and ΔM2

In figure 4.9 and figure 4.10 it is clearly seen that within every rotation of the wheel two peaks in the moment distribution occur. This means that for fatigue life roughly every six hours two stress cycles occur, expressed by ΔM_1 and ΔM_2. For fatigue behaviour it is important that $\Delta\sigma$ is as low as possible. Because of this ΔM should be as low as possible.

Therefore it is checked if the ΔM will decrease when making the supporting structure higher. The results of this study are shown in figure 4.11 below.

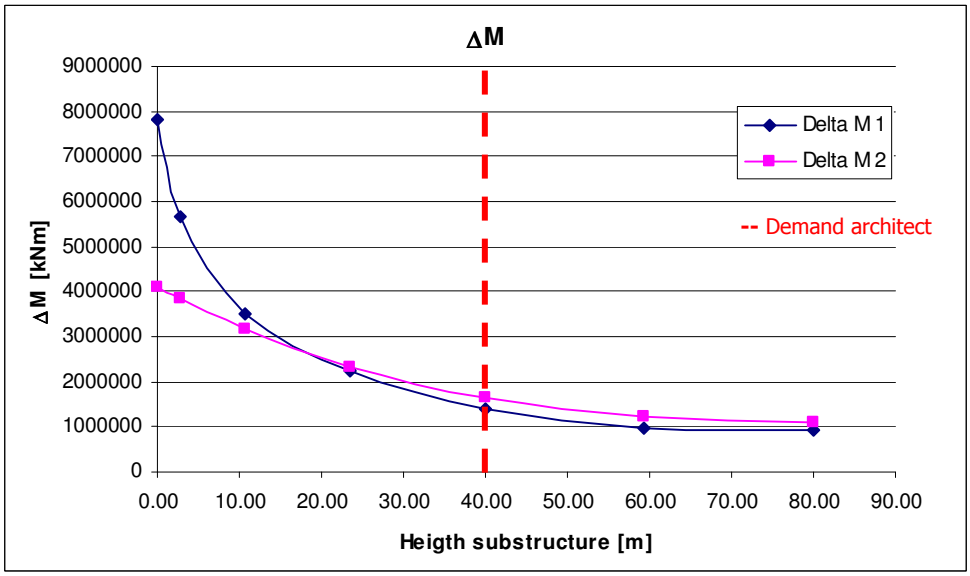

Figure 4.11: Graph ΔM in relation to the height of the supporting structure

It is clearly seen that when increasing the height of the supporting structure the ΔM decreases. The demand of the architect is that the height of the supporting structure does not exceed ¼ times the diameter of the wheel (which is stated at 185m so the maximum height of the supporting structure is 46.25m, because of the simplification of the model the maximum height of the supporting structure becomes 40m). When the height of the supporting structure is increased to 1/3 times the diameter the ΔM decreases with 25% - 30%.

A more important conclusion is that it must be avoided that the height of the supporting structure is lower then ¼ times the diameter, because the slope of the ΔM-graphs increases when the height of the supporting structure is lowered.

H [m]	$\frac{\Delta M_1}{\Delta M_9}$	$\frac{\Delta M_2}{\Delta M_9}$
0.00	5.58	2.48
2.73	4.06	2.33
10.72	2.51	1.91
23.43	1.59	1.41
40.00 = ¼	1.00	1.00
59.29 = ⅓	0.71	0.75
80.00 = ½	0.66	0.68

Table 4.6: Height supporting structure ΔM

4.5.2. Normal forces

For the normal forces in the structure it is expected that when the supporting structure is raised the normal forces will decrease. But not as much as can be seen by the moment analysis chapter 4.5.1. The same analysis as for the moments is made.

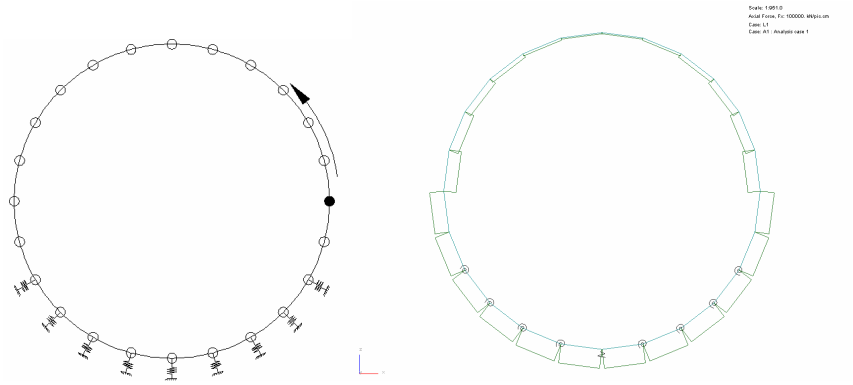

Figure 4.12: Start point rotation and Normal force line

The jump in the normal force diagram seen in figure 4.12 does not mean there is a sign change. This is due to the way OASYS-GSA generates its diagrams. This can be checked by the graph below in which there is no sign change.

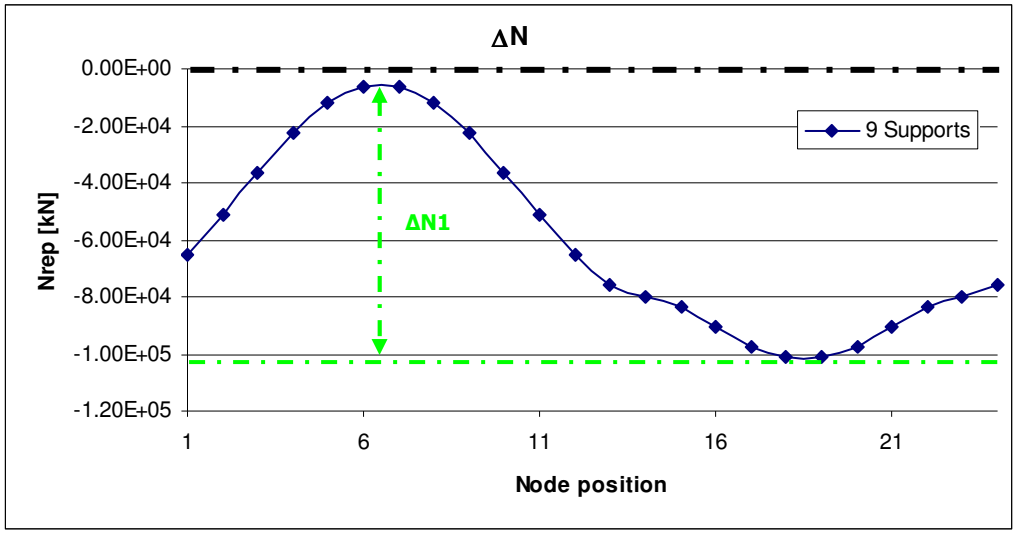

Figure 4.13: Graph of Nrep with 9 Supports, ΔN1

It is seen that the normal forces only have one peak per rotation. In the complete analysis the results show that for 1, 3 and 5 supports two peaks occur. This is explained by figure 4.14.

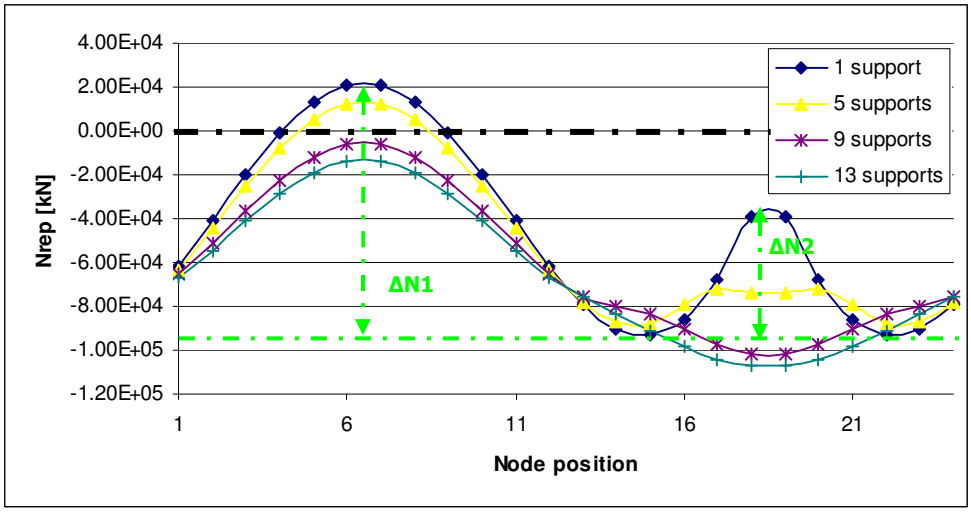

Figure 4.14: Normal Forces by the different support conditions

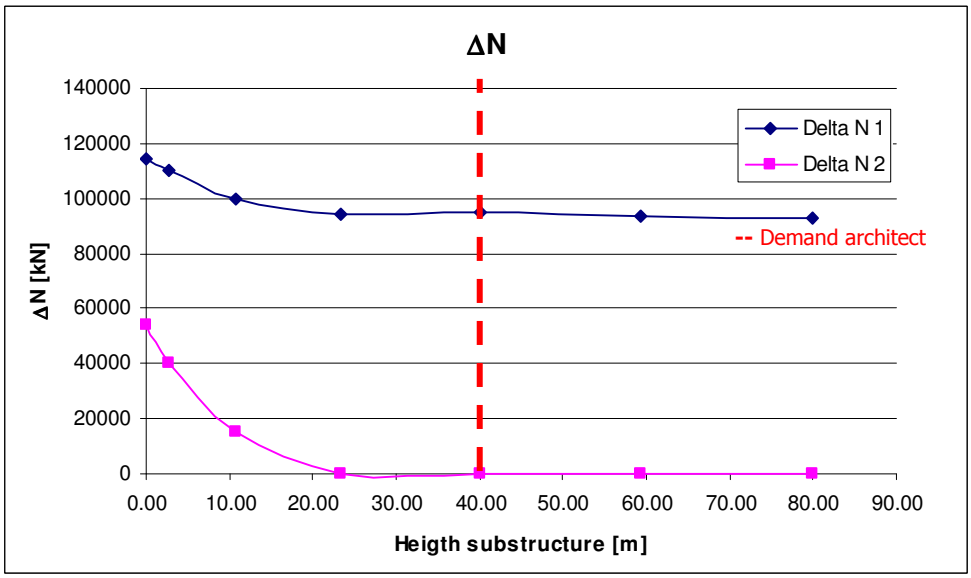

Figure 4.15: Graph ΔN in relation to the height of the supporting structure

When only one support is in place the load is transferred by bending to the support. When the supports are placed until half the diameter of the ring, the top op the ring will act almost like an arch and thus the moments will be reduced and the rest of the load will be transferred to the supports by normal forces. For the more realistic region in which the models with 7, 9 and 11 supports are found, the transfer of the load is by both normal forces and bending moments.

When looking at ΔN it is seen that not much reduction is possible. A big difference is only seen at 1 -5 supports, but for 7 until 13 supports there is not a big difference. This means that the normal force is more or less constant and not greatly affected by the height of the supporting structure, not a great improvement is expected here.

4.5.3. Displacements

The displacements of the ring is looked at in x (horizontal) and z (vertical) direction. For this case the y direction is restraint. As there are no loads placed on the structure in y direction.

- displacement in x direction;

To start the displacement in x direction is analyzed.

In figure 4.16 and figure 4.17 it is seen that the displacements are completely symmetrical. To show this the start point has been set at the top node.

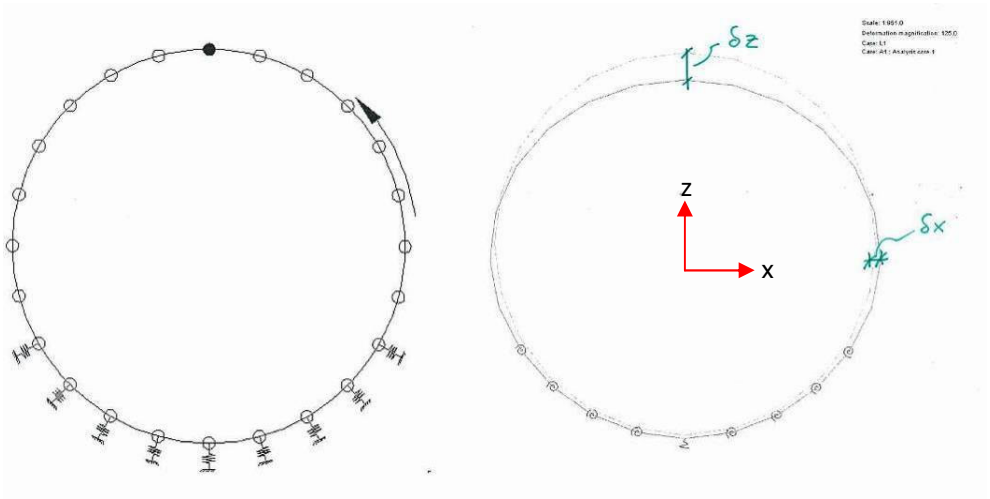

Figure 4.16: Start point rotation and displacements

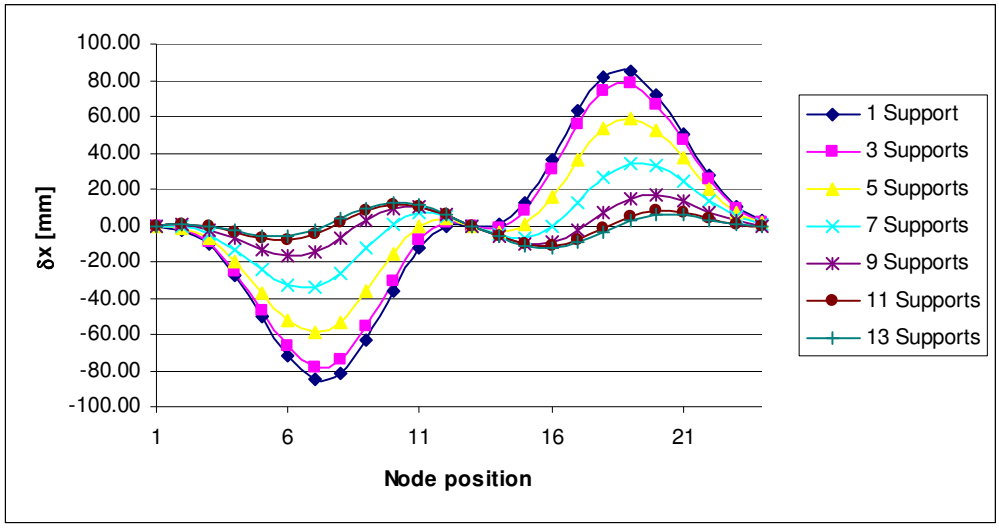

Figure 4.17: Displacements in x direction by the different support conditions

It is seen, in figure 4.17, that raising the height of the supporting structure has a big influence on the displacement in x direction and the displacements are fully symmetrical as expected. Figure 4.18 shows the maximum displacements in x direction in relation to the increase of the height of the supporting structure.

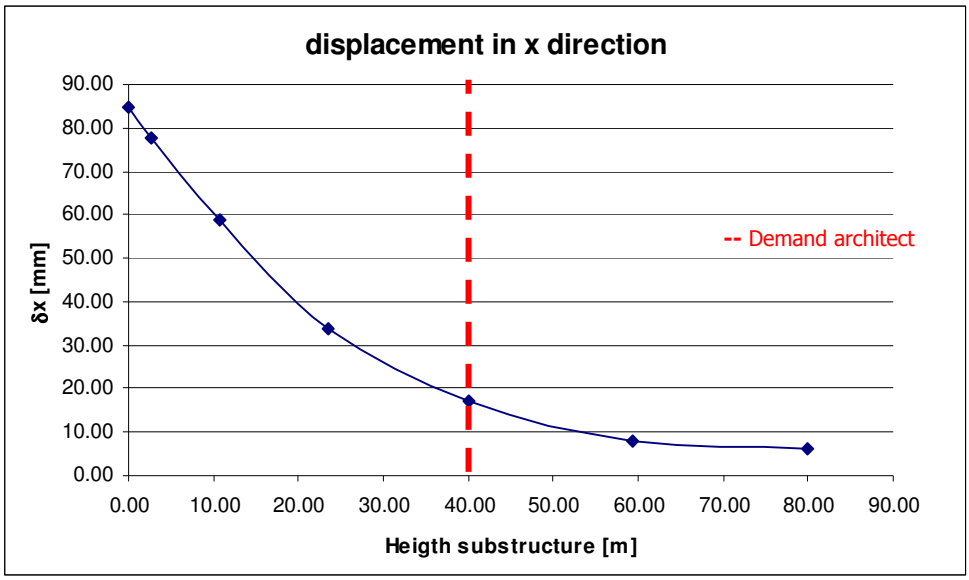

Figure 4.18: Graph δx in relation to the height of the supporting structure

By raising the supporting structure, from 40m to 60m, a reduction of the deflection in x direction of 50% is obtained.

H [m]	$\frac{\delta_x}{\delta_{x;40}}$
0.00	4.98
2.73	4.58
10.72	3.46
23.43	1.99
40.00	1.00
59.29	0.48
80.00	0.35

Table 4.7: Height supporting structure δx

In figure 4.17 and figure 4.18 it is seen that when the height of the supporting structure is increased the displacement in x direction is decreased. If in the final design the governing parameter is the displacement in x direction, than raising the supporting structure is an efficient way to reduce the displacement (the demand for the deflection in x direction is 1/500 * the height of the Great Dubai Wheel). As the decrease in de displacement in x direction is about 50%.

- Displacements in z direction.

In figure 4.19 and figure 4.20 it is clearly seen that the displacements in z direction are completely symmetrical (only loading due to self weight which also is a symmetrical loading). To clearly show this in the graphs the start point has been set at the bottom node. Because springs are used for the supports the results are adjusted for the total z displacement of the system. This is done by subtracting the displacement of the bottom node from all the other displacements. The results is seen in figure 4.20. Just as for the displacements in x direction, also here a reduction of the deflection is possible when increasing the height of the supporting structure.

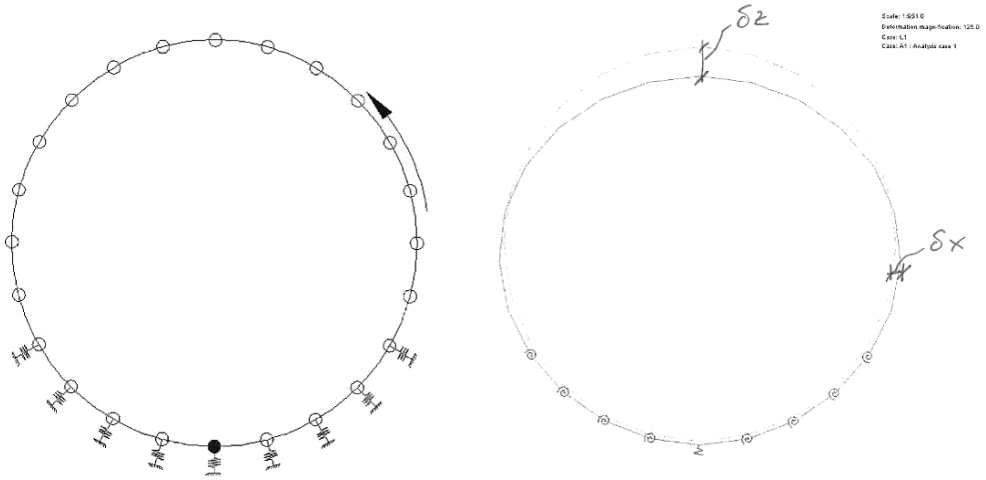

Figure 4.19: Start point rotation and displacements

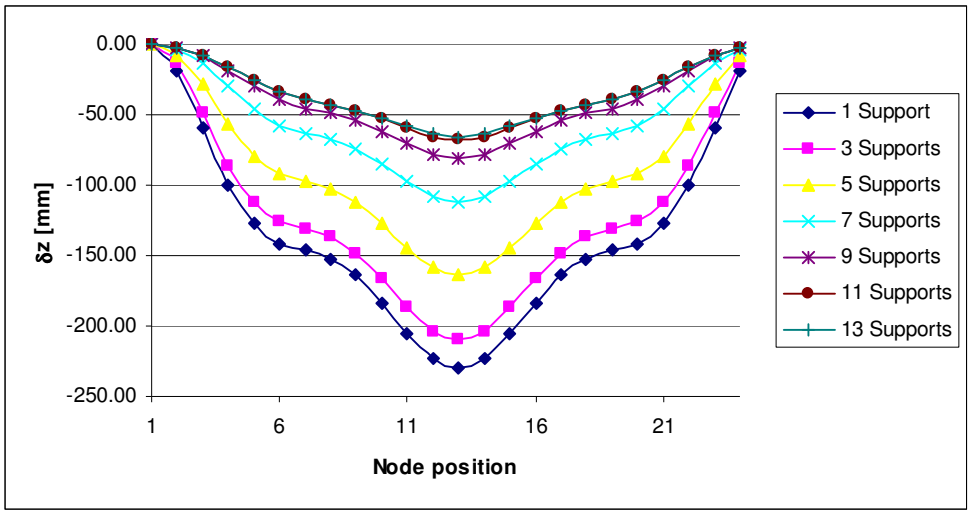

Figure 4.20: Displacements in z direction by the different support conditions

It is clearly seen that raising the height of the supporting structure doesn't have a big influence anymore when the height of the supporting structure gets above the ¼ times the diameter. With the demand for the deflection in z direction of about 1/500 * the height of the Great Dubai Wheel an acceptable value is 370mm. So all the models are acceptable, it is therefore expected that the deflection in z-direction is not a governing parameter.

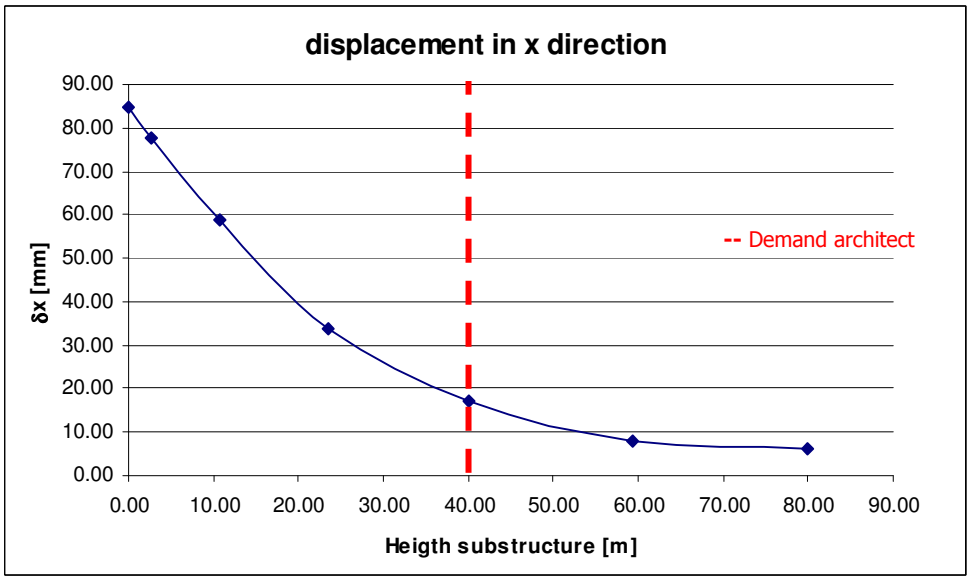

Figure 4.21: Graph δz in relation to the height of the supporting structure

In figure 4.21 it is seen that the displacement in z-direction decreases when the height of the supporting structure is raised. But the gain when the supporting structure increases in height above ¼ times the diameter (40m1) is not very big.

In the table below it is seen that the increase of the height of the supporting structure above ¼ times the diameter will give a decrease of the displacement in z-direction of 16%.

H [m]	$\frac{\delta_z}{\delta_{z;40}}$
0.00	2.84
2.73	2.60
10.72	2.02
23.43	1.39
40.00	1.00
59.29	0.84
80.00	0.81

Table 4.8: Height supporting structure δz

4.5.4. Stresses due to bending and normal force

Because the prior study [13] to the wheel indicated that the wheel is sensitive for fatigue failure the stresses in the wheel need to be known. Of course also for static strength the stresses need to be known but due to the fact that the self weight of the structure is in this project a cyclic load, fatigue plays an important role in the analysis.
To calculate the stresses, and in this case the stress range of the structure the following procedure is followed.

To determine the maximum and minimum stress, the following formulas are applied. The stresses in the inside ring and in the outside ring need to be known. Therefore the two following formulas are used, and the two following graphs are plotted in figure 4.23 and figure 4.24.

$$\sigma_{in;rep} = \frac{N_{rep}}{A} - \frac{M_{rep}}{W_{el}};$$

$$\sigma_{out;rep} = \frac{N_{rep}}{A} + \frac{M_{rep}}{W_{el}};$$

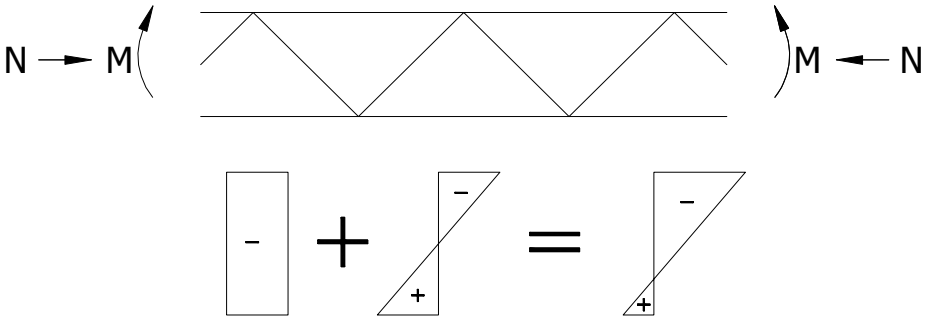

Figure 4.22: Stresses from normal forces and bending moments

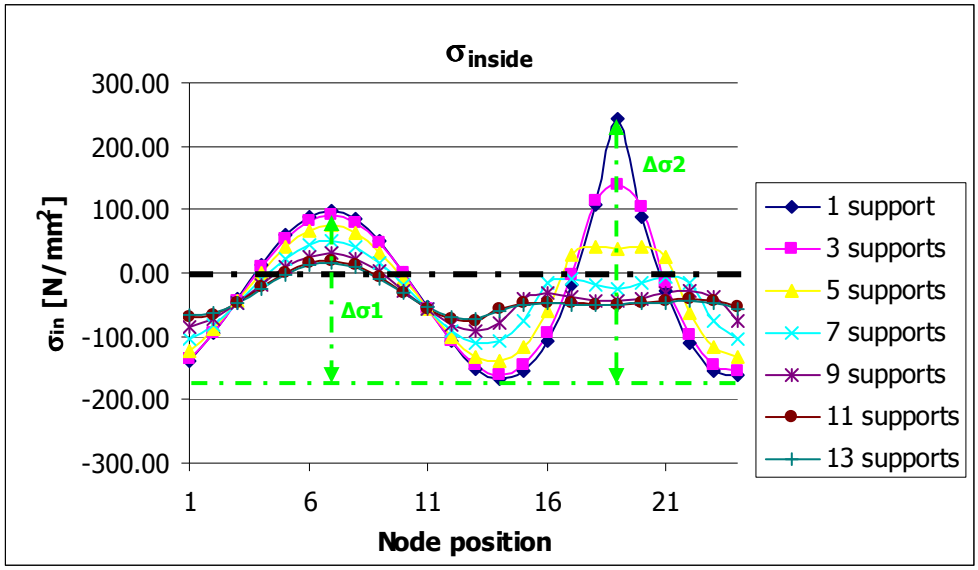

Figure 4.23: Stress distribution nodes inner ring

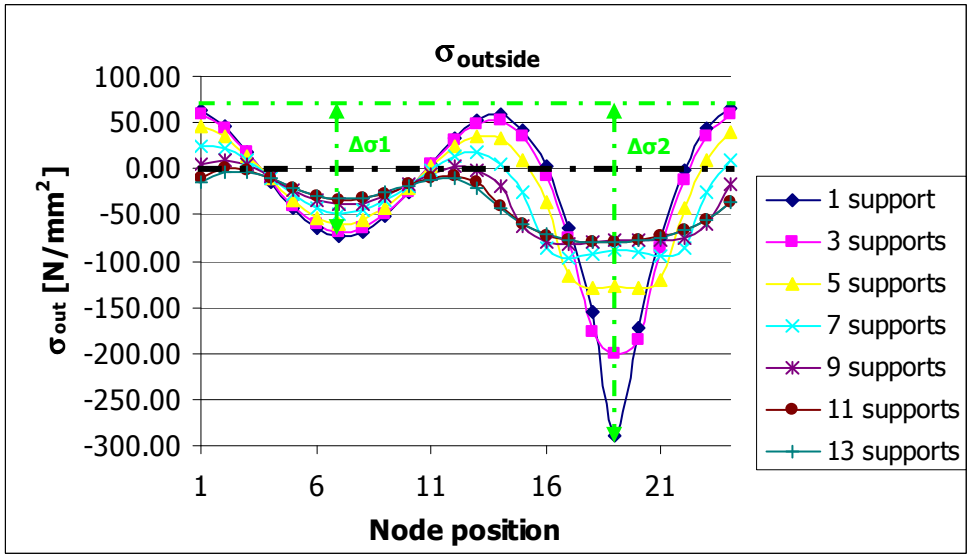

Figure 4.24: Stress distribution nodes outer ring

A remark is made that the stresses are without any safety factor and the stresses are not intended to show the real stress distribution in the structure, the distribution shows only what happens to the stresses in general when the support structure is raised. Because only the self weight of the structure as well as the main capsules are taken into account this gives a good indication what happens to the stress distribution for all the vertical acting loadcases.

In figure 4.23 it can be seen that for 1, 3 and 5 supports two clear stress peaks occur, and for 7, 9,11 and 13 supports only one large stress peak and one smaller stress peak occurs, the same applies for figure 4.24. This means that it is preferable to have more supports in place. In figure 4.25 and figure 4.26 the $\Delta\sigma_{in}$ and $\Delta\sigma_{out}$ are given.

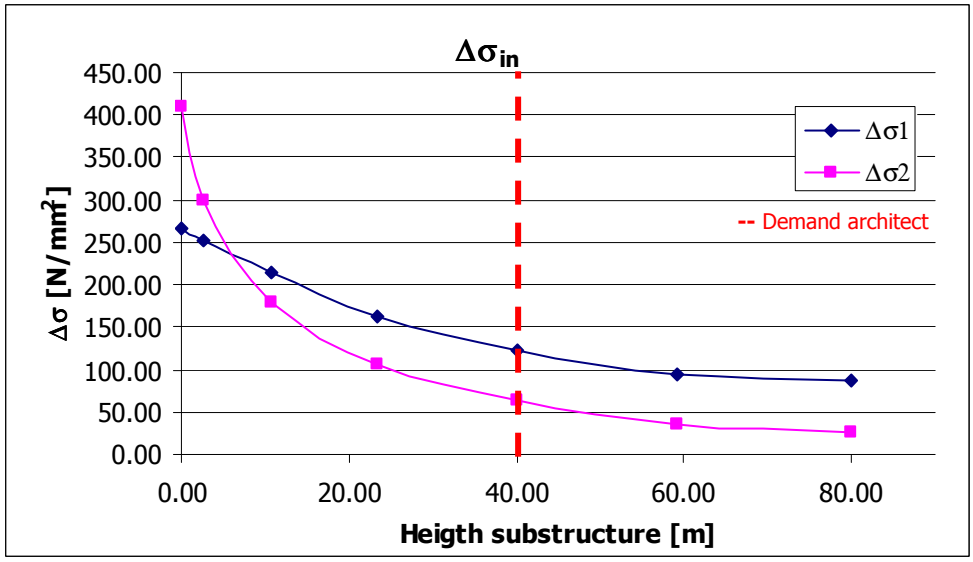

Figure 4.25: $\Delta\sigma_{out}$ in relation to the height of the supporting structure

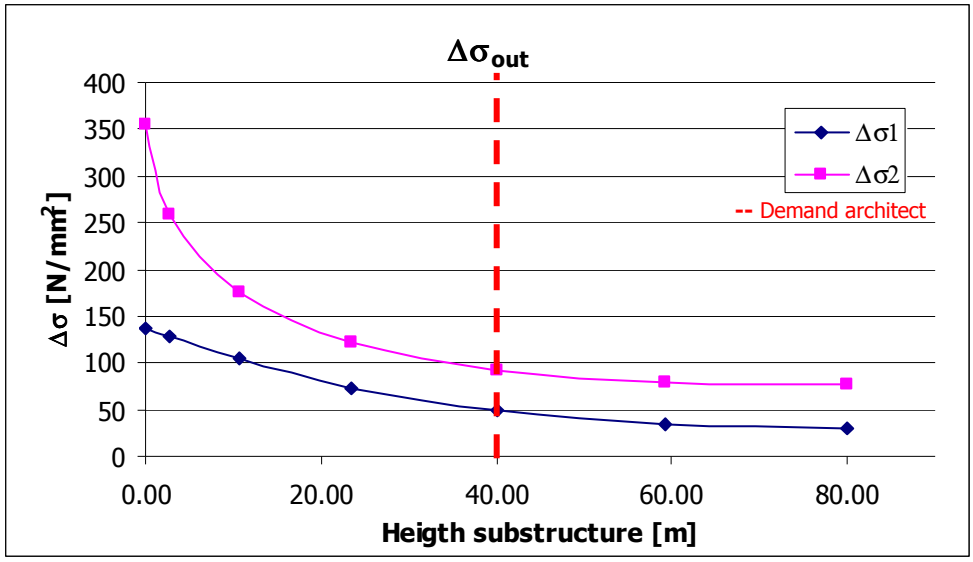

Figure 4.26: $\Delta\sigma_{out}$ in relation to the height of the supporting structure

H [m]	$\frac{\Delta\sigma_{1;i}}{\Delta\sigma_{1;9}}$	$\frac{\Delta\sigma_{2;i}}{\Delta\sigma_{2;9}}$
0.00	2.17	6.51
2.73	2.06	4.74
10.72	1.74	2.85
23.43	1.32	1.67
40.00	1.00	1.00
59.29	0.78	0.55
80.00	0.71	0.43

Table 4.9: $\Delta\sigma_{inner}$ 2D-ring model

H [m]	$\frac{\Delta\sigma_{1;i}}{\Delta\sigma_{1;9}}$	$\frac{\Delta\sigma_{2;i}}{\Delta\sigma_{2;9}}$
0.00	2.75	3.87
2.73	2.59	2.83
10.72	2.13	1.91
23.43	1.47	1.33
40.00	1.00	1.00
59.29	0.70	0.87
80.00	0.60	0.83

Table 4.10: $\Delta\sigma_{outer}$ 2D-ring model

Table 4.9 and table 4.10 make clear that increasing the height of the supporting structure has a positive effect on the stress ranges in as well the inner ring and the outer ring.

4.6. Dynamic response

Because the wheel is constantly rotating and the wind load probably has to be seen as a dynamic loading, it is important to look at how do the natural frequencies change when the height of the supporting structure is increased.

Because the model is a very simple model the question can be asked how useful this information is. Because for the 3D-model a large number of mode shapes will be found, also in torsion etc. But it is important to know the lowest natural frequency as it is most probable that resonance occurs at the lowest natural frequency (for wind the resonance will probably occur at the lowest natural frequencies, for earthquakes the other natural frequencies are of importance too).

Because the model is a 2D-ring model it is chosen to only look at the modes in vertical deformation. This ensures that the same mode shapes to be compared to each other. This is done by adding a support in the top node which supports the model in x direction; this is also done in the bottom node.

For this analysis only the permanent loading caused by self weight of the main structure and the self weight of the main capsules are taken into account.

In the figure 4.27 till figure 4.30 the mode shapes of respectively 1, 5, 9 and 13 supports are given.

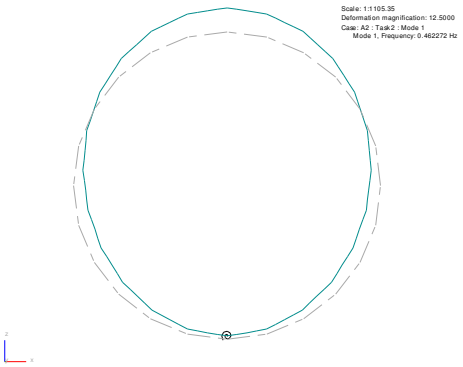

Figure 4.27: Mode shape with 1 support

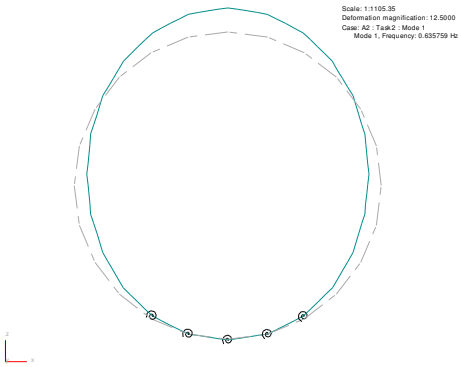

Figure 4.28: Mode shape with 5 supports

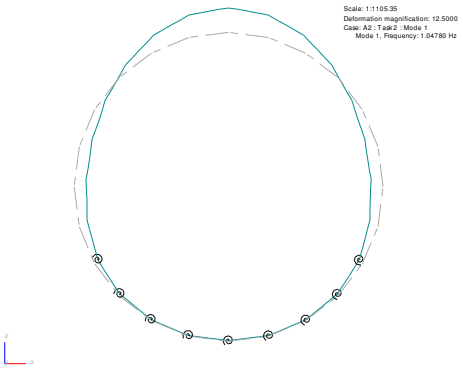

Figure 4.29: Mode shape with 9 supports

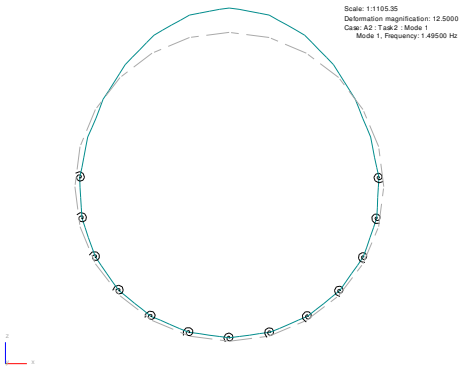

Figure 4.30: Mode shape with 13 supports

In figure 4.31 the lowest natural frequency is put in the graph in relation to the height of the supporting structure. It is almost a completely linear function.

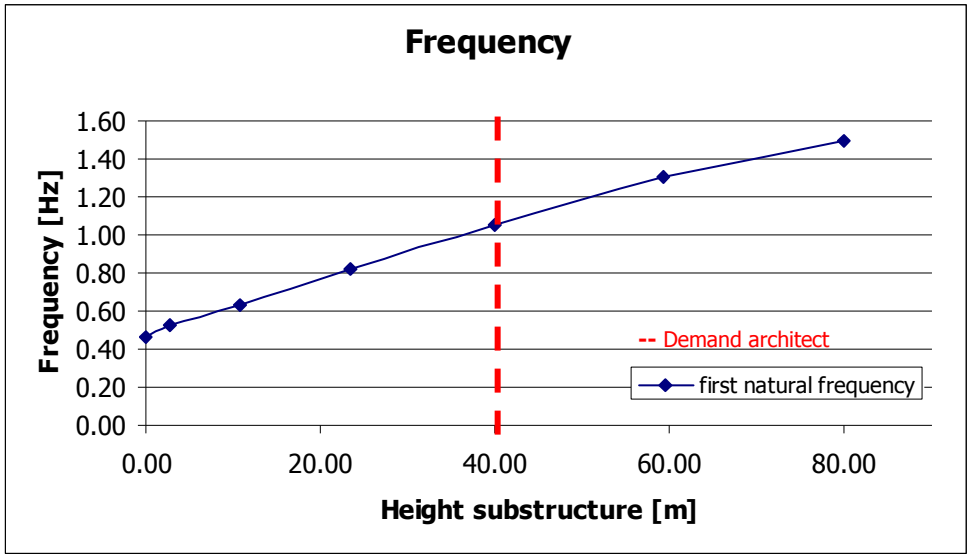

Figure 4.31: Natural frequency in relation to height of the supporting structure

As expected it is seen that by increasing the height of the supporting structure the lowest natural frequency is increased. This is explained by the fact that stiffness is given to the structure by adding supports and when the stiffness is increased the lowest natural frequency will also increase.

H [m]	Mode 1 [Hz]
0.00	0.462
2.73	0.525
10.72	0.636
23.43	0.817
40.00	1.048
59.29	1.306
80.00	1.495

Table 4.11: Natural frequency

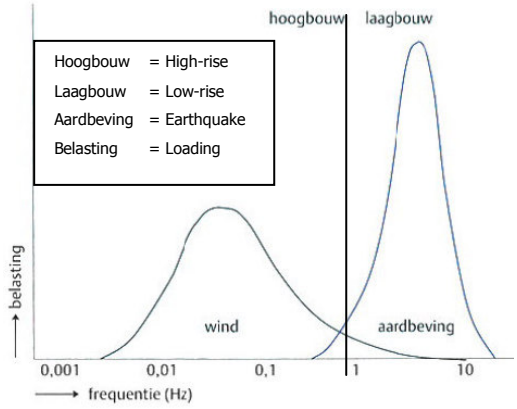

Figure 4.32: Spectrum for wind and earthquakes [13]

It is difficult to say what the effect of the height of the supporting structure is when considering dynamics. This because the wind spectrum has to be taken into account but also the earthquake spectrum, see figure 4.32.

The lowest natural frequencies of the wheel are between 0.5 and 1.5 Hz. This is exactly in between the two peaks for wind and earthquakes. This means that the dynamic loads from these are not big. This of course has to be investigated further when the dynamic behaviour of the 3D-model is investigated. Only then the real natural frequencies of the structure can be determined, and whether the second and maybe third natural frequency also have to be taken into account.

4.7. Conclusion

It is clear that the height of the supporting structure is an important parameter in the design. But more importantly it is clear that the minimum height of the supporting structure can not be stated as an absolute value (like 46.25 m[1]), it has to be stated as the minimum height of the supporting structure is ¼ times the diameter of the wheel as the maximum diameter of the Great Dubai Wheel is searched for. This is because all the graphs previously stated in this chapter show that decreasing the height of the supporting structure below the ¼ demand (stated by the architect) has a big negative influence on the forces and thus the stresses static as well as quasi static. This is illustrated by figure 4.33 and figure 4.34.

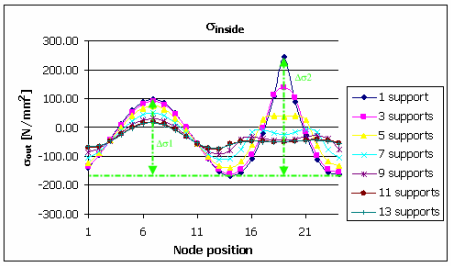

Figure 4.33: Stress distribution nodes inner ring

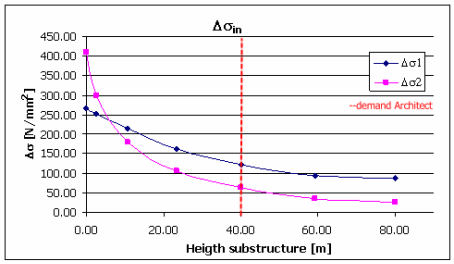

Figure 4.34: $\Delta\sigma_{out}$ in relation to the height of the supporting structure

In figure 4.34 it is seen that the slope of the graph is decreasing when the supporting structure is raised, and also the maximum stresses are decreased. It is therefore beneficial to raise the supporting structure. This will result in lower stresses throughout the entire structure and maybe even more importantly with fatigue behaviour in mind, the stress ranges are lowered when increasing the height of the supporting structure.

The value of ¼ times the diameter is set as a constant. It is chosen to do so, to not affect the total look of the Great Dubai Wheel. But the raising of the supporting structure should still be kept in mind for a possible improvement of the total design of the Great Dubai Wheel.

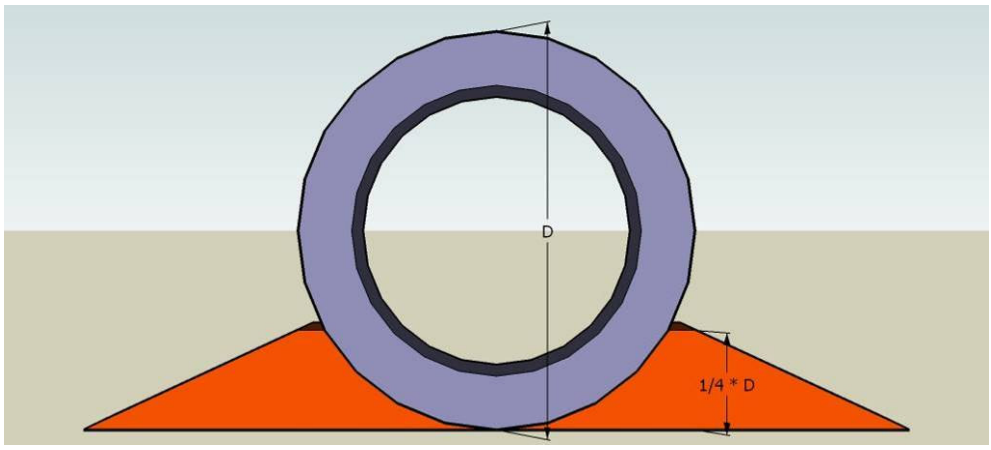

Figure 4.35: Wheel with supporting structure

5. Self weight

Self weight plays an important role in the total stress distribution of the Great Dubai Wheel as is proven in the prior study [13]. This is mainly caused by the fact that the structure is rotating and can thus not be optimized in the sense that more slender profiles can be used at the top of the structure. Another reason why the self weight is so important is because the structure is rotating, the self weight becomes for the structural components a cyclic loading. This chapter of the preliminary calculations is to analyze how the self weight of the structure changes when the diameter of the structure is changed.
The analysis is done by some hand calculations where the "vergeet-me-nietjes" are used. These hand calculations are then verified by the simple model mentioned earlier. Again no specific analysis will be done, just an analysis to gain insight in the bigger picture.

The question to answer is how the self weight of the structure grows when the diameter is increased. To answer this question two different causes of the weight growth have to be taken into account. On one hand the total length of the sections is increased when increasing the height. And on the other hand the needed cross section dimensions have to be increased when increasing the height. To quantify the increase of self weight the standard formulae for deflection (vergeet-me-nietjes) are used.

5.1.1. Length

The increase of the needed section length is linear (π*D), when the diameter is doubled in size and the ring thickness remains constant, the total needed section length is also doubled.

$$D = 160m^1 \rightarrow L_1 = \pi * 160 = 500m^1$$
$$D = 320m^1 \rightarrow L_2 = \pi * 320 = 1000m^1$$
$$\frac{L_2}{L_1} = \frac{1000}{500} = 2$$

5.1.2. Section properties

When the diameter is increased the section properties have to be altered and still comply with the different demands. For this preliminary calculation the following assumptions are made.

- Horizontal deformation at the top due to wind load should be lower then $\frac{1}{500}$ * the diameter;
- Vertical deformation at the top due to self weight should be lower then $\frac{1}{500}$ * the diameter;

The used sections are circular hollow sections. These are applied in the prior study [13], and are easy to compare. The wind load is modelled as an evenly distributed q-load. It is shown in figure 5.1 that this not entirely correct, this is because the surface affected by the wind isn't evenly distributed over the height. This is because the structure is in fact a ring which has more surface area, when looking at the function of the surface area distribution over the height, at the top and bottom less surface area in the middle, see figure 5.1.
But for this preliminary calculation the results should suffice as it is not the exact deflection but the change of deflection when the diameter is increased which is searched at.

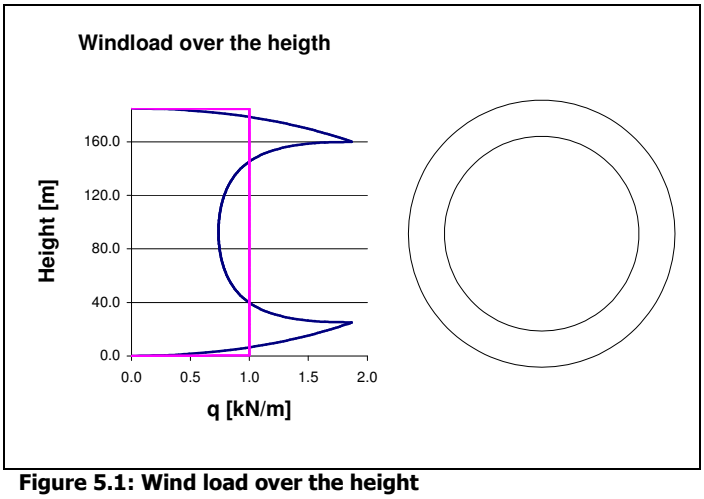

Figure 5.1: Wind load over the height

Also the bending stiffness will not be constant over the height of the structure. This is not taken into account because the nature of the calculation is indicative.

The structure is modelled as a beam clamped on one side.

$$Y_b = \frac{q * l^4}{8 * EI}$$

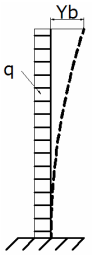

Figure 5.2: Vergeet-me-nietjes

$$Y_L = \frac{q * L^4}{8 * EI_L} \rightarrow EI_L = \frac{q * L^4}{8 * Y_L}$$

$$Y_{L*2} = 2 * Y_L = \frac{q * (2 * L)^4}{8 * EI_{2*L}} \rightarrow EI_{2*L} = \frac{q * 16 * L^4}{8 * 2 * Y_L} = \frac{q * L^4}{Y_L}$$

$$EI_{2*L} = 8 * EI_L$$

To illustrate what the effect of this factor 8 on the cross section, an example calculation with CHS sections is given below.

CHS 200mm with thickness 10mm is applied at first and then when the diameter of the wheel is doubled, a CHS 200mm with thickness of 21mm has to be applied. This means that the cross sectional area is doubled, and thus will be twice as heavy.

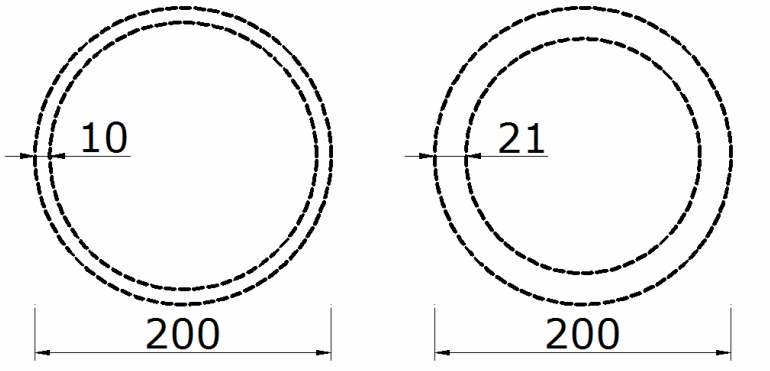

Figure 5.3: CHS 200-10 and CHS 200-21

$$EI_{2L} = 8 * EI_L$$
$$I_{circle(2L)} = 8 * I_{circle(L)}$$
$$I_{circle(L)} = \frac{\pi}{64}\left(D_1^4 - \left(D_1 - 2*t\right)^4\right)$$
$$D_1 = 200mm$$
$$t_L = 10mm$$
$$t_{2L} = ??mm$$
$$8*\frac{\pi}{64}\left(200^4 - \left(200 - 2*10\right)^4\right) = \frac{\pi}{64}\left(200^4 - \left(200 - 2*t_{2L}\right)^4\right)$$
$$t_{2L} \approx 21mm$$

Figure 5.4 show what is needed to enlarge the moment of inertia by a factor 8 as needed for doubling the diameter of the wheel. Of course other options are available, the diameter of the CHS can be enlarged or another type of profile can be used, but for this case of comparison it was chosen to enlarge the thickness, because it shows nicely that the needed steel area is twice as large.

When looking at the deformations at the top of the wheel, the model is a simple supported beam. The deformations can easily be calculated with a "vergeet-me-nietje".

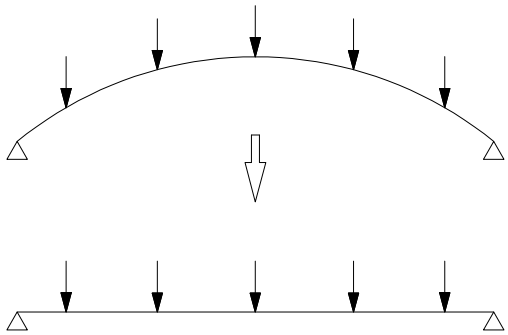

Figure 5.4: Simplification deformation at the top of the wheel

$$Y_b = \frac{5}{384}\frac{q*l^4}{EI}$$

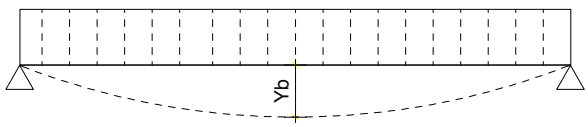

Figure 5.5: Vergeet-me-nietje

Because the wheel is built as a truss girder, the second moment of inertia is calculated as the sum of the own inertia bending moment and the Steiner part. The sections used are circular hollow sections (CHS). Because the Steiner part is of big influence in this structure enlarging the sections doesn't affect the inertia bending moment much. When doubling the section area, the inertia bending moment will double instead of a normal exponential

growth. The only way to increase the inertia bending moment is by changing the thickness of the ring.

Also when increasing the section properties the self weight is increased, but the inertia bending moment is increased too. These two factors influence each other. When looking at these influences it has to be taken into account that the sections will be of reasonable sizes, and not being so big that fabrication is not possible, or not preferable. Because the ring thickness is important in this case, and in this stage of the Master thesis this will not be a variable parameter, the only way to vary the inertia bending moment is by applying bigger profiles. Therefore it will be looked at how the deflection of the wheel changes when increasing the diameter.

In short, the growth of the deflection in z direction is calculated by doubling the diameter.

$$\delta z = \frac{5}{384} * \frac{q * l^4}{E * I}$$

But because ΔA ~ Δq it follows that

$$\delta z = \frac{5}{384} * \frac{A * l^4}{E * I}$$

$$A = \frac{\pi}{4} * \left(D^2 - \left(D - 2 * t \right)^2 \right)$$

$$I_{own} = \frac{\pi}{64} * \left(D^4 - \left(D - 2 * t \right)^4 \right)$$

$$I_{steiner} = A * \left(\frac{a}{2} \right)^2$$

$$I_{total} = 2 * \left(I_{own} + I_{steiner} \right)$$

$$\delta z_{c,I} = \frac{5}{384} * \frac{A_I * L^4}{E * A_I * \left(\frac{a}{2} \right)^2}$$

$$\delta z_{c,II} = \frac{5}{384} * \frac{A_{II} * \left(2 * L \right)^4}{E * A_{II} * \left(\frac{a}{2} \right)^2} = 16 * \delta z_{c,I}$$

This indicates that by doubling the diameter of the wheel the deflection at the top will increase by a factor 16. This means that the growth of the deflection can at one point be the governing parameter.

5.1.3. Stresses

The stresses which act in the structure due to a horizontal load will reduce by a factor 2 when the diameter of the wheel is doubled and the applied section is a factor 8 higher than the original section. This is only for the stress from bending. It is not taken into account that the wind load will increase when the height of the structure is increased.

$$\sigma_L = \frac{-\frac{1}{2} * q * L^2}{W_L} = \frac{-\frac{1}{2} * q * L^2}{\left(\frac{I}{\frac{1}{2} * D}\right)}$$

$$\sigma_{2*L} = \frac{-\frac{1}{2} * q * (2 * L)^2}{W_{2*L}} = \frac{-\frac{1}{2} * q * 4 * L^2}{\left(\frac{8 * I}{\frac{1}{2} * D}\right)} = \frac{-\frac{1}{2} * q * 4 * L^2}{\left(\frac{8 * I}{\frac{1}{2} * D}\right)} = \frac{-\frac{1}{4} * q * L^2}{\left(\frac{I}{\frac{1}{2} * D}\right)}$$

6. 2D-truss model

The truss used is the reason for big forces in the structure (peak forces and moments near the highest support). This is especially in the so called position 2 when the structure is only resting on 8 supports. And the verticals have to take the whole support reaction. This is because the stiffest member takes up most of the load, and the sections are stiffer in compression as in bending. These verticals are therefore critical; these verticals are also not braced in any way (although buckling isn't taken into account in this calculation, it has to be said that for buckling a large system length has to be taken into account). To get a feeling how critical the different members are a 2D-analysis is made. In which the truss girder is completely modelled. This model should give sufficient insight into the forces of the different members.

6.1. Wheel positions

Because the wheel is rotating, different wheel positions are considered. In the start position (position 1) the wheel is supported by 9 supports (24 segments), but when the wheel rotates 7.5 degrees only 8 supports are present, which could lead to a significant increase in reaction forces. The different positions are drawn in figure 6.1.

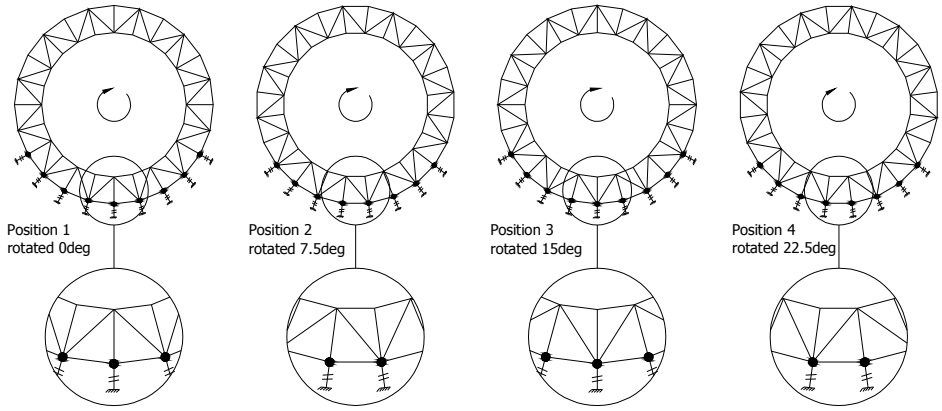

Figure 6.1: Different wheel positions

As is seen in figure 6.1, in position 1 the bottom node is a T-joint and 9 supports are present. In position 2 the wheel is rotated 7.5 degrees clockwise compared to position 1, in this position only 8 supports are present. In position 3 the bottom node is a KT-joint, the wheel is rotated 15 degrees clockwise compared to position 1, and in position 4 the wheel is rotated 22.5 degrees compared to position 1. In position 4 only 8 supports are present (this position is mirror symmetric with position 2).

6.2. OASYS-GSA model

The model is created in OASYS-GSA. For the model to work properly the parameters have to be assigned correctly. Also this model, just like the ring model (chapter 4), is not made to get the exact figures, but to get a better feeling for the influence of the different parameters on the wheel.

6.2.1. Parameters

- Diameter 185m;
- Supports
  - Support height up to ¼ times the diameter is up to 46.25m;
  - Support stiffness 1000MN/m;
- Section properties (section properties from prior study [13]);
  - Outside and inner ring Ø2220 – 40 mm;
  - Diagonals and verticals Ø1440 – 40 mm;
  - Outriggers Ø2220 – 40 mm;

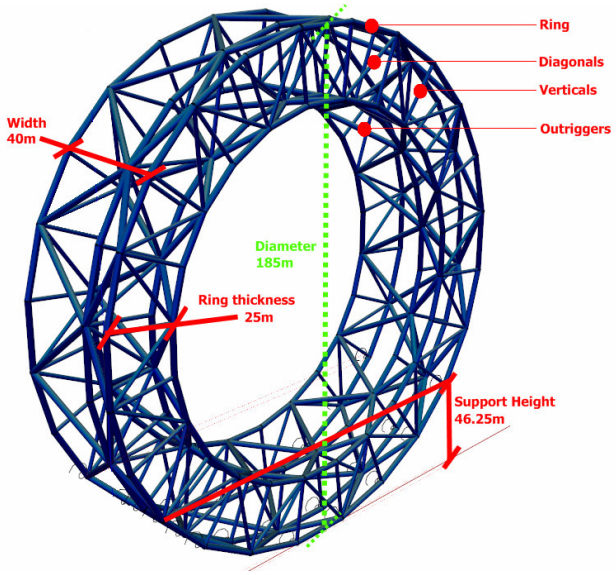

Figure 6.2: Figure parameters

- Loading (only the self weight is taken into account);
  - Because different loadcases give the same kind of results not al loadcases are considered. For example the load case due to self weight is in essence the same as the permanent weight of the main capsules. Therefore only the self weight of the structure is considered. This can be done because the analysis of the 2D-truss model in this chapter is not about finding the exact numbers, but to get insight in the behaviour of the wheel.

6.2.2. Loading

The loading considered for the analysis is:

- Self weight of the wheel (only one ring considered);

6.3. Output

The analysis is about finding the member forces for all different members, and at the relevant nodes.

- Outside ring;
  - OI;
  - OII;
  - OIII;
  - OIV;
- Inside ring
  - I I;
  - I II;
  - I III;
  - I IV;
- Verticals;
  - VA I;
  - VA II;
  - VB I;
  - VB II;
- Diagonals;
  - DA I;
  - DA II;
  - DB I;
  - DB II

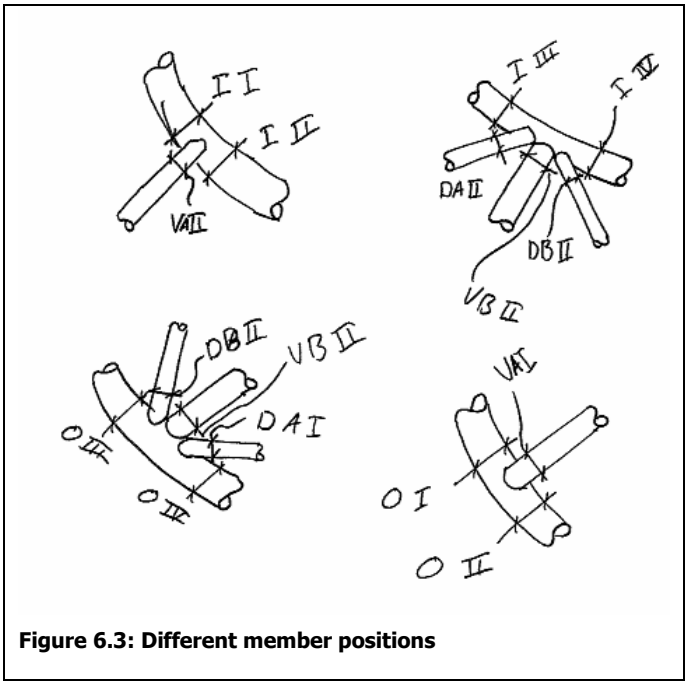

Figure 6.3: Different member positions

For all these member positions the entire 6 hour cycle should be known in relation to the different member forces. This means that for 16 nodes at 48 positions (rotated every 7.5 degrees) with the relevant loadcases (approximately 4) the member forces have to be known. This is at least 16*48*4 = 3072 lines of relevant data output from OASYS-GSA. This means a lot of data has to be considered. With the 2D-model this is still possible. If the 3D-model is analysed in chapter 7, it is possible to determine the relevant data on the bases of the outcome of the analysis of the 2D-model. Because in a rough way the 3D-output should coincide with the 2D-output. When not doing this 2D-model analysis means that with the 3D-model 3 * 16 * 48 *4 = 3456 *4 = 9216 lines of data output has to be considered.
Because of symmetry some member positions are completely symmetrical. This is the case for O I and O II, O III and O IV, I I and I II, I III and I IV, DA I and DB I and the last DA II and DB II. This means that 10 member positions will have to be studied. This still means that 10 member positions times 48 wheel positions times 4 loadcases = 1920 lines of data will have to be considered.

This means that a lot of data is considered. So some automation in the data considering process is necessary.

The goal is to find the peaks in the moments, normal forces and shear forces in a full rotation of the wheel. Also the stresses in the sections will be derived. Not all the graphs will be shown in this report, only the decisive positions. To determine which nodes are decisive the stresses and stress ranges during a full rotation of the wheel are put in graphs and for these decisive positions the normal force, shear and moment diagrams are put in graphs.

6.3.1. Data handling

Programs like OASYS-GSA and SCIA-ESA-PT generate a huge amount of data with a simple click. Of course all this data can be checked but this takes a lot of time. It is therefore necessary to think before acting, which data is needed for the analysis etc. and more importantly which data isn't necessary. Still the data can be a lot to handle.
With OASYS-GSA it is possible to export the data into Excel and check the data automatically. This has to be done with great care because it has to be correct. Also with checking the data in Excel, the Excel-sheet should be readable to others than the author.

In this project the use of interoperability between OASYS-GSA and Excel is extensively used. The output of OASYS-GSA is copied to Excel and handled in Excel.

Because it takes a lot of time to filter the output in OASYS-GSA this is done in Excel with the vlookup function. This is done by assigning reference syntax to the data from OASYS-GSA containing the position number, the node number and the element number (p#n#e#). In this way the data can be easily looked up via the lookup function. This way it is possible to directly copy paste large amounts of data into a sheet, and determine in Excel the relevant data. In this analysis only one loadcase is considered, it is possible to also include the loadcase in the reference syntax (p#n#e#lc#).

6.3.2. Axis

Because OASYS-GSA automatically assigns the local axis of the elements it is not possible to assign this local axis in a way that the wheel can be seen as a continuous girder. The way OASYS-GSA assigns this local axis is it takes the node 1 and node 2, which is the x axis, and the z and y axis are taken in such a way that in the global system the elements always have a positive global y or global z vector. This means that when the elements in the model are vertical the z axis will rotate 180 degrees. This is taken care of by multiplying the moments and shear forces by -1. This way the moments and shear forces can be compared to each other over the desired axis.

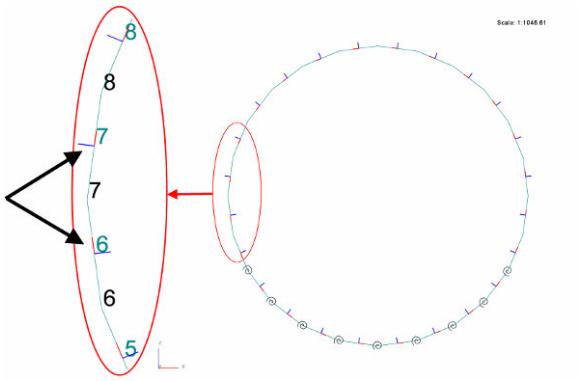

Figure 6.4: Shift in Z-vector of the elements local axis

6.4. Stress ranges

In all the graphs in this paragraph two lines are seen. This is because the stresses on both sides of the sections are determined, see figure 6.5. This way it is possible to see which position is governing, but also which side of the section in that position is governing. C1 is the stress on the inside, and C2 is the stress on the outside of the sections

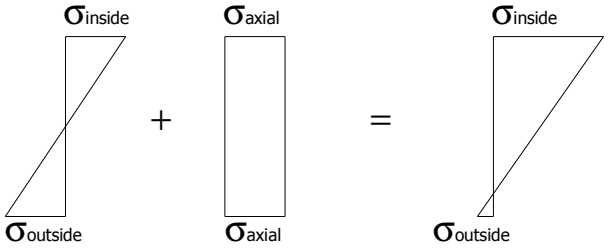

Figure 6.5: Stresses

As mentioned before only the loadcase of self weight is taken into account.

6.4.1. Outside ring I

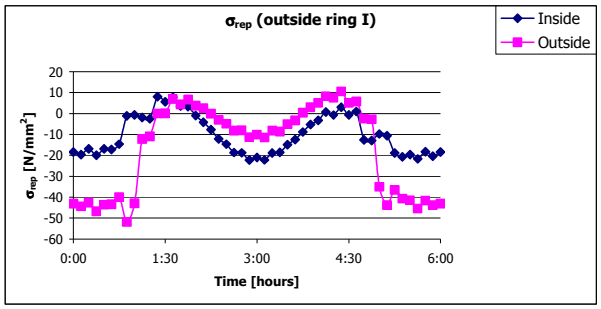

Figure 6.6: Stress range full rotation (Outside ring I)

Stress range O I	C1 [N/mm²]	C2 [N/mm²]
Min σ	-22.25	-51.94
Max σ	8.05	10.54
Δσ	**-30.30**	**-62.48**

Table 6.1: Stress range O I

6.4.2. Outside ring III

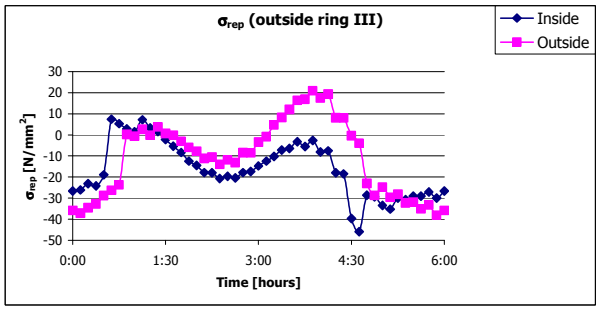

Figure 6.7: Stress range full rotation (Outside ring III)

Stress range O III	C1 [N/mm²]	C2 [N/mm²]
Min σ	-45.89	-38.13
Max σ	7.45	20.97
Δσ	**-53.34**	**-59.10**

Table 6.2: Stress range O III

6.4.3. Inside ring I

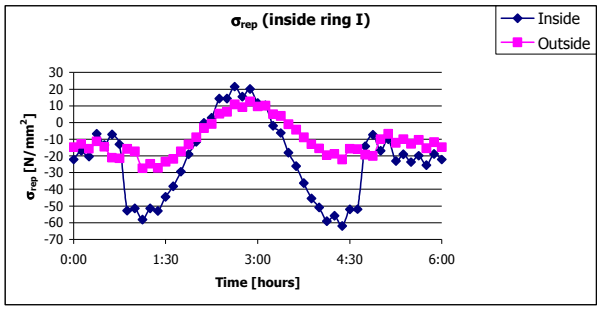

Figure 6.8: Stress range full rotation (Inside ring I)

Stress range I I	C1 [N/mm²]	C2 [N/mm²]
Min σ	-61.86	-27.31
Max σ	21.54	12.58
Δσ	**-83.41**	**-39.88**

Table 6.3: Stress range I I

6.4.4. Inside ring III

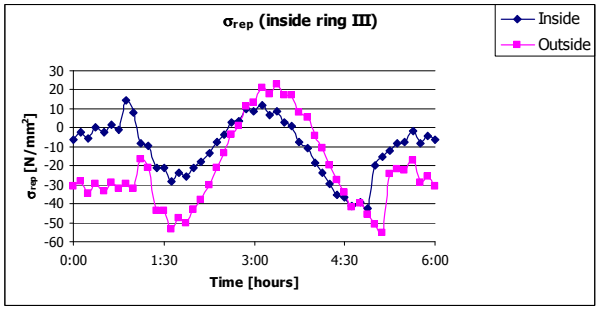

Figure 6.9: Stress range full rotation (Inside ring III)

Stress range I III	C1 [N/mm²]	C2 [N/mm²]
Min σ	-42.24	-55.19
Max σ	14.51	22.80
Δσ	**-56.75**	**-77.99**

Table 6.4: Stress range I III

6.4.5. Vertical A I

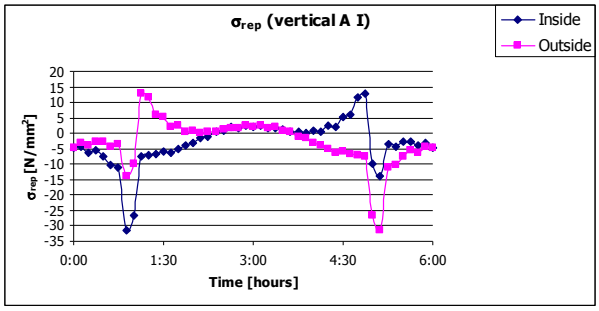

Figure 6.10: Stress range full rotation (Vertical A I)

Stress range VA I	C1 [N/mm²]	C2 [N/mm²]
Min σ	-31.35	-31.35
Max σ	12.79	12.79
Δσ	**-44.14**	**-44.14**

Table 6.5: Stress range VA I

6.4.6. Vertical A II

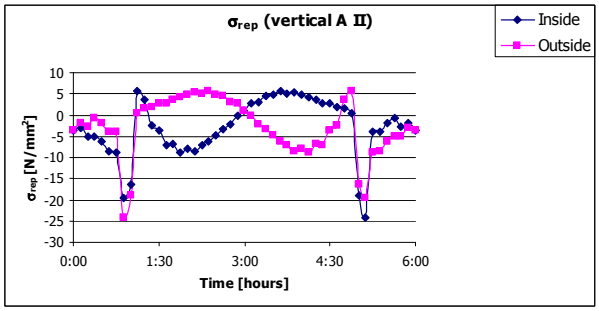

Figure 6.11: Stress range full rotation (Vertical A II)

Stress range VA II	C1 [N/mm²]	C2 [N/mm²]
Min σ	-24.06	-24.06
Max σ	5.66	5.66
Δσ	**-29.72**	**-29.72**

Table 6.6: Stress range VA II

6.4.7. Vertical B I

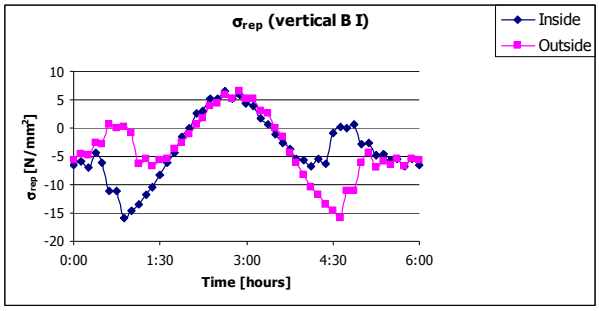

Figure 6.12: Stress range full rotation (Vertical B I)

Stress range VB I	C1 [N/mm²]	C2 [N/mm²]
Min σ	-15.94	-15.94
Max σ	6.47	6.47
Δσ	**-22.41**	**-22.41**

Table 6.7: Stress range VB I

6.4.8. Vertical B II

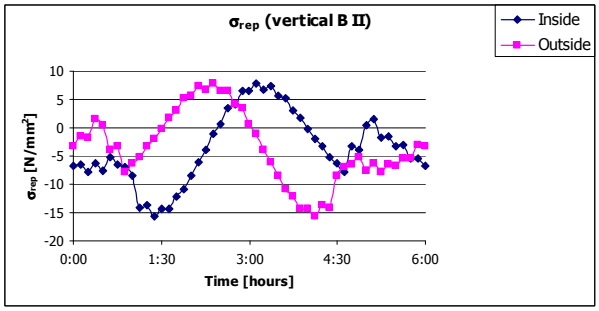

Figure 6.13: Stress range full rotation (Vertical B II)

Stress range VB II	C1 [N/mm²]	C2 [N/mm²]
Min σ	-15.65	-15.65
Max σ	7.83	7.83
Δσ	**-23.49**	**-23.49**

Table 6.8: Stress range VB II

6.4.9. Diagonal A I

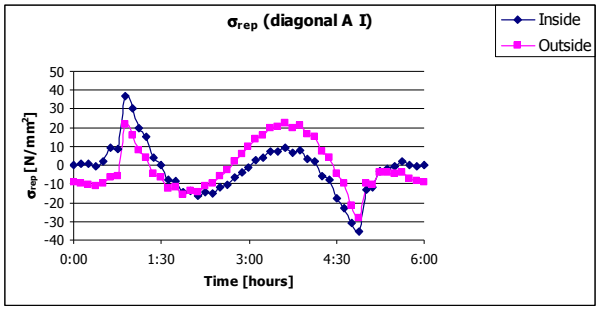

Figure 6.14: Stress range full rotation (Diagonal A I)

Stress range DA I	C1 [N/mm²]	C2 [N/mm²]
Min σ	-35.63	-28.31
Max σ	36.86	22.58
Δσ	**-72.49**	**-50.89**

Table 6.9: Stress range DA I

6.4.10. Diagonal A II

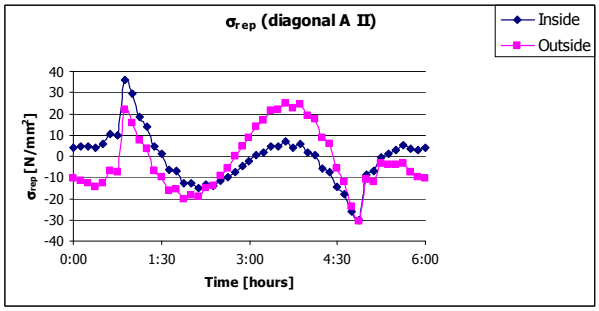

Figure 6.15: Stress range full rotation (Diagonal A II)

Stress range DA II	C1 [N/mm²]	C2 [N/mm²]
Min σ	-30.36	-30.56
Max σ	35.74	25.13
Δσ	**-66.10**	**-55.69**

Table 6.10: Stress range DA II

6.4.11. Governing position

The previous paragraphs show that the governing position for the maximum compression stress and for the largest stress range is position inside ring I (I I).

Stress range I I	C1 [N/mm²]	C2 [N/mm²]
Min σ	-61.86	-27.31
Max σ	21.54	12.58
Δσ	**-83.41**	**-39.88**

Table 6.11: Stress range I I

The governing position for maximum tensile stress is position DA I.

Stress range DA I	C1 [N/mm²]	C2 [N/mm²]
Min σ	-35.63	-28.31
Max σ	36.86	22.58
Δσ	**-72.49**	**-50.89**

Table 6.12: Stress range DA I

It is also important and interesting at which point in the rotation the maximum stresses occur. For the maximum compression stress at I I the point in time in a rotation at which the maximum stress occurred is 4:22. And for the maximum tensile strength in DA I the point in time is 0:52. The position on the wheel is seen in figure 6.16 and figure 6.17.

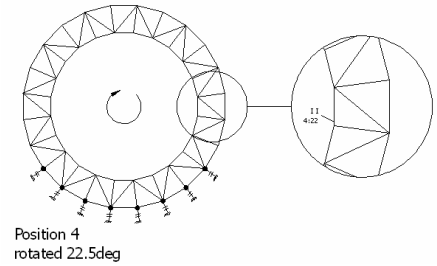

Figure 6.16: Position governing compression stress

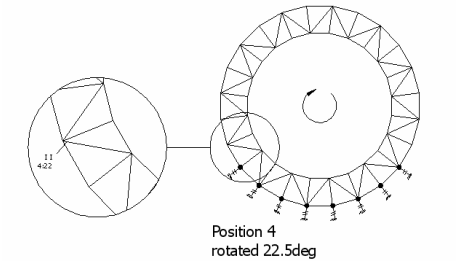

Figure 6.17: Position governing tensile stress

6.4.12. Stress distribution

The flow of stresses in the Great Dubai Wheel is seen in figure 6.18. It is clearly seen that the stresses are distributed along the stiffest parts of the structure (the stresses are mainly distributed by normal forces) as expected.

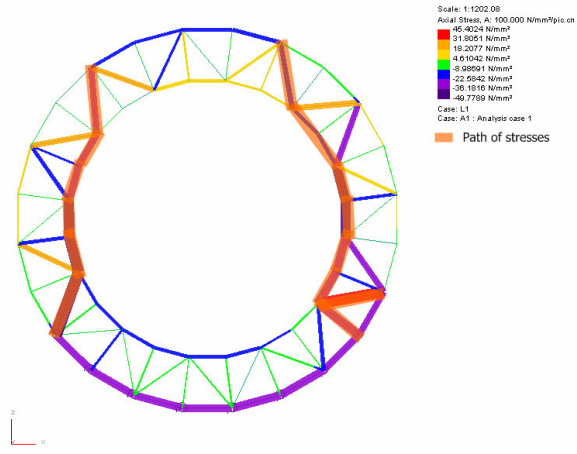

Figure 6.18: Axial stresses ring C

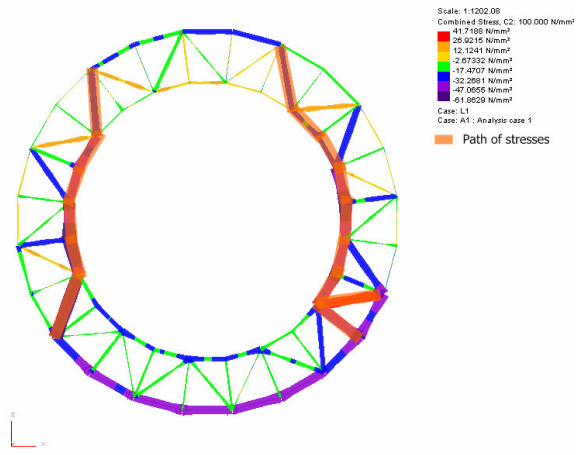

Figure 6.19: Combined stresses ring C

It can also be seen that the diagonals are loaded in maximum tensile stress at the most right support and when the wheel rotates the same diagonal is loaded at maximum compression stress at the most left support. This is kept in mind in the fatigue analysis (chapter 9).

The biggest part of the forces in the Great Dubai Wheel is routed to the supports by normal forces. This is seen by comparing figure 6.18 and figure 6.19. In figure 6.18 the normal forces are given and in figure 6.19 the combined stresses are given. Figure 6.18 and figure 6.19 show roughly the same path of the stresses to the supports. Also the magnitude of the stresses is mainly influenced by the normal force action in the structure, and for a much smaller part by the moment action. This is the case because the moment of inertia of the truss is much bigger than the moment of inertia of the tubes.

6.5. Position inner ring I

For the governing position which is I I, when looking at the biggest stress and biggest stress range, the normal force, shear force and moment diagrams are given for a full rotation, see figure 6.20, figure 6.21 and figure 6.22.

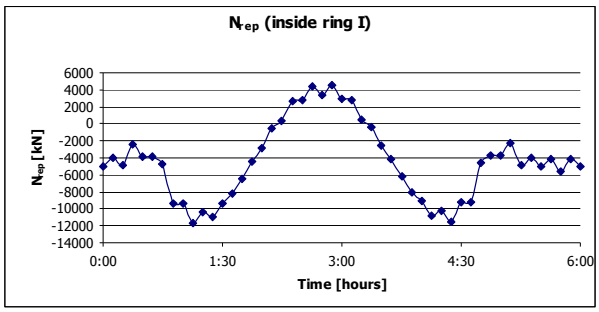

Figure 6.20: Normal force diagram position I I

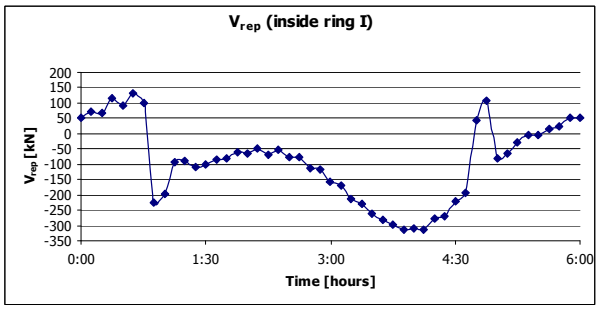

Figure 6.21: Shear force diagram position I I

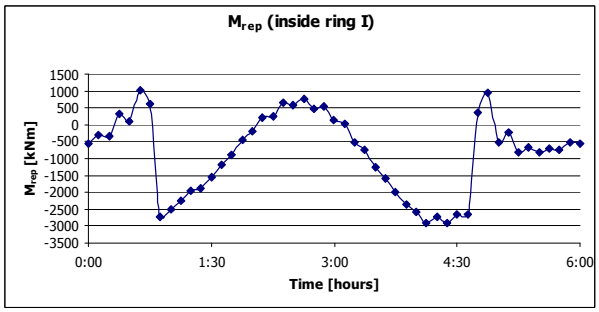

Figure 6.22: Moment diagram position I I

6.5.1. Stress distribution

In figure 6.23 and figure 6.24 the stress distribution of position I I is given. It can be seen that for the governing stresses on the inside of the section the stresses from the normal forces are governing in the total stress distribution. This was also expected by the fact that it is a vertical beam in which the normal force is governing in a load case self weight.

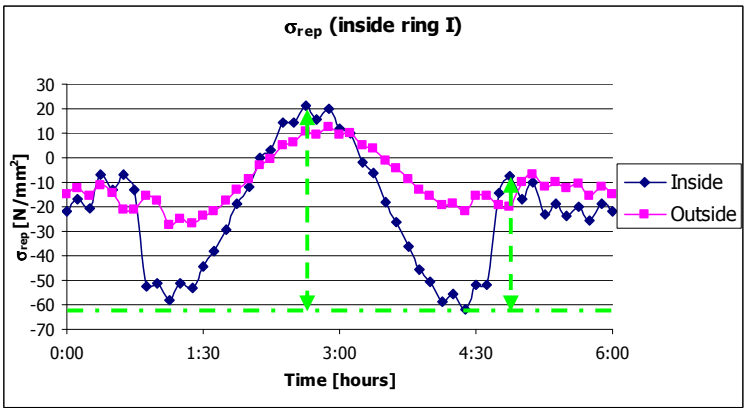

Figure 6.23: Stress distribution position inside ring I, combined stresses inside and outside

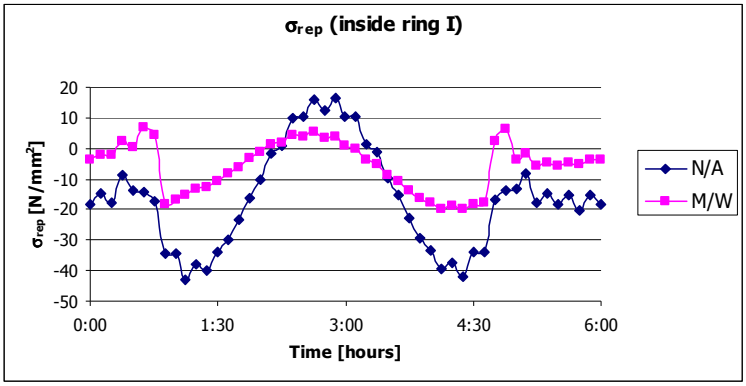

Figure 6.24: Stress distribution position inside ring I, axial stresses and bending stresses

It can be seen in figure 6.23 and figure 6.24 that the stresses from normal force action are the most important stresses. It is the stresses from the normal force that are the cause of the biggest stress range and largest stresses.

7. 3D-frame model

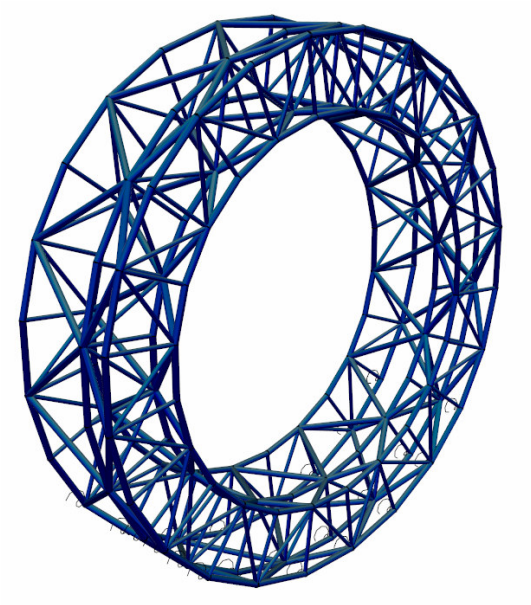

Figure 7.1: 3D-model Great Dubai Wheel

7.1. Segmentation

In the original design the number of segments in the Dubai wheel was set to 38 or 40. In the prior study [13] the number of segments was reduced to 36, this was done because the panorama wheel had 36 capsules, but only 24 main capsules are present.

- With this segmentation a problem arose. How do the forces of the 24 capsules have to be transferred to the main structure? Because the Great Dubai Wheel is made out of a truss girder, the forces have to act on the nodes.
- The self weight of the Great Dubai Wheel plays an important role in the design of the Great Dubai Wheel. Because the self weight also acts as a fatigue load it should be kept as low as possible.

Therefore it is chosen to decrease the number of segments to 24, as there are 24 main capsules.

7.2. Parametric model

To do this research a parametric model is made. This model can also be used in the later analysis of the Great Dubai Wheel. A structural analysis program which allows for a parametric design is OASYS-GSA. The normal procedure is to make an Excel-sheet which calculates the nodes and elements orientation and copy-paste this into the graphical interface of OASYS-GSA. Also the loads and support conditions can be copy-pasted. When the analysis is done, the output can also be copy-pasted into an Excel-sheet to automatically analyze the results.
For this project the normal procedure is followed. The remark is made that the model is made in a way that a comparison with the prior study is as easy as possible. For example the loads are based on the prior study [13], as well as the geometry of the different positions. In the prior study [13] SCIA-ESA-PT is used, as this software does not allow parametric design, it is chosen to use OASYS-GSA for this Master thesis a full description of the parametric Excel-sheet is given in chapter 11.3.

7.2.1. Parameters

- Diameter;
- Ring thickness;
- Spring constant;
- Y coordinate Ring A, B and C;
- Wheel-position;

7.3. Loadcases

- Self weight main structure LC1;
- Self weight main capsules LC2;
- Self weight panorama wheel LC3;
- Variable load main capsules LC4;
- Variable load main capsules momentaan LC5;
- Variable load panorama wheel LC6;
- Variable load panorama wheel momentaan LC7;
- Wind Ring A LC8;
- Wind Ring C LC9;

All of the loading mentioned in the following paragraphs are serviceability loadings.

7.3.1. LC1 Self weight main structure

The self weight is calculated by OASYS-GSA.

7.3.2. LC2 Self weight capsules

The weight of the capsules is 360 ton (3600kN). This load is spread out over the nodes in Ring B and C. So the load of each capsule is spread out over 4 nodes (3600/4 = 900kN).

- 24 segments 900kN;

7.3.3. LC3 Self weight panorama wheel

The panorama wheel is attached to the main structure via wheels. This way only forces perpendicular to the sections can be transferred. The forces are derived in the following way:

- A model is made of the panorama wheel, see figure 7.2. The supports in this model are present in all the outer nodes, and act perpendicular to the structure. This is done because the panorama ring is supported by wheels to the main structure. The reaction forces of this model are also the forces acting on ring A in the whole structure.

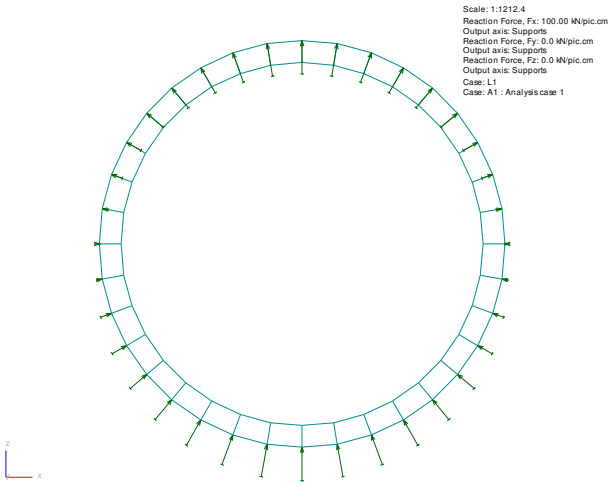

Figure 7.2: Panorama wheel model, with support reactions

- Because the panorama wheel consists of 36 segments (36 small capsules) the results have to be recalculated when the forces are applied to the 24 segment model. This is done by increasing the reaction forces by a factor of 36/24 = 3/2. This is checked by removing half of the supports in the panorama model and the reaction forces increased by a factor 2).

The load is a sinusoidal load with the following formula.

$$F_{24} = F_{top} * \tfrac{36}{24} * \cos\left(\frac{\pi}{\left(\frac{24}{2}\right)} * \left(stramien - 1 \right) \right);$$

In which the F_{top} is taken from the output of the panorama wheel model. The axis in which these nodal forces act is the cylindrical axis.

7.3.4. LC4 Variable load main capsules

The variable loads from the capsules are derived from the variable loads mentioned in the report of the prior study [13]. The total variable load from the main capsules is 24760kN. These nodes are equally distributed over the loads in ring B and C. The nodal lodes thus become:

- 24 segments 258kN;

7.3.5. LC5 Variable load main capsules momentaan

The variable loads from the capsules are derived from the variable loads mentioned in the report of the prior study [13]. The total variable load from the main capsules is 24760kN. These nodes are equally distributed over the loads in ring B and C. For the momentaan factor (ψ) 0.35 is chosen. This value is chosen because the wheel consists of 20 hotel capsules and 4 restaurant capsules. For hotels a ψ-factor of 0.4 is taken into account and for restaurants a ψ-factor of 0.25 is taken into account. The factor for the Great Dubai Wheel is set to ψ=0.35.

The nodal lodes thus become:

- 24 segments 0.35 * LC 4 = 90.3kN;

7.3.6. LC6 Variable load panorama wheel

The analysis is similar to chapter 7.3.3. only the size of the forces is altered.

$$F_{24} = F_{top} * \tfrac{36}{24} * \cos\left(\frac{\pi}{\left(\frac{24}{2}\right)} * \left(stramien - 1\right)\right);$$

7.3.7. LC7 Variable load panorama wheel momentaan

The analysis is similar to chapter 7.3.3. only the size of the forces is altered.

$$F_{24} = F_{top} * \tfrac{36}{24} * \cos\left(\frac{\pi}{\left(\frac{24}{2}\right)} * \left(stramien - 1\right)\right);$$

7.3.8. LC8 and LC9 Wind loading

The total wind load on the structure is 39500 kN. It is said that the wind loading is constant over the height of the structure and is spread out evenly over the total structure. The total area of one side of the Great Dubai Wheel is:

$$A_p = \frac{\pi * D_{outer}^{\ 2}}{4} - \frac{\pi * D_{inner}^{\ 2}}{4};$$

$$A_p = \frac{\pi * 185^2}{4} - \frac{\pi * 135^2}{4};$$

$$A_p = 12566 m^2;$$

The friction surface of the Great Dubai Wheel is:

$$A_f = \pi * D_{outer} * W_{ring} + \pi * D_{inner} * W_{ring};$$

$$A_f = \pi * 185 * 40 + \pi * 135 * 40;$$

$$A_f = 40212 m^2;$$

In which

W_{ring} = width ring;

D_{outer} = outer diameter;

D_{inner} = D_{outer} – 2*Ring thickness

The wind load is considered as a constant distributed loading on the Great Dubai Wheel. In reality the wind load will have a logarithmic distribution but for this analysis the modelling by a constant distributed load is sufficient.

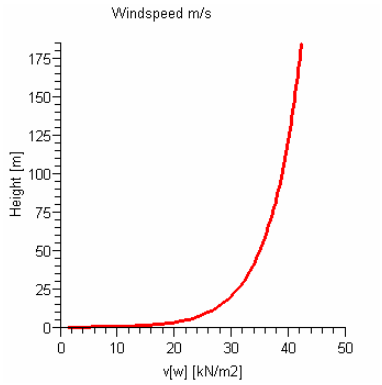

Figure 7.3: Logarithmic wind speed

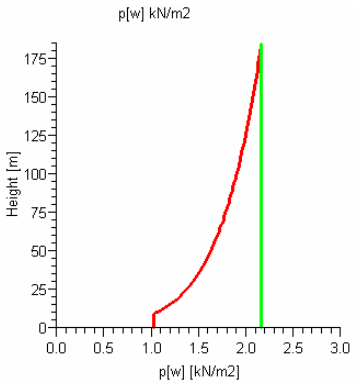

Figure 7.4: Logarithmic pressure and modelled pressure of the wind

In the parametric Excel-sheet the wind load is calculated in accordance to the maximum height of the structure. The wind load per square meter is calculated at 2.14kN/m^1 (in chapter 10 the logarithmic wind loading is implemented in the analysis).

Because the model is a truss girder the wind load is modelled to act on the nodes. This is not entirely correct but for this stage of the analysis it is sufficient. Because the model consists of three rings the total wind loading, for the case for wind acting perpendicular on ring A, is distributed in the following way, see figure 7.5:

- Ring A 5 m friction and wind pressure
- Ring B 20 m friction
- Ring C 15m friction and wind suction

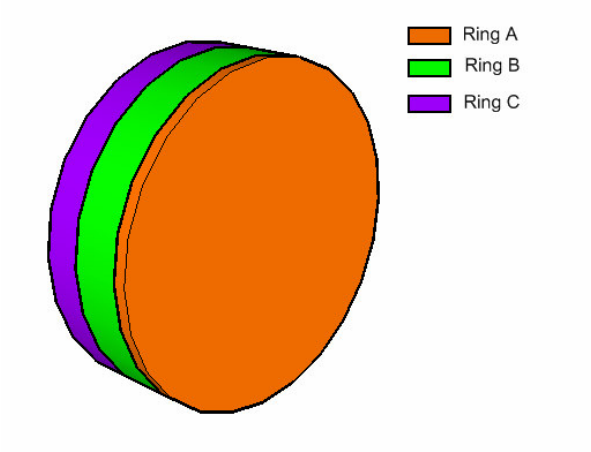

Figure 7.5: Friction area per ring

Two cases are considered in one case the wind load will act perpendicular on Ring A, and in the other case the wind load will perpendicular on ring C. This is done because the cross section of the Great Dubai Wheel is not symmetrical.

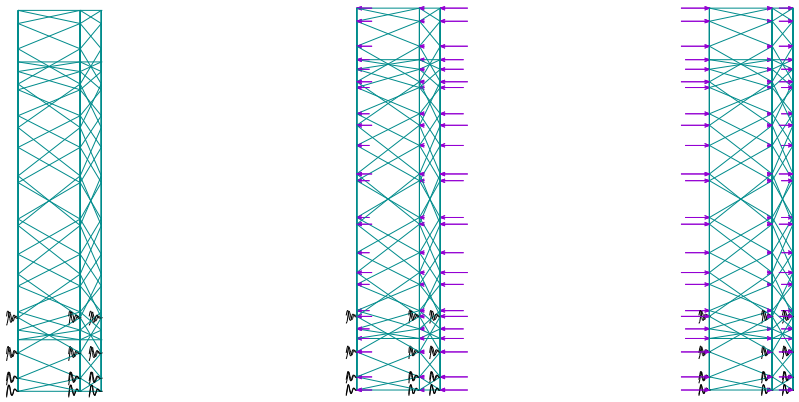

Figure 7.6: Non-symmetrical cross section of the Great Dubai Wheel

7.4. Load combinations

The different loadcases are combined in load combinations.

Linear load combinations	LC1	LC2	LC3	LC4	LC5	LC6	LC7	LC8	LC9
C1: ULS per	1.35	1.35	1.35	0	0	0	0	0	0
C2: ULS per +var	1.2	1.2	1.2	1.5	0	1.5	0	0	0
C3: ULS per + var + wind a	1.2	1.2	0.9	0	1.5	0	0	1.5	0
C4: ULS per + var + wind c	1.2	0.9	1.2	0	0	0	1.5	0	1.5
C5: SLS per + var + wind a	1.0	1.0	1.0	0	1.0	0	0	1.0	0

Table 7.1: Linear load combinations

The stresses in the output of OASYS-GSA make clear that the governing ring of the Great Dubai Wheel is ring C. This was expected because ring C has to take roughly the same loading as ring A and B together. Also as expected combination 3 is the governing load combination, as in this loadcase ring C takes the wind load all by itself see figure 7.7.

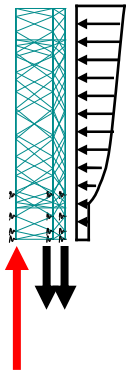

Figure 7.7: Wind load on ring A (LC8)

The results from the model are used for the analysis of the static joint strength and the fatigue behaviour.

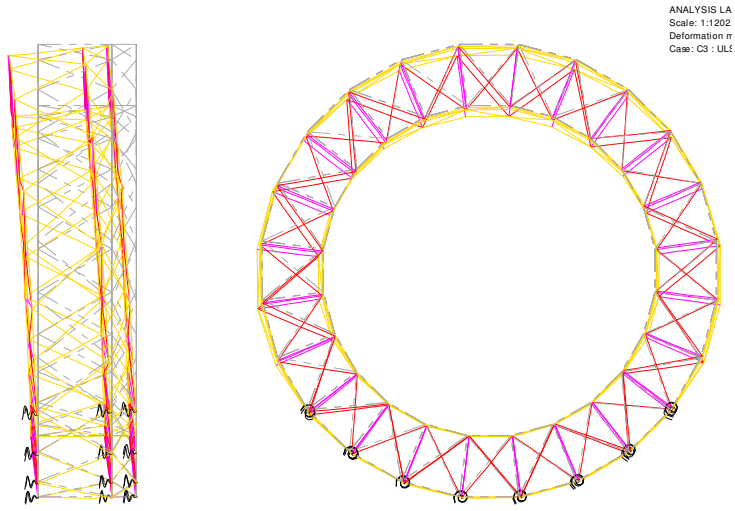

Figure 7.8: Deformations due to load combination 3

8. Static strength joints

The joints in the Great Dubai Wheel will be a critical factor. It is not only in the joints where the forces will be transmitted from one member to another but also the support reactions will act directly on these joints. The joints will not only have to be able to withstand the (quasi) static loading, but also have sufficient fatigue behaviour to withstand the cyclic loading due to the rotation of the wheel.

This means that for the entire Great Dubai Wheel the stresses in the members should not exceed the yield stress. However this demand is not even strict enough. Because the Great Dubai Wheel is a truss girder in which the joints are modelled as fully rigid joints. The braces can only be loaded until a certain percentage of the yield stress, due to the fact that the joint will not be able to fully withstand the yield stress of the material. This is caused by the fact that the joint is not 100% stiff in all places of the joint and in all directions. Because of this the capacity of the joint has to be calculated, this capacity of the joint can be redefined to a parameter C_e which is called the joint efficiency.

The chosen sections and joints in the prior study [13] which are used as a guide throughout this preliminary research will not have a large joint efficiency as these are sections with large γ values and very unfavourable β values for T-joints.

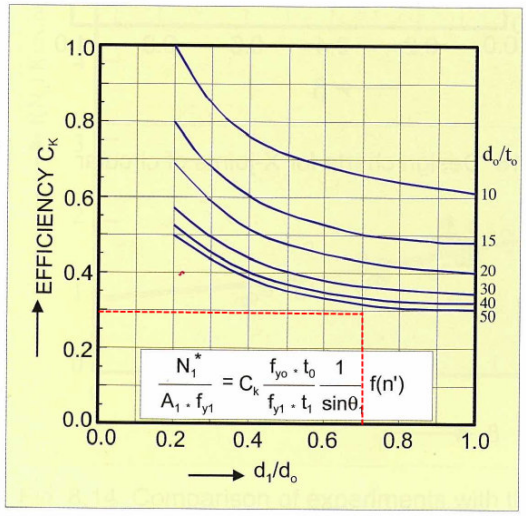

Figure 8.1: Efficiency coefficient K-joint [5]

As an example the joint efficiency design chart for a K-joint with overlap has been given in figure 8.1, in which the dotted line shows the joint efficiency of the chosen sections. It can be seen that the joint efficiency is only about 30%. This would mean that the maximum stress in the braces should only be 30% * 355 = 106.5N/mm^2.

8.1. Types of joints

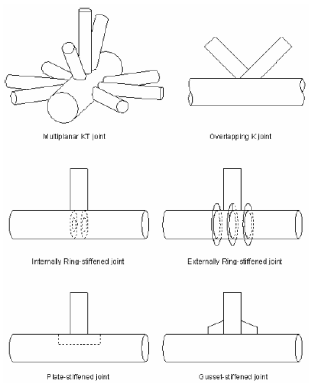

Figure 8.2: Examples of complex joints

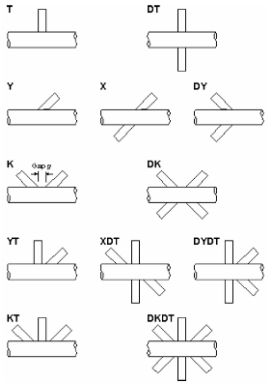

Figure 8.3: Tubular joints geometric classification

Dr. A. Romeijn, TU-Delft, "Fatigue Dictaat deel 1" CT5126, September 2006 [6]

In the original design of the Great Dubai Wheel only 3 types of joints appear namely a simple T-joint, a multiplanar double KT-joint and a multiplanar triple KT-joint.

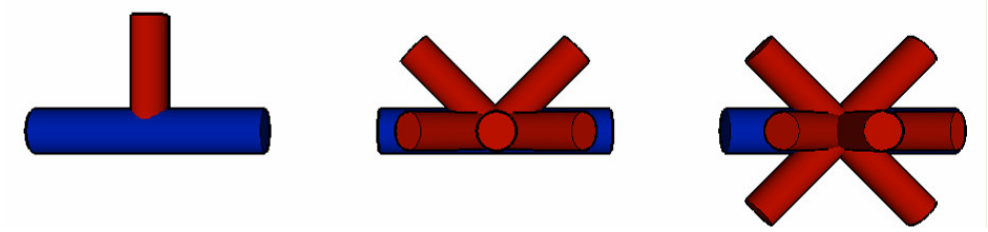

Figure 8.4: T, multiplanar K-KT and multiplanar K-K-KT-joints

For each of these 3 joints the capacity has to be known. The T-joint can be calculated via the normal ways. But for the other joint types no standard ways exist. This has to be done via literature. Literature [6] says that the complex joints can be broken down into their simple uniplanar constituent parts. These uniplanar constituent parts are less stiff and therefore less able to withstand the forces. It is therefore conservative to calculate those multiplanar joints in a uniplanar way. In the next paragraphs the governing joints T- and KT-joints are calculated. It is expected that the T-joint is the governing joint; this is because in the KT-joints the joints are stiffened by the braces.

8.2. Joint efficiency

For a T-joint and a KT-joint the joint efficiencies are calculated. The calculations are found in appendix A. With the joint efficiencies known it is easy to conclude if the joints are strong enough or not.

8.2.1. T-joint

The efficiency of the T-joint is calculated. This calculation is found in appendix A. The efficiency of a T-joint as in the Great Dubai Wheel is a meagre 18 %., see figure A.1. This with the almost constant normal force in the inner and outer rings the efficiency becomes 14%.

8.2.2. KT-joint

The KT-joint has a higher efficiency than the T-joint. This is because the braces stiffen the chord, which will then be less prone to deform. The calculation is found in figure A.4. It is seen that the efficiency of the KT-joint is 38%.

8.3. Conclusion static strength joints

It is concluded that the T-joint is the governing joint in the Great Dubai Wheel, and the capacity of the joint is far too small. The calculated joint efficiency of 18% (14% if the chord loading is taken into account) is worrisome. Especially because the chosen truss system (modified Warren truss) is also supported under the T-joints and large normal forces will be present in all the verticals at some time during a full rotation of the wheel.

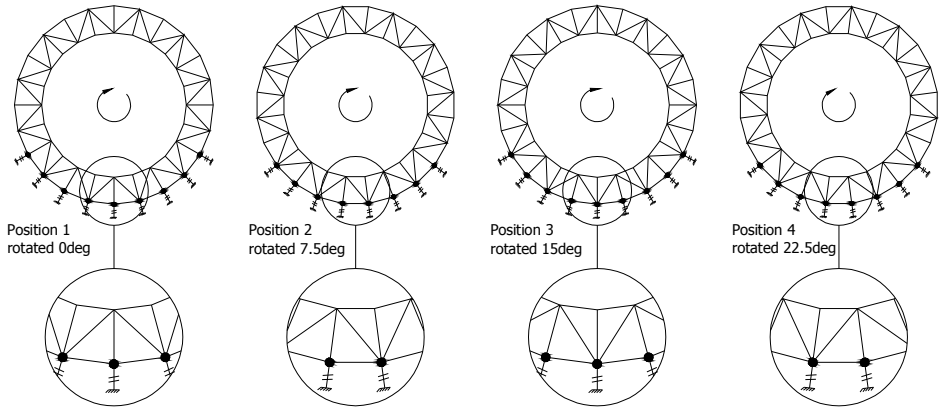

Figure 8.5: Different wheel positions

Therefore the conclusion is drawn that the joints will have to me modified in some way, because an efficiency of 18% is not an economical solution and for the Great Dubai Wheel not a workable solution due to the large stresses present at the joints.

8.3.1. Possible improvements

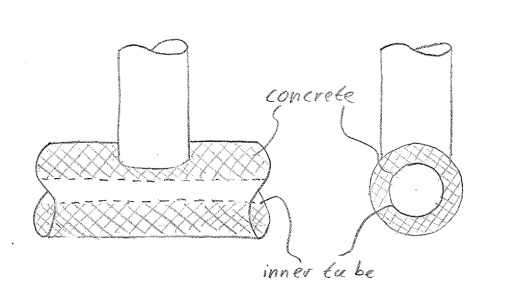

Figure 8.6: Concrete filling of joints

The joint strength can be improved by for instance putting an inner tube inside the main tube and fill the space in between with concrete. The joint will get stiff and the joint efficiency will increase. For tension the increase in joint-efficiency will be less than for compression, but there is an increase.

Figure 8.7: Cast steel joint [6]

Also the use of cast steel joints is an option. More material is put where it's needed the most. Another possibility is to weld in plates to stiffen the connection

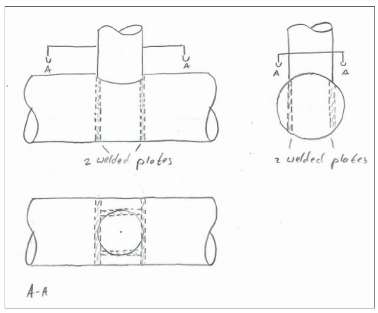

Figure 8.8: Plates to stiffen connection

How much is gained by the three examples stated is not yet known. What is known is that these three possible solutions mean that more weight is put in the joints and probably the sections can be optimized. The total weight of the wheel should therefore be smaller. Another option is to optimize the sections and use more economical sections, such as rectangular hollow sections or I-profiles.

9. Fatigue

Fatigue can be a challenge in structures with fluctuating stresses. For example in steel railway bridges, every time a train passes the stress increases in the structure. The stress fluctuations in the steel sections in the Great Dubai Wheel are a result of the rotation of the entire structure. All the steel sections will undergo a full stress cycle which is a somewhat unique feature. To understand how this rotation affects the fatigue life of the wheel a fatigue analysis is made. In which it is meant to find the maximum stress range of the structure. In this preliminary design it is not meant to find an exact solution or an optimum stress range per section and/or joint. But to find an indication how big the stress ranges are that can be taken by the joints. At the end of this chapter some optimizations possibilities are given, which increase the fatigue life.
Different approaches can be used to find the fatigue life of the structure. For this introduction of the fatigue behaviour of the Great Dubai Wheel the hot-spot stress approach is used. The applicable S-N curves for tubular joints have been taken from the Eurocode 3.

It is not intended to do a full fatigue study, this can and is a Master thesis on itself. It is intended here to give an approximation of the fatigue strength. This is done by clearly stating the Δσ. And to look which joints have the worst stress concentration factors (SCF's).

9.1. SCF's joints

Problems with fatigue are first expected in the joints. In the joints peak stress occur, this peak stress/stresses are taken into account by stress concentration factors. The joints in the Great Dubai Wheel are all multiplanar KT-joints or simple T-joints see figure 8.2 and figure 8.3. For the T-joint the SCF's are determined in appendix B.5.

9.2. Stress range

When the SCF's are known the geometrical stresses are easily calculated by $\sigma_{geom} = SCF * \sigma_{nom}$. For hollow section joints an S-N curve is made (Eurocode 3), see figure 9.1. It is seen that a thickness correction has to be applied. In the Great Dubai Wheel a thickness of 40mm is used throughout the whole structure. This thickness correction factor is determined in appendix B.2.

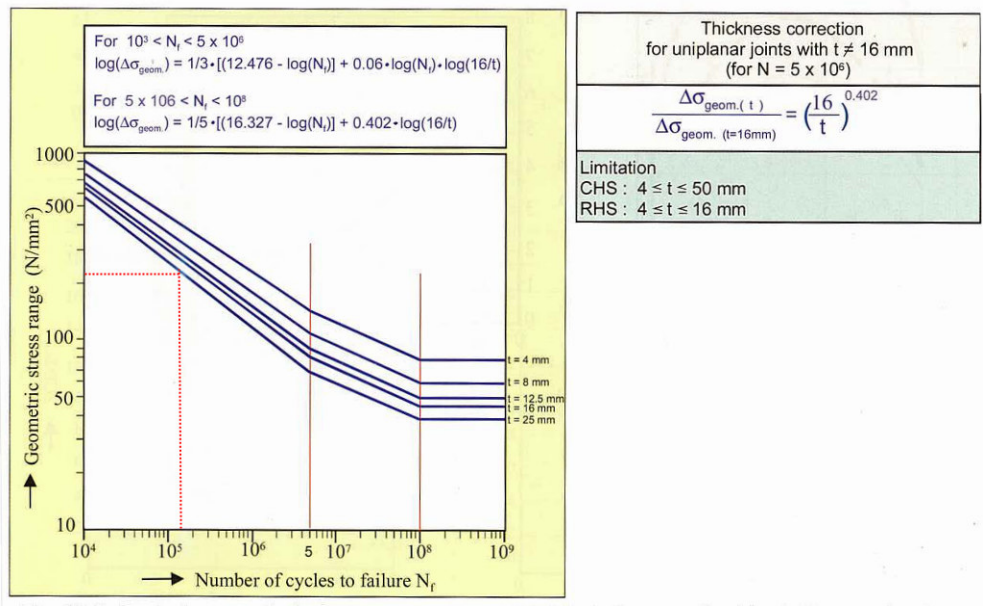

Figure 9.1: S-N curve for hollow section joints [5]

To be able to give the Δσ for the Great Dubai Wheel, the number of stress cycles has to be known. It is chosen to estimate the number of stress cycles by taking the number of rotations and multiply this by two (symmetrical loading).

$$\left(\left((2*4)_{day} * 365\right)_{year} * 50\right)_{lifetime} = 146000 \text{ cycles.}$$

The allowable Δσ becomes:

$$\log\left(\Delta\sigma_{geom.(t)}\right) = \tfrac{1}{3} * \left[12.476 - \log\left(N_f\right)\right] + 0.06 * \log\left(N_f\right) * \log\left(\tfrac{16}{t}\right)$$

$$\log\left(\Delta\sigma_{geom.(40)}\right) = \tfrac{1}{3} * \left[12.476 - \log\left(146000\right)\right] + 0.06 * \log\left(146000\right) * \log\left(\tfrac{16}{40}\right)$$

$$\Delta\sigma_{geom.(40)} = 206\, {}^{N}\!/_{mm^2}$$

This means that the geometrical stress range must be less then 206 N/mm^2.

9.3. T-joint

The problems in the structure are first expected in the joints and when considering the joints the problems are first expected in the T-joint. T-joints are the most sensitive for failure due to fatigue because this is the least stiff connection. To find the SCF's for the T-joint in the Great Dubai Wheel the design guide 8 of CIDECT has been followed: "Design Guide 8. For circular and Rectangular hollow section welded joints under fatigue loading" [2]. In figure 9.2 the relevant parameters for the calculation of the SCF's for a T-joint are stated.

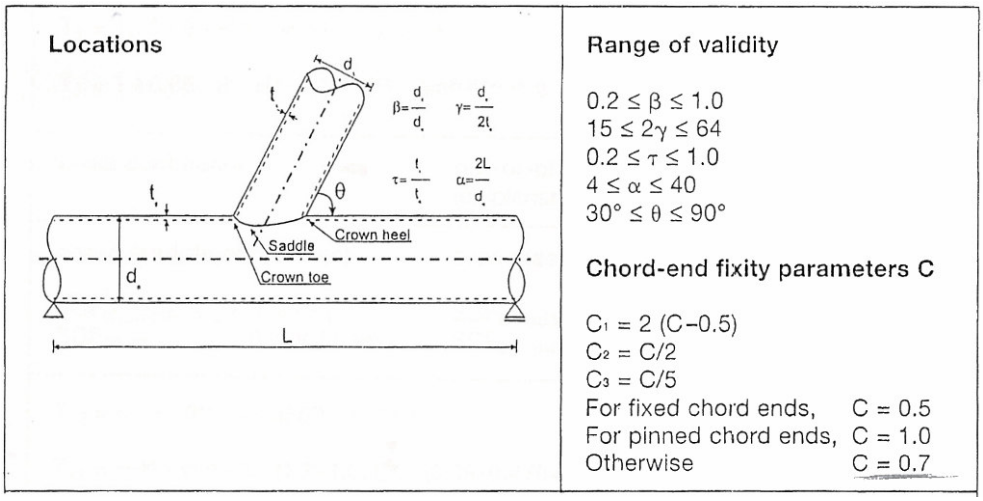

Figure 9.2: CIDECT 8 T-joint parameters [2]

With these parameters the SCF's for a T-joint are calculated and it can be seen, in appendix B.6, (figure B.4, figure B.5 and figure B.6), that the SCF values are high. This is mainly caused by the β-ratio. Because the wall thickness of the chord member is low in comparison with the diameter of the chord member the stiffest part of the connection will take most of the load because it is deformed relatively easily.

9.3.1. Allowable stress range T-joint

The maximum SCF for a T-joint is 21.1 as can be seen in appendix B.6 at the chord saddle position under axial loading. This means that at that position a stress range of

$$\sigma_{geom} = SCF * \sigma_{nom} \rightarrow \sigma_{nom} = \frac{206.5}{21.11} = 9.8 \text{ N/mm}^2$$ is allowed. This is only for the case where there is no bending moment. So the maximum allowable stress range will be a bit different but for simplicity and because the allowable stress range is only 4% of the real stress range, this simplification was thought to be justified.

The stress range for a T-joint on the outer ring is (for stresses due to the normal forces):

Node #	Element #	N/A [N/mm2]
101	**245**	+33.6
109	**253**	+9.0
117	**261**	-158.8

Table 9.1: Stress range T-joint

The stress range is $+33.6-(-158.8)=192.4$ N/mm^2.

Unity check stress range:

$$\frac{192.4}{9.8} \leq 1.0$$
$$19.63 \lhd 1.0$$

The "unity check" above does not comply, obviously. The stress range is a factor 20 too large.

Because of these large SCF's it is the question if the proposed solution of the joints is a feasible solution. Therefore just as for the static strength of the joints for the fatigue strength improvements must be made. The same type of solutions as for the static strength can be applied here (filling the chord with concrete, applying cast steel joints and weld in plates as described in chapter 8.3.1).

Because the T-joint has a very bad fatigue behaviour the KT joint hasn't even been checked.

9.4. Section fatigue behaviour

The sections in the Great Dubai Wheel are so large that the sections are fabricated from 40mm thick plates which will be welded together. Therefore there is a chance of fatigue failure in the sections themselves. It is therefore important to keep the stress range in the members as low as possible. Also increasing the thickness of the plates will possibly decrease the stress range, but due to the thickness effect a reduction in the allowable stress range has to be taken into account the reduction factor is given in appendix B.2.

10. Maximum diameter current design

The maximum diameter of the wheel with its current design is determined in this chapter.

10.1. Static strength

The static strength of the Great Dubai Wheel is dominated by the strength of the joints. The joint efficiency determines what stress can be taken by the joint. These are calculated in chapter 8. The maximum allowable stresses are determined in the next paragraph (10.1.1). To find the maximum diameter on these criteria a graph is plotted in which for the different members the maximum occurring stress is plotted, and by the dotted lines the maximum allowable stresses are plotted.

10.1.1. Maximum allowable stresses

With the joint efficiency of only 14% the maximum allowable stress in the verticals is only $f_{d;ver} = C_t * f_y = 14\% * 355 = 49.7$ N/mm^2.

In the diagonals with a joint efficiency of 36% the maximum allowable stress in these members is $f_{d;diag} = C_{kt} * f_y = 36\% * 355 = 127.8$ N/mm^2. And for the members in the ring the maximum allowable stress for inside and outside ring is equal to the yield stress $f_{d;ring} = 355$ N/mm^2.

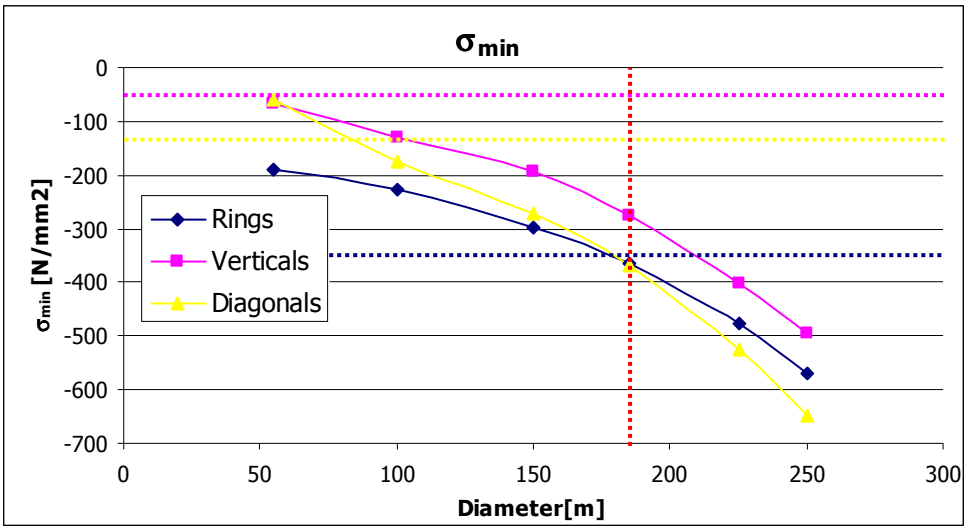

Figure 10.1: σ_{min} in the rings

It is seen in figure 10.1 that the occurring stress is far outranged by the allowable stress for the design diameter of 185m. It is also seen that the stresses do not comply no matter what the diameter is.

10.2. Fatigue strength

For the analysis of the fatigue strength it was concluded that just as for the static strength, the joints are the governing elements of the Great Dubai Wheel. The SCF's found in chapter 9 show that the allowable stress range with a diameter of 185m is about 10 N/mm^2. This proved to be far too small as the stress range was about 300 N/mm^2. In figure 10.2 the allowable stress ranges are plotted by a dotted line, it is seen that none of the members satisfy the demands on fatigue behaviour.

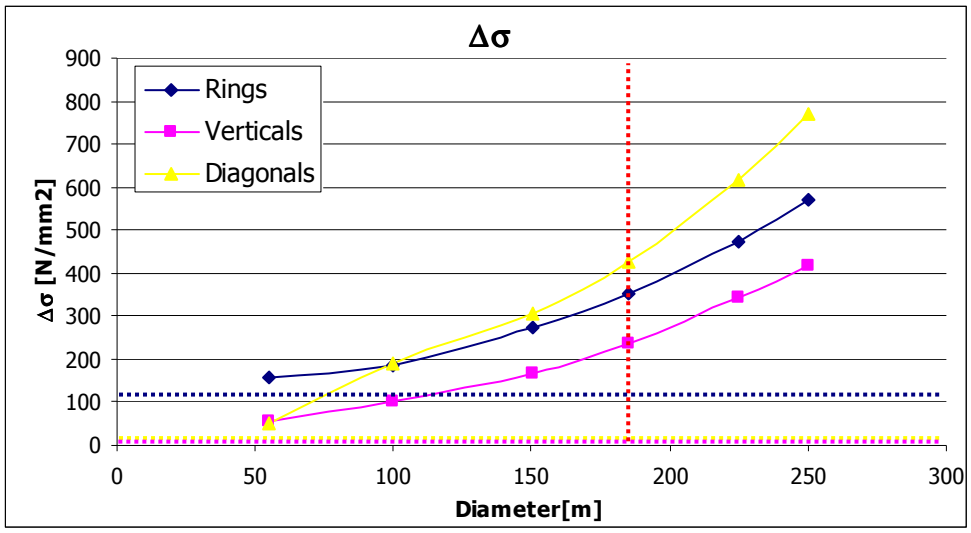

Figure 10.2: Δσ in the rings

10.3. Conclusion

The main challenges in the Great Dubai Wheel from a structural point of view lie in the inefficient material usage. This means that the Great Dubai Wheel is too heavy and that the usage of material has to be more efficient to a great extend. The usage of material in the joints is not efficient. Especially the joint efficiency of the T-joints (14%) is worrisome. Based on these observations it is concluded that the Great Dubai Wheel in its current design isn't feasible. The challenge in this Master thesis is to find the maximum diameter of the Great Dubai Wheel, so what is the maximum diameter of the Great Dubai Wheel with its current design?
The two previous paragraphs proved that for the current design for the static strength the maximum diameter is about 50m (full closed ring, almost the classic Ferris wheel concept) and for the fatigue behaviour the maximum diameter is even below the 50m.

It is concluded that the design of the prior study [13] is not a feasible design. The biggest challenge is to increase the efficiency of the used material.

But why are the stresses this large? The stresses are so large because the self weight plays a very important role. When the reaction forces are analyzed, the total reaction force in the global z direction is 327MN, and from the self weight of the main structure 201MN. This means that 62% of the loading comes from the self weight of the main structure. This also means that with the 14% T-joint efficiency the structure can not even stand up by itself (resist its own self weight).

10.4. Possible improvements

Therefore improvements to the Great Dubai Wheel have to be made if the truss girder concept is kept in place:

- The material in the Great Dubai Wheel should be used more efficient;
  - Change in truss geometry, instead of a Warren truss a cross truss.
- Wind loading should be defined more in detail, see figure 10.3;

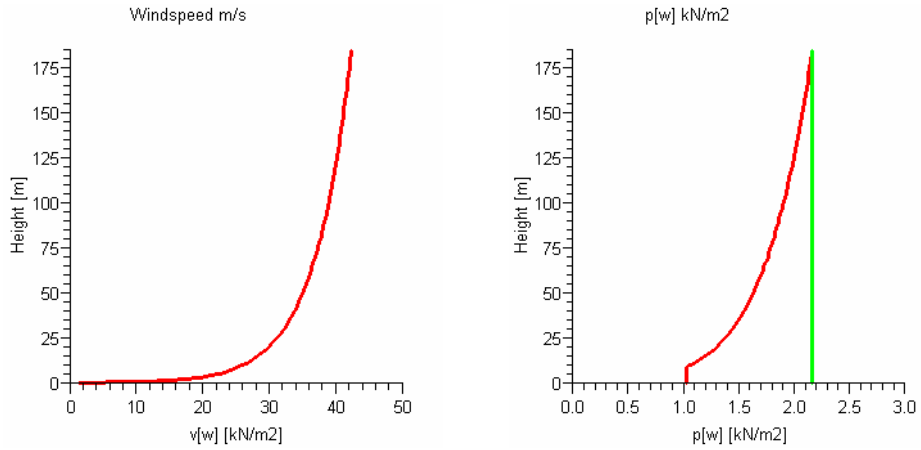

Figure 10.3: Detailed wind load analysis

- Less or lighter main capsules;
- The joint efficiencies will have to be increased (filling with concrete, cast steel joints, use of stiffeners, gusset plates see figure 8.6, figure 8.7 and figure 8.8);

11. Sensitivity analysis

In the previous chapters the focus of this Master thesis was on the limitations of the design. In the following chapters the focus will be on the possibilities of the design. In the following chapters stress ranges will not be a designing factor. This can be dealt with in another Master thesis that will focus on the fatigue behaviour of the Great Dubai Wheel. This does not mean that the stress ranges are not taken into account but it is not attempted to lower the stress ranges. It is expected that by lowering the stress levels in the Great Dubai Wheel the stress ranges also drop.

It is clear that the current design is not feasible as proven in chapter 10, but in chapter 3 (Out of the box thinking), some possible solutions have been mentioned which could lead to a design that is feasible.

The final recommendation for the geometry of the Great Dubai Wheel will be a combination of several possible solutions.

- Number of segments;
- Ring thickness;
- Releases in diagonals and verticals;
- Cross truss;
- Bracing;
- Combined solutions;
- Other optimizations;
    - Stiffness foundation;
    - Cables for diagonals;

Which combination of solutions is investigated in this chapter 11.10. One option isn't investigated and that's making the wheel stationary. When the wheel is made stationary the unique feature of the Great Dubai Wheel of the totally rotating structure is thrown away. It is therefore not considered as an option to make the Great Dubai Wheel a stationary structure on which the capsules ride over on a rail.

11.1. Definition members

In this report different member names are mentioned; in figure 11.1 the different members are pointed out and named.

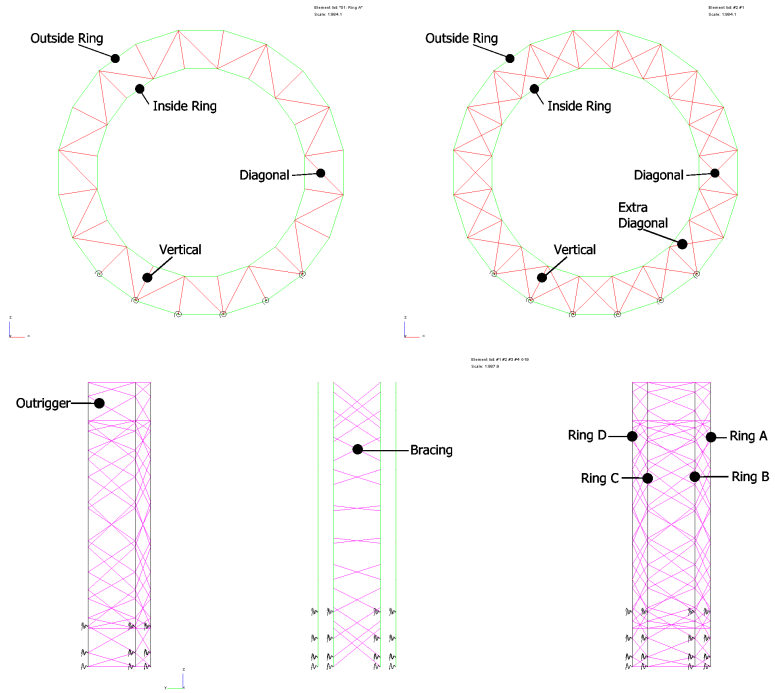

Figure 11.1: Different elements

11.1.1. Section properties different elements

Ring elements:	CHS 2220-40
Vertical elements	CHS 1440-40
Diagonal elements	CHS 1440-40
Outrigger elements	CHS 2220-40
Bracing elements	CHS 1440-40

11.2. Design parameters

For the analysis the member sizes are not changed. This because it is needed to measure the effect of a possible solution compared to the original design. This comparison is done via the stresses. It was also possible to do the comparison in a way that the maximum stresses in the structure is set to a certain level, and that total tonnage of required steel is compared between the different models, but because the total material usage is of less importance in this project, and the effectiveness of the possible improvements is looked after it is chosen to compare the models via the stresses.

What are the design parameters which are of great importance in the design for the Great Dubai Wheel? In chapter 10 it can be seen that the static strength of the structure is not sufficient. This is mainly due to the joint efficiency which is very low (14%). This joint efficiency can be improved by using cast steel joints or in some other way. A joint efficiency of 80 to 100% should be possible.
The other important design parameter is the stress range. For the fatigue analysis the stress range can't be bigger then a certain value, this in order to get a certain fatigue life (number of cycles until failure).
These two parameters, maximum stress and stress range, are the two structural design parameters which will be focussed on. Not in a form that these values should be lower as a predetermined value, but the stress and the stress range should be as low as possible. In chapter 12 the stress and stress range should be below a certain value in order to find the maximum diameter.

Of course thousands of design parameters can be thought of, but because the project is still in a preliminary phase it is important to find a structure that will keep standing instead of the original design which was not feasible. Therefore the functional demands are not designing parameters, and the focus is put on the static structural design (maximum stresses).

11.3. Parametric design

Parametric design is an essential facet in this Master thesis. To be able to do the sensitivity analysis it is essential to quickly compute models and analyse them. The Great Dubai Wheel for structural analysis is just a simple space frame model. It is therefore relatively easy to program the geometry by defining the node coordinates and to put elements between these nodes. Also the output of the structural analysis program needed to be analysed in a quick and efficient way. Therefore an automated Excel-sheet is made in which the output from the structural analysis program (OASYS-GSA) is copied, and the maximum stresses and stress ranges are determined. This is explained further in this paragraph.

11.3.1. Parametric design tools

Excel-sheet

The different models which are analyzed are all compared to each other. To be able to do this comparison the models are created in a systematic way. First of all the parameters which are constant are described. Because the models are created via the parametric design Excel-sheet, it is very easy to create all these different models.

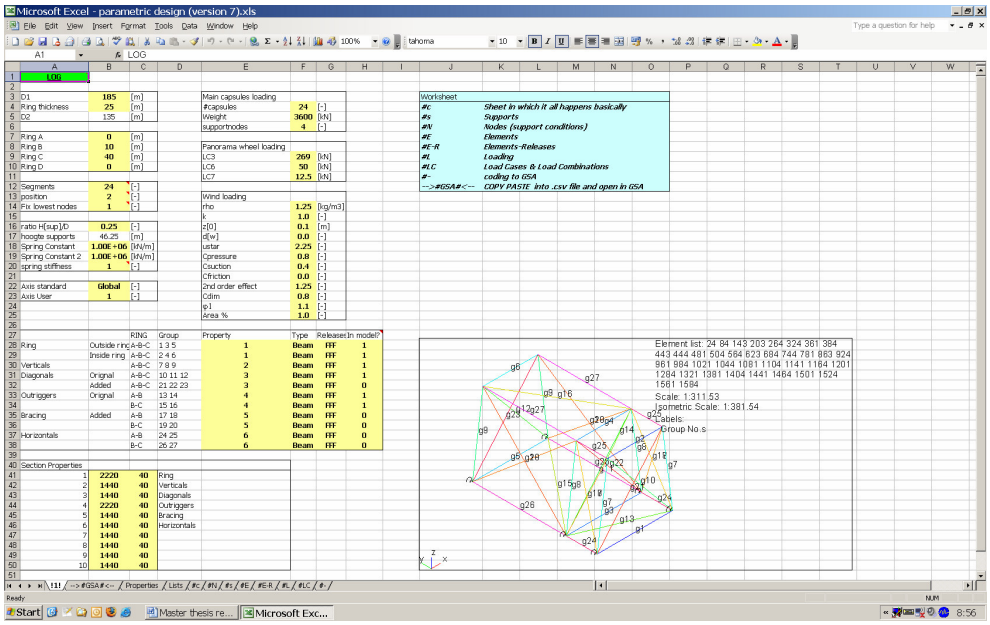

Figure 11.2: Parametric Excel-sheet

The input sheet is divided into four parts. The left top part contains the main parameters such as diameter, number of segments, user axis for OASYS-GSA, and spring stiffness. The top right part of the input sheet contains the loading. These should not normally be touched as the file itself automatically corrects for change in diameter and width. The middle part is the part which gives the model its shape. And in the bottom part the section properties can be assigned. This way it is easy to add the diagonals for the cross truss, as seen in figure 11.3, or to remove it again. The sheet above is the model used in the previous chapters of this report; this model will be referred to as model #0.

Modified Warren truss **Cross truss**

Figure 11.3: Modified Warren truss and cross truss

Excel is also used for the analysis of the different models. The output of OASYS-GSA can directly be copied from OASYS-GSA to Excel and via an automated Excel-sheet analyzed on the set criteria.

Structural analysis program

For the structural analysis OASYS-GSA (figure 11.4) is chosen, this because OASYS-GSA is able to copy and paste its geometry and output from and to Excel. It is even possible to fully define all the input for OASYS-GSA in Excel and copy this into a *.csv-file and directly run this file in OASYS-GSA.

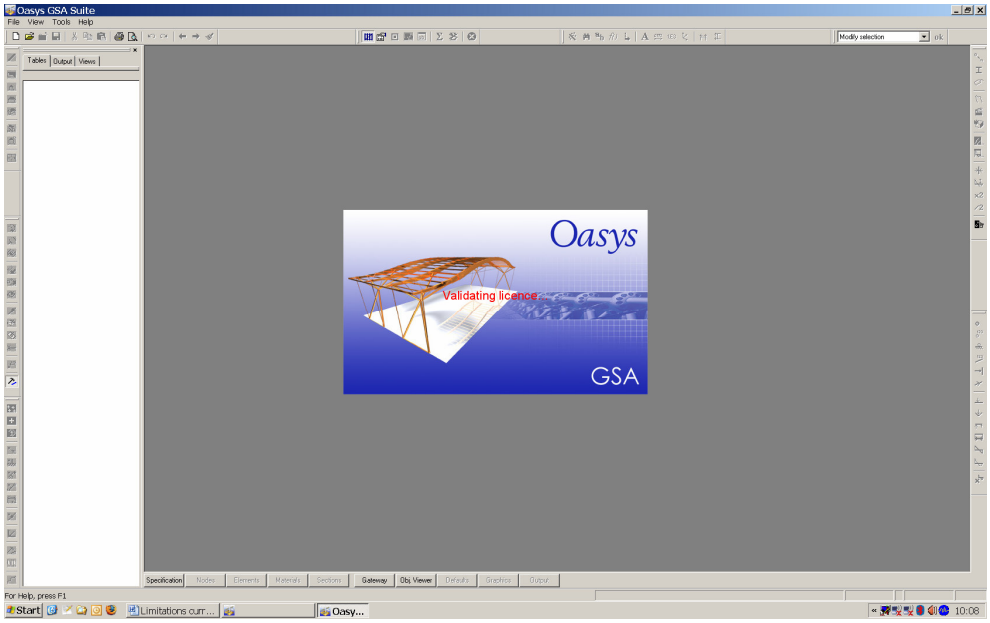

Figure 11.4: OASYS-GSA

Text editor

The final sheet in the Excel-file is the input for the structural analysis program. In order to make this input-file the last sheet is copied, and pasted into a simple text editor. For this an open source freely available program has been used, namely Notepad++. The main advantages of this program above the normal Notepad, available in Windows itself, is that Notepad++ can open multiple files in tabs and it is a portable version so it can be put on an USB-stick and worked with anywhere.

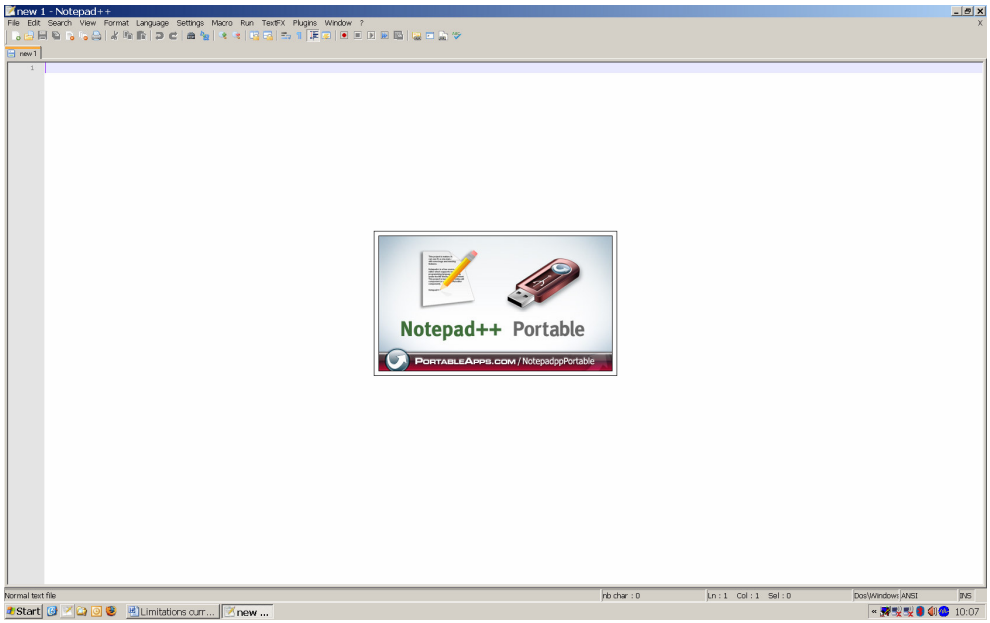

Figure 11.5: Notepad++

11.3.2. Parametric design procedure

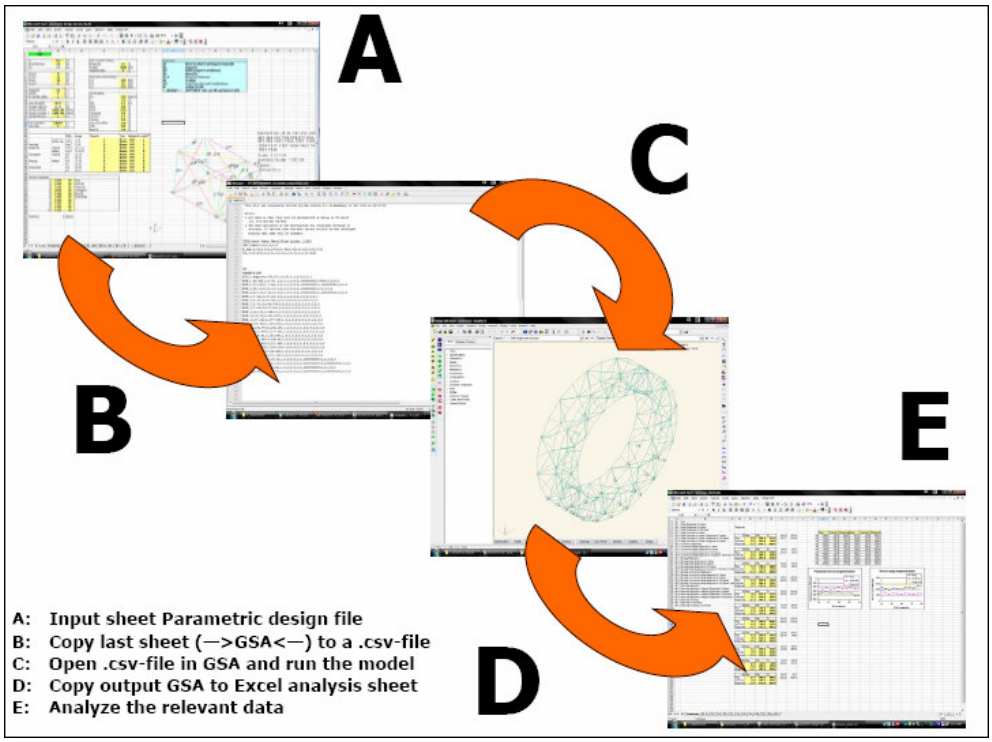

Figure 11.6: From Excel to OASYS-GSA and back

In figure 11.6 the procedure to analyze one model is stated. The procedure consists of 5 steps. The first step is to define the geometry of the model. This is done by filling in some parameters. Step two is to copy the last sheet of the Excel-file into a *.csv-file and save this. In the third step the *.csv-file is opened directly into OASYS-GSA. The program sees this file as a normal OASYS-GSA-file, this file is then analyzed by the program. The fourth step is to copy the relevant data from OASYS-GSA to Excel this can easily be done by copy-pasting. The fifth and final step is to analyze this relevant data in Excel or by hand. Either by a fully automated Excel-sheet or by simple hand calculations deriving the relevant data and take those values like stresses, displacements or forces.

With this procedure creating a model and analyze it by OASYS-GSA only takes a minute or two. This fast handling of different models is critical in this Master thesis as the number of different models which are analyzed is large. Because Excel is used to define the geometry and the loading, some limitations exist on what can be altered on the geometry, for instance the adding of an extra 5^{th} ring will require some rewriting of the Excel-sheet.

Options of Excel-sheet

The parametric design sheet has many options, many parameters can be changed. In figure 11.7 – figure 11.10 the different parts of the Excel-sheet are given. In appendix XXX the

	A	B	C
1	**LOG**		
2			
3	D1	**210**	[m]
4	Ring thickness	**25**	[m]
5	D2	160	[m]
6			
7	Ring A	**0**	[m]
8	Ring B	**10**	[m]
9	Ring C	**40**	[m]
10	Ring D	**50**	[m]
11			
12	Segments	**24**	[-]
13	position	**2**	[-]
14	Fix lowest nodes	**1**	[-]
15			
16	ratio H[sup]/D	**0.25**	[-]
17	hoogte supports	52.5	[m]
18	Spring Constant	**1.00E+06**	[kN/m]
19	Spring Constant 2	**1.00E+06**	[kN/m]
20	spring stiffness	**1**	[-]
21			
22	Axis standard	**Global**	[-]
23	Axis User	**1**	[-]

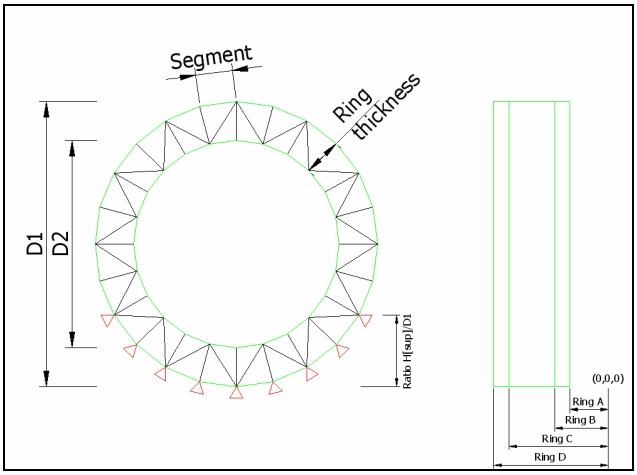

Figure 11.7: Top left part of the input sheet with geometry parameters

The option to fix the lowest nodes in the model is put in because the models tend to rotate which does not happen, the supports added to the lowest nodes will not take loading, they are merely present for modelling purposes only.

The option spring constant 1 and 2 are present to be able to vary the spring constants easily to see if these influence the structural behaviour of the wheel, together with the option spring stiffness the spring stiffness can vary from a constant spring stiffness to a sinusoidal spring stiffness along the width of the Great Dubai Wheel.

The axis options are merely there for the correct nomenclature for OASYS-GSA.

Main capsules loading		
#capsules	**24**	[-]
Weight	**3600**	[kN]
supportnodes	**4**	[-]
Panorama wheel loading		
LC3	**269**	[kN]
LC6	**50**	[kN]
LC7	**12.5**	[kN]
Wind loading		
rho	**1.25**	[kg/m3]
k	**1.0**	[-]
z[0]	**0.1**	[m]
d[w]	**0.0**	[-]
ustar	**2.25**	[-]
Cpressure	**0.8**	[-]
Csuction	**0.4**	[-]
Cfriction	**0.0**	[-]
2nd order effect	**1.25**	[-]
Cdim	**0.8**	[-]
φ1	**1.1**	[-]
Area %	**1.0**	[-]

#capsules is number of main capsules in the Great Dubai Wheel. Support nodes is number of nodes that support one single main capsule.

Panorama wheel loading is the loading that is taken from the panorama wheel model.

Wind loading is the wind loading from the Dutch NEN 6702 Code. The wind loading is calculated with the logarithmic wind loading as can be seen in figure 10.3. The cell with area % is put in to decrease the area of the Great Dubai Wheel as the wind can blow threw the Great Dubai Wheel. For the wind load a 2nd order effect of 1.25 is taken into account. And a dynamic amplification factor of 1.1 is used. Derived from the prior study [13].

Figure 11.8: Top right part of the input sheet with the loading parameters

The loadcases mentioned in figure 11.8, are the loadcases mentioned in chapter 7.3.

26			RING	Group	Property	Type	Releases	In model?
27	Ring	Outside ring	A-B-C	1 3 5	**1**	**Beam**	**FFF**	**1**
28		Inside ring	A-B-C	2 4 6	**1**	**Beam**	**FFF**	**1**
29	Verticals		A-B-C	7 8 9	**2**	**Beam**	**FFF**	**1**
30	Diagonals	Orignal	A-B-C	10 11 12	**3**	**Beam**	**FFF**	**1**
31		Added	A-B-C	21 22 23	**3**	**Beam**	**FFF**	**1**
32	Outriggers	Orignal	A-B	13 14	**4**	**Beam**	**FFF**	**1**
33			B-C	15 16	**4**	**Beam**	**FFF**	**1**
34	Bracing	Added	A-B	17 18	**5**	**Beam**	**FFF**	**0**
35			B-C	19 20	**5**	**Beam**	**FFF**	**0**
36	Horizontals		A-B	24 25	**6**	**Beam**	**FFF**	**0**
37			B-C	26 27	**6**	**Beam**	**FFF**	**0**

Figure 11.9: Middle part of the input sheet with section properties

In figure 11.9 it is possible to enter for different elements, as seen in figure 11.1, the element properties as they will be copied to OASYS-GSA. When in the last column of figure 11.9 a 1 is put in, than that element is put in the OASYS-GSA-model, when a 0 is put in than that element will not be in the OASYS-GSA-model.

39	Section Properties			
40	1	**2220**	**40**	Ring
41	2	**1440**	**40**	Verticals
42	3	**1440**	**40**	Diagonals
43	4	**2220**	**40**	Outriggers
44	5	**1440**	**40**	Bracing
45	6	**1440**	**40**	Horizontals
46	7	**1440**	**40**	
47	8	**1440**	**40**	
48	9	**1440**	**40**	
49	10	**1440**	**40**	

Figure 11.10: Bottom part of the input sheet with section properties

In figure 11.10 it is seen that it is possible to change the dimensions of the sections used. Throughout the Master thesis only CHS sections are used, this is done because the moments in both directions are of importance.

11.4. Number of segments

The original design which won the contest consisted of 40 segments. In this Master thesis it was changed to 24 segments because there are 24 main capsules. But the question still remains, from a structural point of view, what the best segmentation is, and more importantly whether the segmentation influences the maximum stresses and the stress ranges. To research this, the parametric model is adapted to be able to vary the number of segments, from 20 to 60. It is chosen to not check models with a lower number of segments then 20, because the Great Dubai Wheel becomes more sharp-edged than round. The analysis is done, to limit the number of models to be analyzed, on models from 20 to 60 segments with steps of 4 segments each time, so 20, 24 … 56, 60 segments. The results are shown figure 11.11 below and show the results for the ring, vertical and diagonal elements in separate lines.

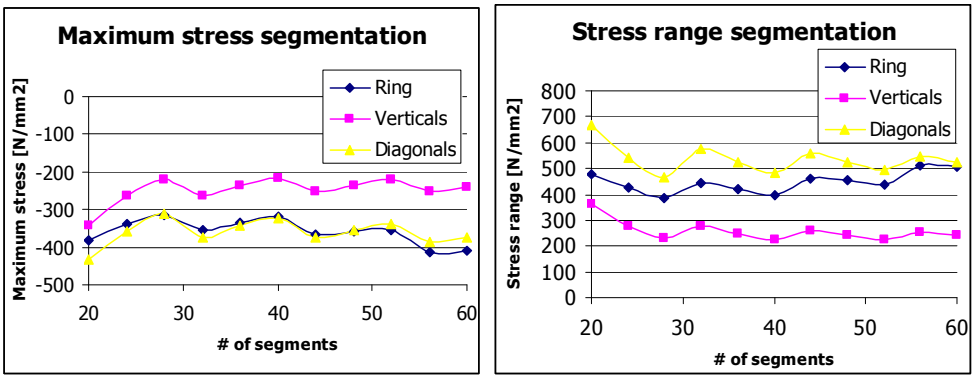

Figure 11.11: Maximum stresses and stress ranges by different segmentation

In figure 11.11 a relatively small variation on stresses is seen when increasing the number of sections. A slightly different trend is observed in case of a number of segments close to 20. For a number of segments above approximate 30 the lines oscillate around a constant value which is mainly caused by local effects in relation to the angle of the diagonals and the verticals at the highest support (local effects outrange the effect of the number of segments). It therefore has to be checked if the model is not on one of the peaks of the graphs. But it can not be said what the optimum number of segments is because the local effects outrange the effect of the number of segments.

11.5. Ring thickness

The thickness of the ring, in other words the height of the truss, is from an aesthetics point of view an important parameter. But for a structural point of view it might also be an important parameter. It has been checked in this paragraph if the ring thickness influences the stresses in a way that it is advantageous to change the ring thickness. The models analyzed are shown in figure 11.12.

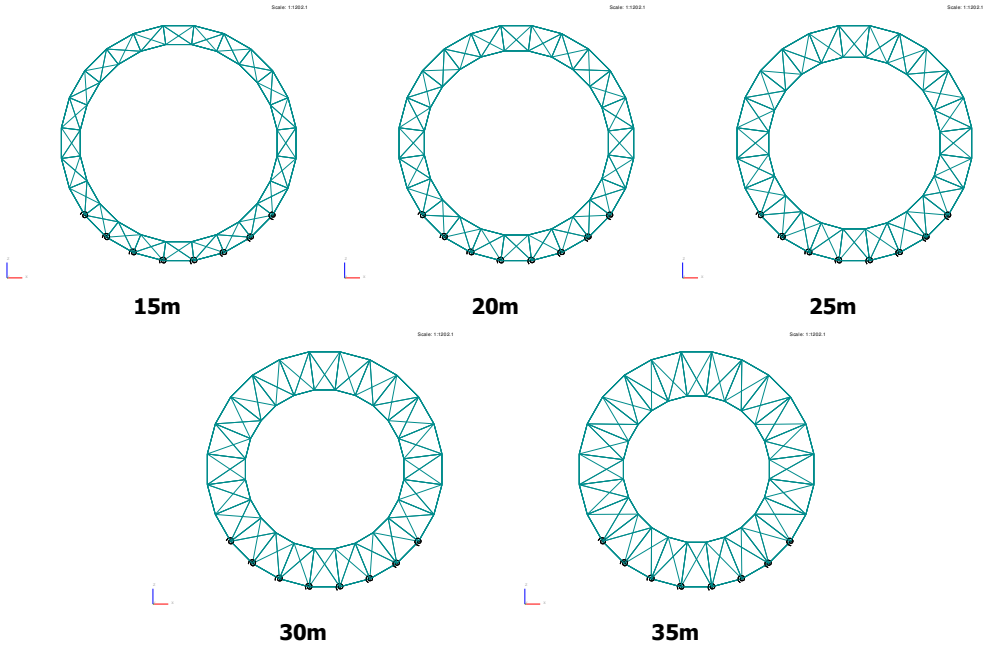

Figure 11.12: Models ring thickness

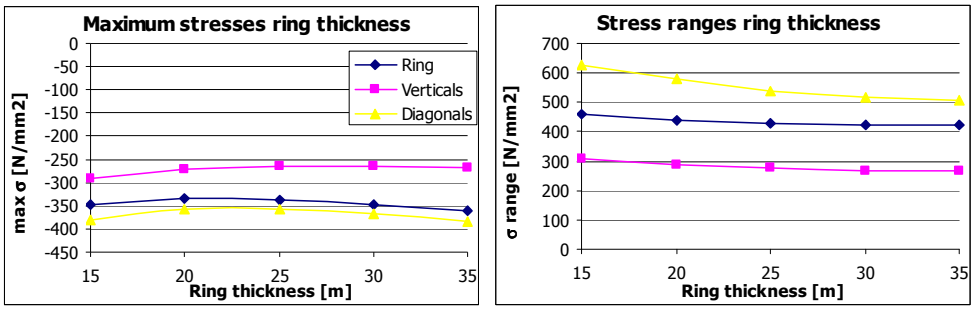

Figure 11.13: Stresses and ring thickness

In figure 11.13 it is seen that the ring thickness doesn't have a big effect on the stress distribution in the Great Dubai Wheel. It seems that the optimum, if you can say there is an optimum, lays around 25 to 30m. The ring thickness at the current design is 25m. When the diameter is enlarged it is expected that the above numbers are changed a bit but it is not necessary to change the ring thickness. When a final design is done the most preferable ring thickness should of course be determined.

11.6. Releases in diagonals and verticals

The stress distribution in the structure shows that moment action in the elements are a significant part of the total stress distribution namely as shown next 20%.

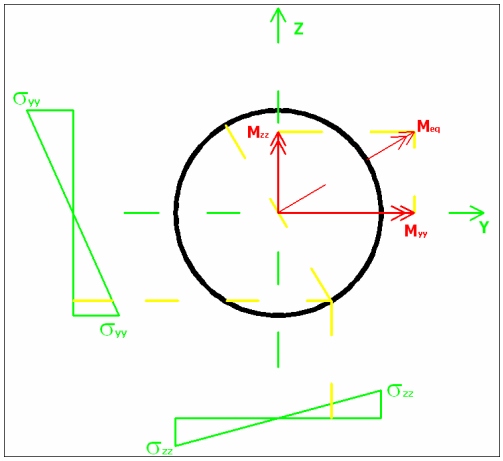

Figure 11.14: Equivalent bending stress

Because the sections used in the Great Dubai Wheel are all circular hollow sections. It is possible to determine the maximum stress by adding the stress of the M_{yy} and M_{zz} via linear interpolation. This is possible because the inertia bending moment is equal for all directions. The same results are achieved by calculating the equivalent bending moment of M_{yy} and M_{zz} and calculate the bending stress of this equivalent moment. OSAYS-GSA gives an output of bending stresses in local y- and z-axis, the total bending stress is therefore determined by the following formula. The values are taken from the maximum stress in the Great Dubai Wheel see table 11.1.

Elem	Case	Pos	A	By +ve z	Bz +ve y	C2
664	C3	244	-282.7	**22.76**	**-71.53**	-357.5

Table 11.1:Maximum bending stress

$$\sigma_{tot;d} = \sigma_{A;d} + \sqrt{\sigma_{yy,d}^{\ 2} + \sigma_{zz,d}^{\ 2}}$$

$$\frac{\sqrt{\sigma_{yy,d}^{\ 2} + \sigma_{zz,d}^{\ 2}}}{\sigma_{tot;d}} *100\%$$

$$\frac{\sqrt{22.8^2 + 71.5^2}}{357.5} *100\% = 20\%$$

It should therefore be possible if the joints are fabricated as hinges to lower the stresses. This will be checked in this paragraph. For this analysis several models are made. The models are given in the table below with their model number and their description. The original model is the starting model and is referred to as model #0.

MODEL NR.	Description
#0	Start
#1.1	Hinge Diagonals in Y-plane
#1.2	Hinge Diagonals in Z-plane
#1.3	Hinge Diagonals in Y&Z-plane
#2.1	Hinge Verticals in Y-plane
#2.2	Hinge Verticals in Y-plane + Diagonals in Y plane
#2.3	Hinge Verticals in Y-plane + Diagonals in Y&Z plane
#2.4	Hinge Verticals in Y-plane + Diagonals in Z plane

Table 11.2: Model descriptions releases

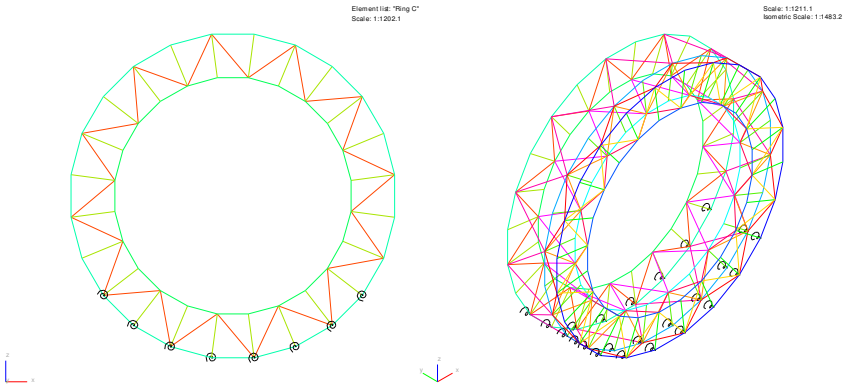

Figure 11.15: Model #0 front view and isometric view

The model is started with the diagonals as these are the elements in which the highest stresses occurred in the original model #0.

11.6.1. Diagonals

To get a good idea what the best improvement is, the analysis is done in three steps. The first step is to take the original model and apply releases (a hinge in OASYS-GSA is called a member release), in the local Y-plane of the sections. This is then repeated but this time the release is applied in the local Z-plane, and for the last step the releases are applied in the both the Y and Z plane. This is given in figure 11.16.

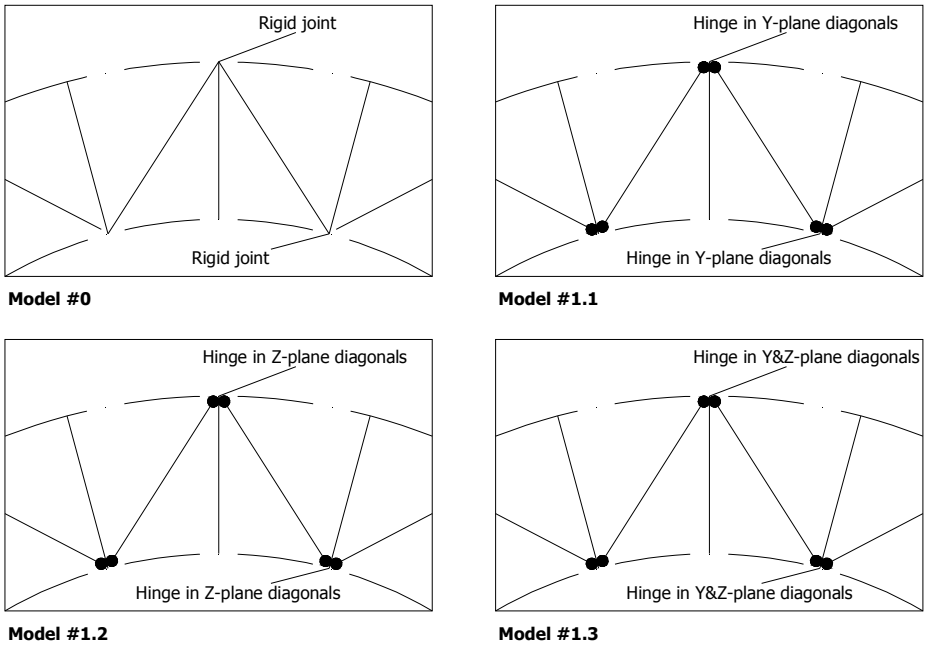

Figure 11.16: Releases applied to the original model

The outcome of the analysis consists of a lot of data. To quickly compare the models to each other and to quickly find out if the proposed solutions indeed lower the stresses in the structure, an automated Excel-sheet is created. The Excel-sheet gives the maximum and minimum and the stress range of three different types of sections namely ring members, verticals and the diagonals. These stresses are compared to the original model. The results of the analysis are given in table 11.3.

#0	**Min σ**			**Δσ**	
Ring	-338.0			426.0	
Verticals	-264.3			275.9	
Diagonals	-357.5			539.1	

#1.1	**Min σ**	**+/- #0**		**Δσ**	**+/- #0**
Ring	-336.6	**-**		426.3	**-**
Verticals	-264.4	**-**		276.8	**-**
Diagonals	-354.3	**-1%**		540.5	**-**

#1.2	**Min σ**	**+/- #0**		**Δσ**	**+/- #0**
Ring	-341.1	**+1%**		430.4	**+1%**
Verticals	-301.3	**+14%**		296	**+7%**
Diagonals	-305.8	**-14%**		506.9	**-6%**

#1.3	**Min σ**	**+/- #0**		**Δσ**	**+/- #0**
Ring	-339.6	**-**		430.6	**+1%**
Verticals	-301.5	**+14%**		296.9	**+8%**
Diagonals	-282.8	**-21%**		501.8	**-7%**

Table 11.3: Stress and stress ranges releases in diagonals

In table 11.3 it is seen that applying a hinge in the Y-direction of the diagonals (model #1.1) does not influence the maximum stresses at all. In the columns next to the minimum stress and stress range the difference in percentages to #0 is given. When applying a hinge in the local Z-plane (model #1.2) the maximum stress reduces in the diagonals but a negative consequence is that the maximum stress in the verticals increases. When a hinge is applied in the Y&Z-planes (model #1.3) the reduction of the stresses in the diagonals is about 20%. But in this case the verticals are stressed more than in the original model and the ring sections are loaded about the same as in the original model.

11.6.2. Verticals

The same type of analysis as for the diagonals has been done for the verticals.

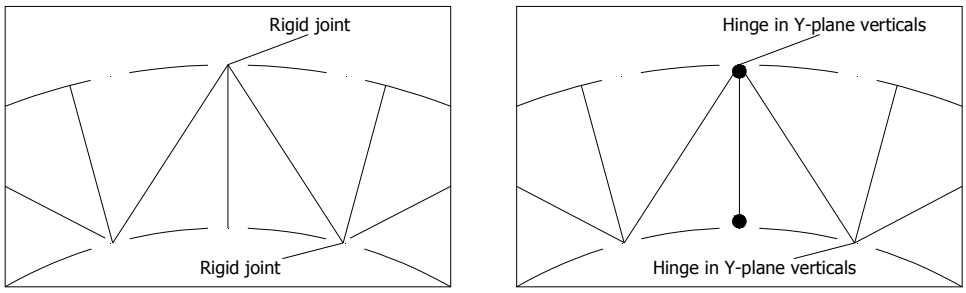

Model #0 Model #2.1

Figure 11.17: Releases applied to the original model

The Great Dubai Wheel is in lateral direction designed using portal frames instead of a lattice structures, therefore it was not possible to assign the releases in the local Z-plane; this would have meant that a mechanism of instability, so called singularity, was created.

#0	**Min σ**			**Δσ**	
Ring	-338.0			426.0	
Verticals	-264.3			275.9	
Diagonals	-357.5			539.1	

#2.1	**Min σ**	**+/- #0**		**Δσ**	**+/- #0**
Ring	-336.1	**-1%**		423.8	**-1%**
Verticals	-253.0	**-4%**		268.2	**-3%**
Diagonals	-361.8	**+1%**		544.5	**+1%**

Table 11.4: Stress and stress ranges releases in verticals

It is clearly seen in table 11.4 that the reduction in stresses is almost negligible.

11.6.3. Diagonals and verticals

Finally models are analyzed in which the releases in the diagonal and vertical elements are combined, as seen in figure 11.18.

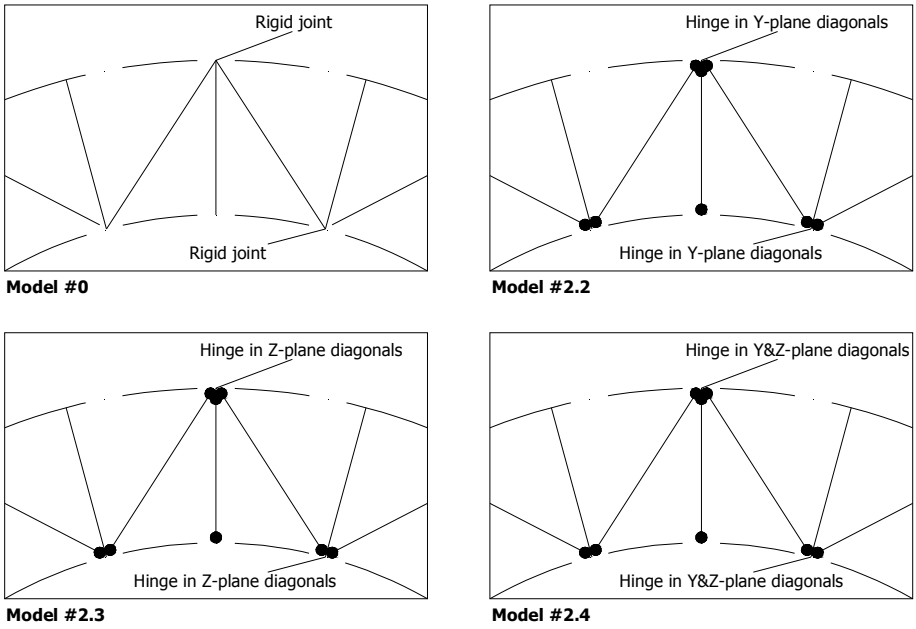

Figure 11.18: Releases applied to the original model

#0	**Min σ**			**Δσ**	
Ring	-338.0			426.0	
Verticals	-264.3			275.9	
Diagonals	-357.5			539.1	

#2.2	**Min σ**	**+/- #0**		**Δσ**	**+/- #0**
Ring	-333.7	**-1%**		423.6	**-1%**
Verticals	-253.3	**-4%**		269.2	**-2%**
Diagonals	-357.3	**-**		546.5	**+1%**

#2.3	**Min σ**	**+/- #0**		**Δσ**	**+/- #0**
Ring	-339.3	**-**		428.1	**-**
Verticals	-293.0	**+11%**		290.0	**+5%**
Diagonals	-312.5	**-13%**		511.9	**-5%**

#2.4	**Min σ**	**+/- #0**		**Δσ**	**+/- #0**
Ring	-336.8	**-**		427.9	**-**
Verticals	-293.3	**+11%**		291.1	**+6%**
Diagonals	-285.8	**-20%**		507.7	**-6%**

Table 11.5: Stress and stress ranges releases in diagonals and verticals

Also in these cases it is clearly seen in table 11.5 that the reduction in stresses is almost negligible.

11.6.4. Conclusion releases

The results of the analysis of the usage of member releases, expressed by hinges, instead of stiff connections are somewhat disappointing. It was expected that the reduction of the stresses and stress ranges would be bigger. From the results obtained it is concluded that already for the initial design the axial stiffness of the members influences the stress distribution much more than the bending stiffness of the members. This means that the load distribution is mainly based on axial forces instead of bending moments. It also seems that by adding the releases to the elements under consideration the stiffness of the structure is reduced which almost entirely compensates for the positive effect of the releases, so the forces are redistributed.

This means that by applying releases to the different elements, the Great Dubai Wheel doesn't get any more feasible and another solution has to be looked at. But the releases should still be taken into account, because for the diagonals a positive effect is certainly present. Also, for optimization of fabrication costs, a detailed study is needed on the meaning of rigid versus hinged connections.

11.7. Cross truss

MODEL NR.	Description
#0	Start
#3.1	Cross truss rigid joints

Table 11.6: Model descriptions cross truss

The original design of the truss is a modified Warren truss. In figure 11.19 it is seen that the elements which are most heavily loaded are the diagonals which connect to the highest supports (diagonal members in the circles in figure 11.19). Therefore it is logical to apply more elements in some way which lighten the loading on these diagonals.

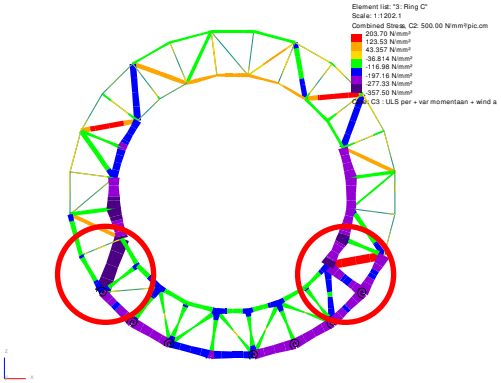

Figure 11.19: Model #0 location peak stresses

One solution is to apply a cross truss instead of the modified Warren truss. For the cross truss more elements are present in the area of the highest supports. This is seen in figure 11.20.

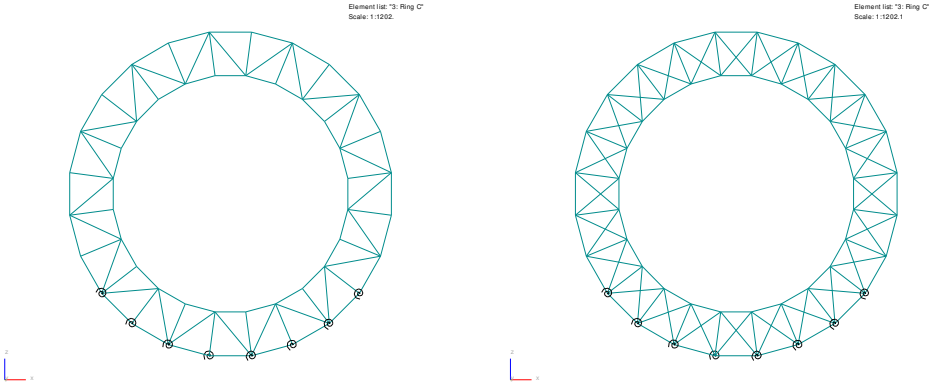

Model #0 **Model #3.1**

Figure 11.20: Modified Warren truss and cross truss

Also this analysis was performed with the automated Excel-sheet mentioned before. The results of the analysis are given in table 11.7. It is seen that a serious stress reduction is achieved.

#0	**Min σ**			**Δσ**	
Ring	-338.0			426.0	
Verticals	-264.3			275.9	
Diagonals	-357.5			539.1	

#3.1	**Min σ**	**+/- #0**		**Δσ**	**+/- #0**
Ring	-264.3	**-22%**		359.9	**-16%**
Verticals	-144.1	**-45%**		144.4	**-48%**
Diagonals	-265.3	**-26%**		327.8	**-39%**

Table 11.7: Stress and stress ranges cross truss

Table 11.7 shows that the cross truss leads to considerably lower stresses in the structure. A remark has to be made that the cross truss consists of the same sections as the modified Warren truss and that thus more material is used in the cross truss. But because material usage is of less importance in this project the extra material usage is not taken into account, as the designing factor is the maximum stress.

11.8. Bracing

MODEL NR.	Description
#0	Start
#4.1	Bracing rigid joints
#4.1 (2)	Bracing rigid joints (single bracing)
The models are illustrated in figure 11.21.	

Table 11.8: Model descriptions bracing

In figure 11.21 it is seen that the cross section of the Great Dubai Wheel (model #0) is a non-braced portal frame (Vierendeel truss). This means the presence of large horizontal displacements and it also means that the joints are heavily loaded. It is thought that by bracing the frame with diagonal members the stiffness, as seen in figure 11.21, is increased and hence the horizontal deformation will reduce and especially the contribution of bending stresses are reduced by a great extend.

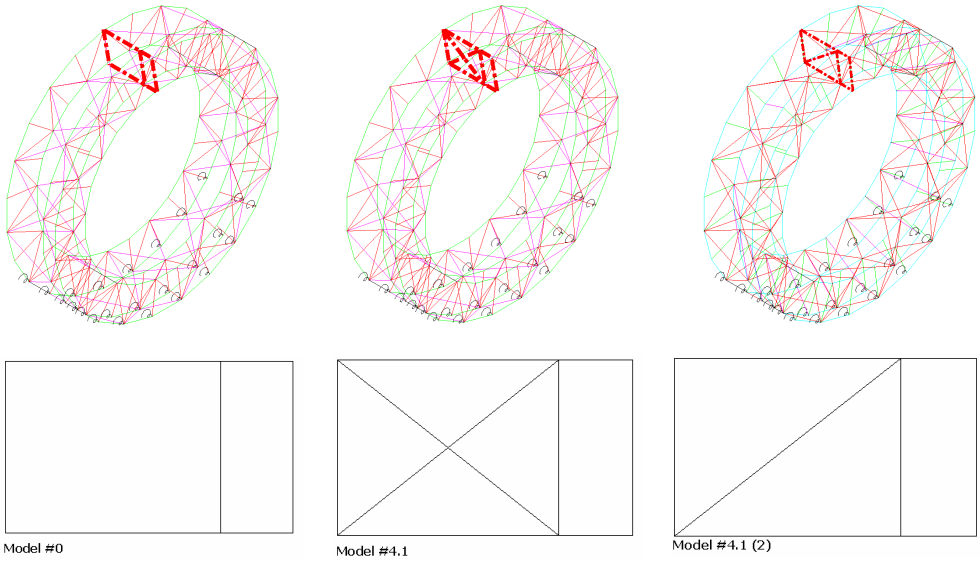

Figure 11.21: Cross section model #0, #4.2 (Bracing) and #4.2 (2) (single bracing)

The displacements shown in table 11.9 are located at the highest possible point of the structure, in table 11.9 it can be seen that indeed the horizontal deformation is reduced.

Model	**Horizontal deformation [mm]**
Model #0	587
Braced frame	454
Single braced frame	467

Table 11.9: Horizontal deformation at the top node

The results of the analysis are given in table 11.10. It shows that a serious stress reduction is achieved. But the stress reduction is not that great compared to the cross truss improvement.

#0	**Min σ**			**Δσ**	
Ring	-338.0			426.0	
Verticals	-264.3			275.9	
Diagonals	-357.5			539.1	

#4.1	**Min σ**	**+/- #0**		**Δσ**	**+/- #0**
Ring	-305.9	**-9%**		369.7	**-13%**
Verticals	-230.7	**-13%**		245.7	**-11%**
Diagonals	-326.0	**-9%**		505.8	**-6%**

#4.1 (2)	**Min σ**	**+/- #0**		**Δσ**	**+/- #0**
Ring	-323.5	**-4%**		386.5	**-9%**
Verticals	-238.8	**-10%**		260.0	**-6%**
Diagonals	-324.7	**-9%**		514.7	**-5%**

Table 11.10: Stress and stress ranges bracing

11.9. Extra ring

MODEL NR.	Description
#0	Start
#6.1	Extra ring rigid joints 50m
#6.1 (2)	Extra ring rigid joints 40m
The models are illustrated in figure 11.23	

Table 11.11: Model descriptions extra ring

Figure 11.22 shows the stresses in ring A to ring C in front view. It shows that the most heavily loaded ring is ring C. This is obvious as the other two rings will work together as they are spaced more closely to each other.

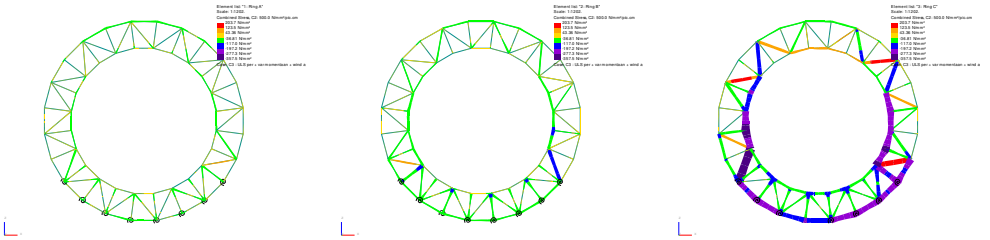

Ring A **Ring B** **Ring C**

Figure 11.22: Cross section model #0 stress levels

Therefore the adding of an extra ring has been proposed as a possible solution. The extra ring makes the structure symmetrical. This means that the structure behaves in the same manner whether the wind blows from the left or from the right.

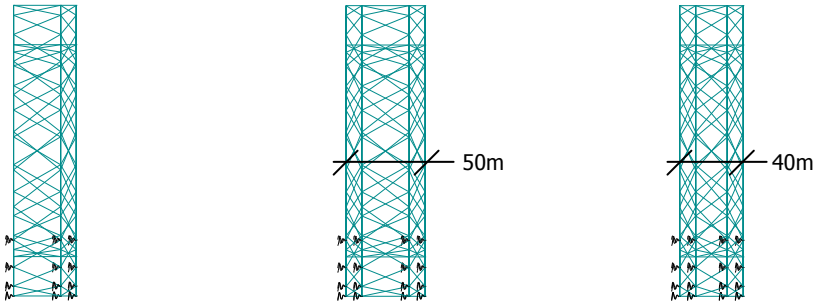

Original model #0 **Extra ring added #6.1 (50m)** **Extra ring added #6.1 (2) (40m)**

Figure 11.23: Alternatives for geometry extra ring

And as for the two closely spaced rings in model #0, the two other rings will work together and spread the loading more or less evenly. This should lead to lower stresses.

The geometry of model #0 is maintained, and the extra ring is added to the structure. This means that the width of the structure will increase from 40m to 50m. Another model in which the width remained 40m is also checked and gives slightly higher stresses which are expected by the decreased leverage arm. Both models are analysed to make sure the increase of width isn't the basis for the decrease in stresses but the extra ring is the basis for it.

#0	Min σ			Δσ	
Ring	-338.0			426.0	
Verticals	-264.3			275.9	
Diagonals	-357.5			539.1	

#6.1	Min σ	+/- #0		Δσ	+/- #0
Ring	-215.1	**-36%**		275.6	**-35%**
Verticals	-187.2	**-29%**		207.9	**-25%**
Diagonals	-241.3	**-33%**		370.2	**-31%**

#6.1 (2)	Min σ	+/- #0		Δσ	+/- #0
Ring	-230.0	**-32%**		294.1	**-31%**
Verticals	-192.7	**-27%**		217.3	**-21%**
Diagonals	-261.0	**-27%**		404.3	**-25%**

Table 11.12: Stress and stress ranges extra ring

The adding of the extra ring greatly influences the maximum stresses and the stress ranges in the Great Dubai Wheel. As seen in figure 11.24 ring C and D work together to take the loading instead of the situation in the original model in which only ring C took the load.

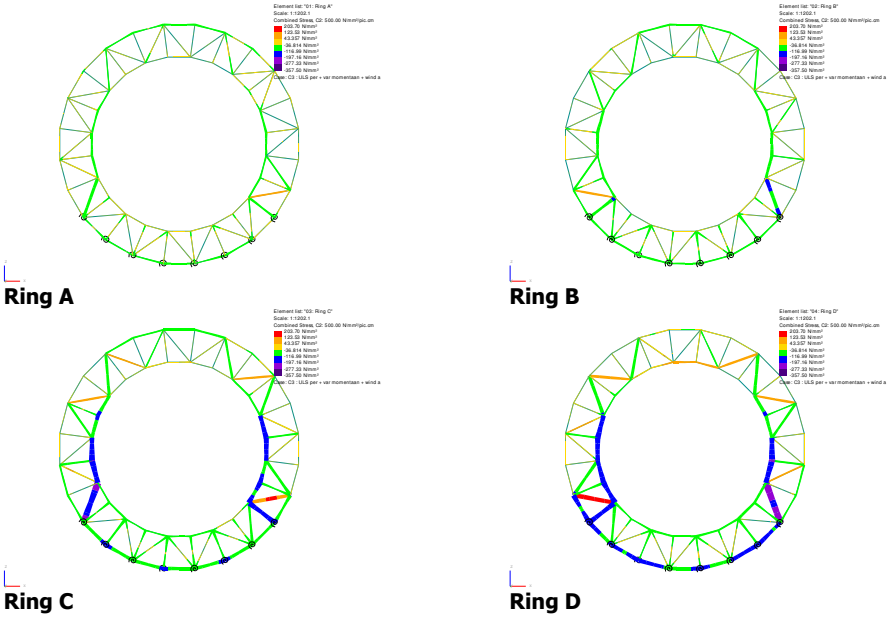

Ring A **Ring B**

Ring C **Ring D**

Figure 11.24: Cross section model #6.1 stress levels

The conclusion which is drawn from the analysis on the model with the extra ring is that the extra ring greatly influences the stress distribution in the Great Dubai Wheel. By adding the ring the maximum stresses in the Great Dubai Wheel reduces by 29% - 36% compared to the original model. And because of the similar results for both models (40m and 50m) it can be said with certainty that the extra ring is a serious alternative to reduce the stresses.

11.10. Combined solutions

Because this Master thesis is about finding the maximum diameter for the Great Dubai Wheel, it is needed to find the optimum solution for the geometry. This means that it could be preferable to combine some of the improvements given in the previous paragraphs (11.7 - 11.9).

- Bracing + cross truss;
- Extra ring + bracing;
- Extra ring + cross truss;
- Extra ring + bracing + cross truss;

MODEL NR.	Description
#0	Start
#5.1	Bracing + cross truss rigid joints
#7.1	Extra ring + bracing
#8.1	Extra ring + cross truss
#9.1	Extra ring + bracing + cross truss

Table 11.13: Model descriptions combined solutions

11.10.1. Bracing + cross truss

Figure 11.25 shows that the adding of the brace and cross elements will make the Great Dubai Wheel less transparent. This is not preferable because a main function of the Great Dubai Wheel is to provide a panoramic view of the surrounding area. But before this panoramic view is achieved there first has to be a feasible solution for the main bearing structure, and when a feasible model is chosen the sections can be optimized and the structure becomes more transparent again.

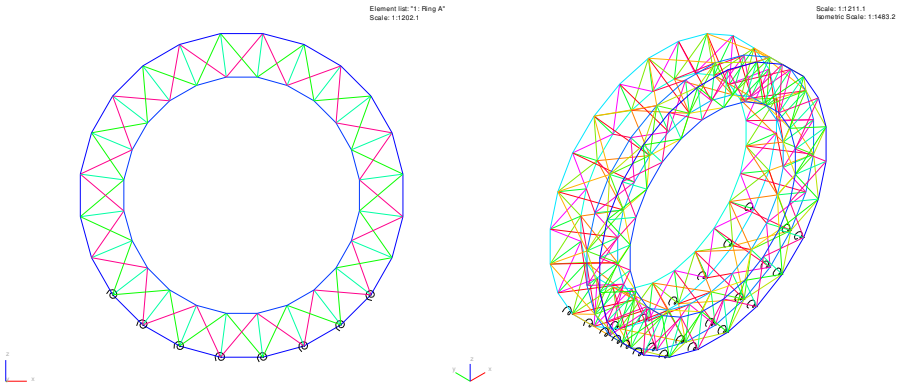

Figure 11.25: Bracing + cross truss

In table 11.14 the results of the analysis are shown. The results for the original model but also for the model with only a cross truss and the model with only the added bracing are given. Table 11.14 shows that both the maximum and minimum stresses as well as for the stress ranges the combined model is greatly improved compared to the original model.

#0	**Min σ**			**Δσ**	
Ring	-338.0			426.0	
Verticals	-264.3			275.9	
Diagonals	-357.5			539.1	

#5.1	**Min σ**	**+/- #0**		**Δσ**	**+/- #0**
Ring	-253.1	**-25%**		321.2	**-25%**
Verticals	-90.9	**-66%**		97.2	**-65%**
Diagonals	-236.4	**-34%**		307.1	**-43%**

Table 11.14: Stress and stress ranges bracing + cross truss

11.10.2. Extra ring + bracing;

In figure 11.26 the model with an extra ring and bracing is shown. Just as for the previous model (Bracing + cross truss) the model is less transparent when the extra ring and the bracing is added. But it is expected that because of the increased stiffness due to the increased leverage arm and the adding of the braces the stress reduction is significant.

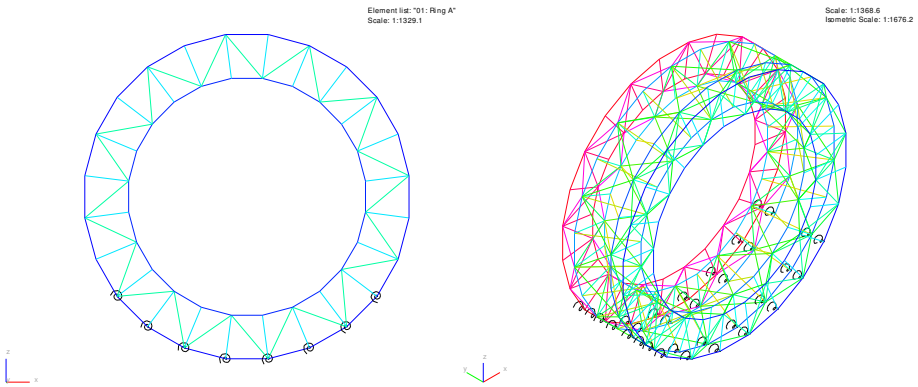

Figure 11.26: Extra ring + bracing

In table 11.15 the results of the analysis of the model are given. The results show that significant stress reductions are achieved.

#0	**Min σ**			**Δσ**	
Ring	-338.0			426.0	
Verticals	-264.3			275.9	
Diagonals	-357.5			539.1	

#7.1	**Min σ**	**+/- #0**		**Δσ**	**+/- #0**
Ring	-211.0	**-38%**		254.5	**-40%**
Verticals	-173.1	**-35%**		188.2	**-32%**
Diagonals	-237.5	**-34%**		381.6	**-29%**

Table 11.15: Stress and stress ranges extra ring + bracing

11.10.3. Extra ring + cross truss

In figure 11.27 the model with the extra ring and cross truss is shown. It is expected that because of the increased stiffness due to the increased leverage arm and the adding of the cross truss the stress reduction is significant.

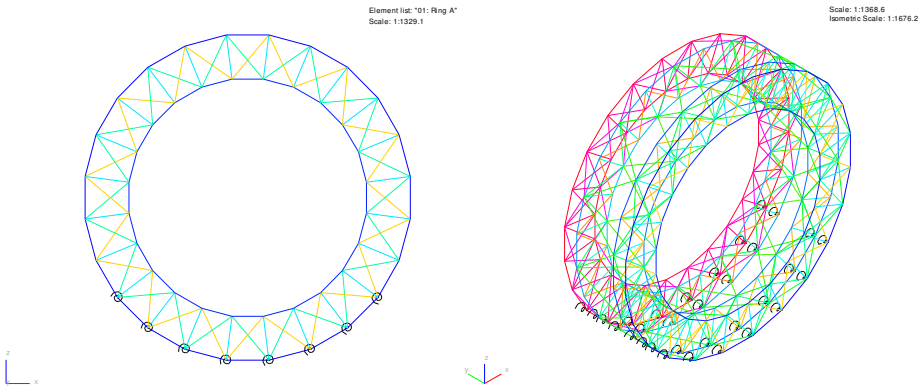

Figure 11.27: Extra ring + cross truss

In table 11.16 the results of the analysis of the model are given. The results show that a significant stress reduction is achieved.

#0	**Min σ**			**Δσ**	
Ring	-338.0			426.0	
Verticals	-264.3			275.9	
Diagonals	-357.5			539.1	

#8.1	**Min σ**	**+/- #0**		**Δσ**	**+/- #0**
Ring	-176.9	**-48%**		241.4	**-43%**
Verticals	-106.3	**-60%**		105.9	**-62%**
Diagonals	-177.0	**-50%**		212.9	**-61%**

Table 11.16: Stress and stress ranges extra ring + cross truss

11.10.4. Extra ring + bracing + cross truss

In figure 11.28 the model with the extra ring and cross truss is shown. It is expected that this model is the model which would lead to the lowest stresses and the lowest stress ranges. This is expected due to the fact that optimal use is made of axial stiffness of all members. But just as for the other combined models the transparency of this model is not great.

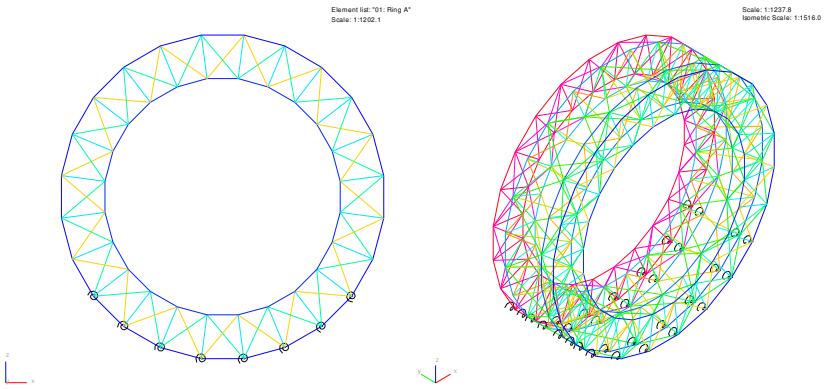

Figure 11.28: Extra ring + bracing + cross truss

In table 11.17 the results of the analysis of the model are given. The results show that a significant stress reduction is achieved.

#0	**Min σ**			**Δσ**	
Ring	-338.0			426.0	
Verticals	-264.3			275.9	
Diagonals	-357.5			539.1	

#9.1	**Min σ**	**+/- #0**		**Δσ**	**+/- #0**
Ring	-184.2	**-46%**		237.7	**-44%**
Verticals	-79.6	**-70%**		95.6	**-65%**
Diagonals	-171.3	**-52%**		223.7	**-59%**

Table 11.17: Stress and stress ranges extra ring + bracing + cross truss

11.11. Conclusion optimization

The original model (model #0) was not feasible. However, including a number of modifications can result in a large reduction on maximum stresses as well as stress range is obtained. In table 11.18 and table 11.19 the different combined models with their results are shown.

MODEL NR.	Description
#0	Start
#5.1	Bracing + cross truss rigid joints
#7.1	Extra ring + bracing
#8.1	Extra ring + cross truss
#9.1	Extra ring + bracing + cross truss

Table 11.18: Model number and description

#0	**Min σ**			**Δσ**	
Ring	-338.0			426.0	
Verticals	-264.3			275.9	
Diagonals	-357.5			539.1	

#5.1	**Min σ**	**+/- #0**		**Δσ**	**+/- #0**
Ring	-253.1	**-25%**		321.2	**-25%**
Verticals	-90.9	**-66%**		97.2	**-65%**
Diagonals	-236.4	**-34%**		307.1	**-43%**

#7.1	**Min σ**	**+/- #0**		**Δσ**	**+/- #0**
Ring	-211.0	**-38%**		254.5	**-40%**
Verticals	-173.1	**-35%**		188.2	**-32%**
Diagonals	-237.5	**-34%**		381.6	**-29%**

#8.1	**Min σ**	**+/- #0**		**Δσ**	**+/- #0**
Ring	-176.9	**-48%**		241.4	**-43%**
Verticals	-106.3	**-60%**		105.9	**-62%**
Diagonals	-177.0	**-50%**		212.9	**-61%**

#9.1	**Min σ**	**+/- #0**		**Δσ**	**+/- #0**
Ring	-184.2	**-46%**		237.7	**-44%**
Verticals	-79.6	**-70%**		95.6	**-65%**
Diagonals	-171.3	**-52%**		223.7	**-59%**

Table 11.19: Stress and stress ranges different models

It table 11.19 it is shown that model #9.1 is the model in which the lowest stresses occur, although in model #8.1 the stresses are about the same. So the adding of the braces in the combined model doesn't make a serious difference. Regarding the consequences of

alternatives studied the largest impact on stress reduction is the adding of the diagonal members which makes the truss into a cross truss girder, and the adding of the extra ring. This makes sure that the wind load is taken by two rings instead of one ring as used in the original model, see figure 11.29.

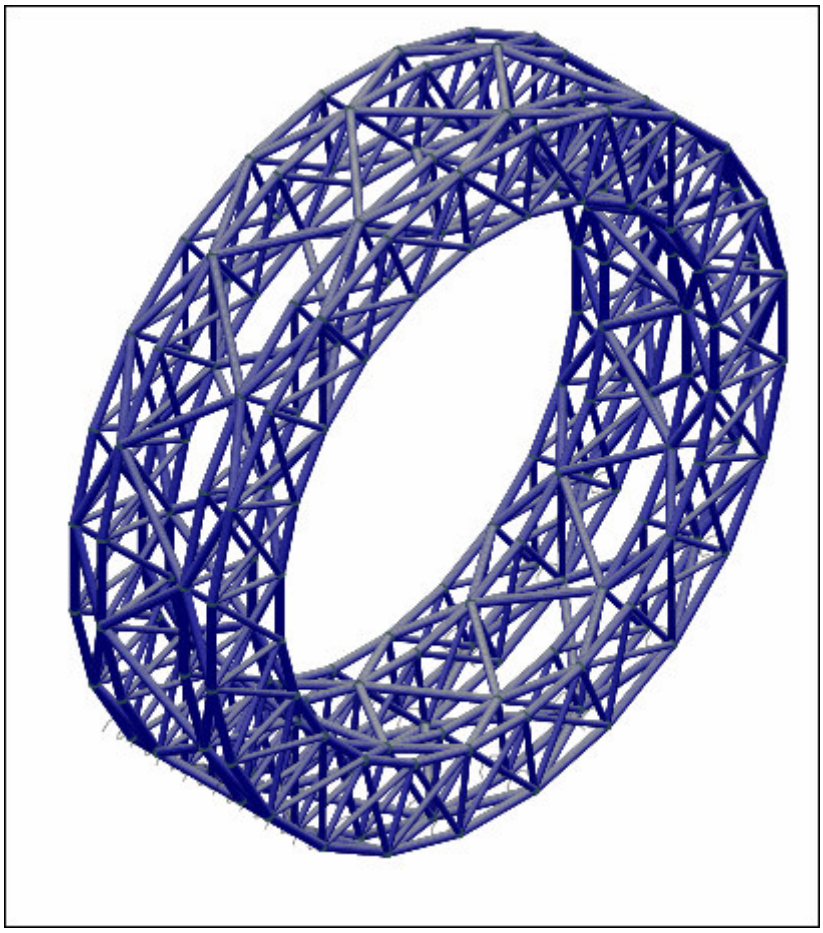

Figure 11.29: 3D-model extra ring + cross truss

11.12. Other optimizations

The models as mentioned in the previous paragraphs are not all the models analyzed. There are some more models which are analyzed but the results of these where not worth to mention here fully. For a complete review they will be summarised shortly.

- Varying stiffness of foundation, almost no difference in stresses in the structure are found.

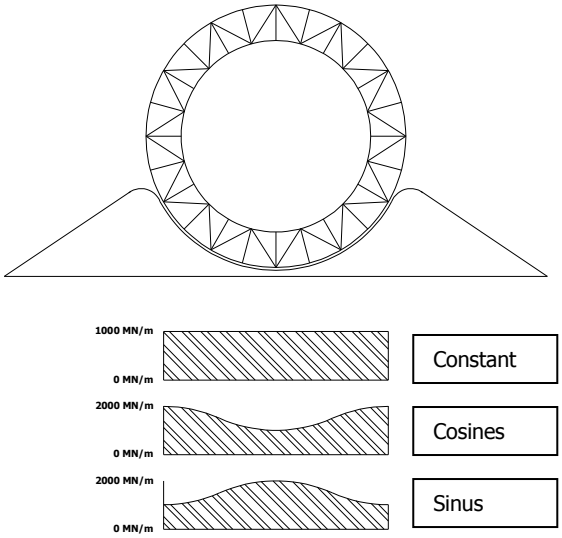

Figure 11.30: Spring stiffness

- Cables instead of steel sections for the diagonals.
  - Cables needed to be of a diameter of 400mm. This was thought to be not feasible, this was because no compression is allowed in cables and the prestressing needed to not get compression was almost 1000 N/mm^2, which only left 350 N/mm^2 to take the loading.

12. Maximum diameter improved design

In chapter 10 it was made clear that the current design wasn't feasible. For static strength the stresses were just too large and the joint efficiency was far too low. For fatigue strength the occurring stress range far outreached the allowable stress range. In chapter 11 it was said to focus on the static strength of the Great Dubai Wheel and to leave the fatigue strength for what is was. The static strength and the fatigue strength are mainly due to the T-joints which are present in this design. Therefore it is decided that for the final design the joints are made of cast steel. The joint efficiency will increase, in what extend is not researched.

In chapter 11 possible solutions are discussed. This research made clear that the large stresses in the Great Dubai Wheel are effectively reduced by adding an extra ring to the structure and to add extra diagonals so a cross truss is formed. This is mainly due to the fact that the wind loading is the governing load case, and with the adding of the extra ring the wind load is spread over two rings and the cross truss makes sure the forces near the highest supports are spread out over more members. When the diameter of the Great Dubai Wheel is increased the wind loading will play an even bigger role as the total wind load on the structure will increase.

With these two adaptations a large stress reduction is achieved. A slightly higher stress reduction is found by also adding bracing to the portal frames, but adding members at these places greatly influences the transparency of the structure. The transparency of the structure already is far less then it was in the original design by the extra ring and the extra diagonals as seen in figure 12.1.

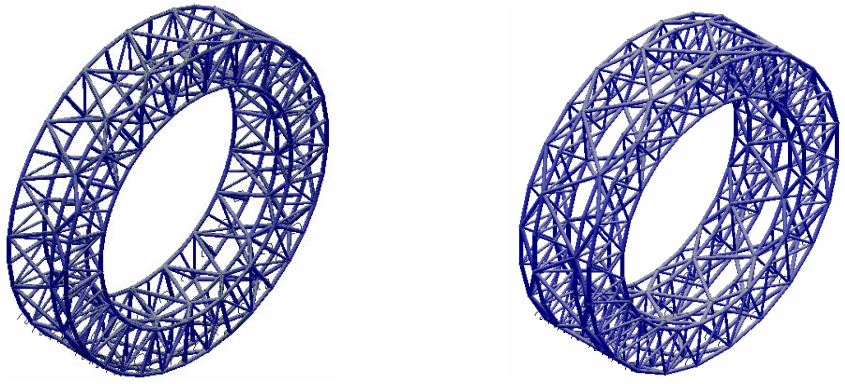

Figure 12.1: Original and improved 3D-model

12.1. Requirements

For the structural analysis only two requirements are given:

[1] The maximum and minimum stresses;

[2] The stress range;

It is chosen to have only two restrictions in the structural analysis, because these two restrictions covered the most important facets of the design. Of course other restrictions are used for the analysis but not in a way that a parameter should not exceed a certain value. An example of this is that the support reactions can only be in compression.

12.1.1. Maximum allowable stress

The requirement for the maximum stress is set at 280 N/mm^2, this value is chosen because when the joints are improved with for instance cast steel joints, concrete filling or stiffener plates (figure 8.6, figure 8.7 or figure 8.8), a joint efficiency of 80% is feasible (80% * 355 N/mm^2 = 284 N/mm^2).

12.1.2. Allowable stress range

For the stress range the S-N-curve has to be looked at. For maximizing the fatigue life, it is assumed that the joints are made out of cast steel joints. This means that the values for the stress concentration factors are 1. So no stress concentration has to be taken into account. In chapter 9 (fatigue, figure 9.1), it is seen that the maximum stress range is:

$$\log\left(\Delta\sigma_{geom.(t)}\right) = \tfrac{1}{3}*\left[12.476-\log\left(N_f\right)\right]+0.06*\log\left(N_f\right)*\log\left(\tfrac{16}{t}\right)$$

$$\log\left(\Delta\sigma_{geom.(40)}\right) = \tfrac{1}{3}*\left[12.476-\log\left(146000\right)\right]+0.06*\log\left(146000\right)*\log\left(\tfrac{16}{40}\right)$$

$$\Delta\sigma_{geom.(40)} = 206\ {}^{N}\!/_{mm^2}$$

The nominal stress range with a plate thickness of 40mm then becomes 200 N/mm^2. When the plate thickness is lowered the stress range is increased, a plate thickness of 30mm gives a stress range of 225 N/mm^2 and a plate thickness of 20mm gives a stress range 255 N/mm^2. This is all with the assumption of the 146.000 stress cycles (see chapter 9) which is the number of cycles in the lifetime of the Great Dubai Wheel. For the fatigue analysis the analysis is done with the same load case as for the static analysis. This is done because in the calculations are still of a preliminary nature and not all the parameters are fully known. So a conservative approach is taken. This means that the full wind load is taken into account when analysing the stress range. This is of course not true. Because the maximum wind load with safety factor will not act during a full rotation of the Great Dubai Wheel, the wheel is stopped because the safety of the guests has to be guaranteed. Therefore a second case is considered in which only the self weight of the structure and the variable loading, so the wind loading is not taken into account. The safety factors are still taken into account because still a somewhat conservative approach is thought to be needed.

12.2. Parameters

The variable parameter used in this chapter is the diameter. The other parameters are kept constant. This is done because that the original design should not be altered too much. It is proven for instance in chapter 4 that raising the supporting structure is beneficial for the stress distribution in the Great Dubai Wheel. But by raising the height of the supporting structure the total look of the Great Dubai Wheel is changed. It is therefore chosen to keep the ratio between the diameter and the height of the supporting structure constant.

The thickness of the ring is kept constant. This is done because in chapter 11 it is proven that the stresses are not greatly reduced when changing the ring thickness. The total look of the structure will change somewhat, but the structure becomes more slender when the diameter is increased.

The width of the structure is also kept constant. It is felt like the width of the structure only should be increased when the diameter increases by such an extent that for stability reasons the width should be increased.

12.3. Maximum diameter

With the requirements and the parameters mentioned in the previous paragraphs the maximum possible diameter is determined.
The allowable stress in the Great Dubai Wheel is set to 280 N/mm^2, see chapter 12.1.1, with this demand a maximum diameter of about 235m is feasible.

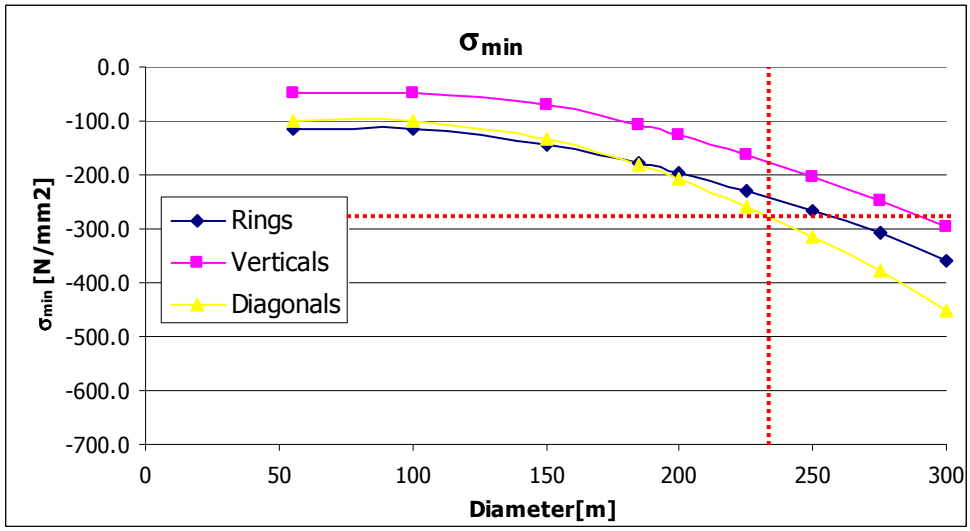

Figure 12.2: σ_{min}

The allowable stress range is 200 N/mm^2, see chapter 12.1.2. With this demand a maximum diameter of about 150m is feasible, see figure 12.3. But as explained before, this demand of the stress range is thought to be too conservative. Therefore a graph without the wind load is given in figure 12.4. This would mean that a design of 210m would be feasible.

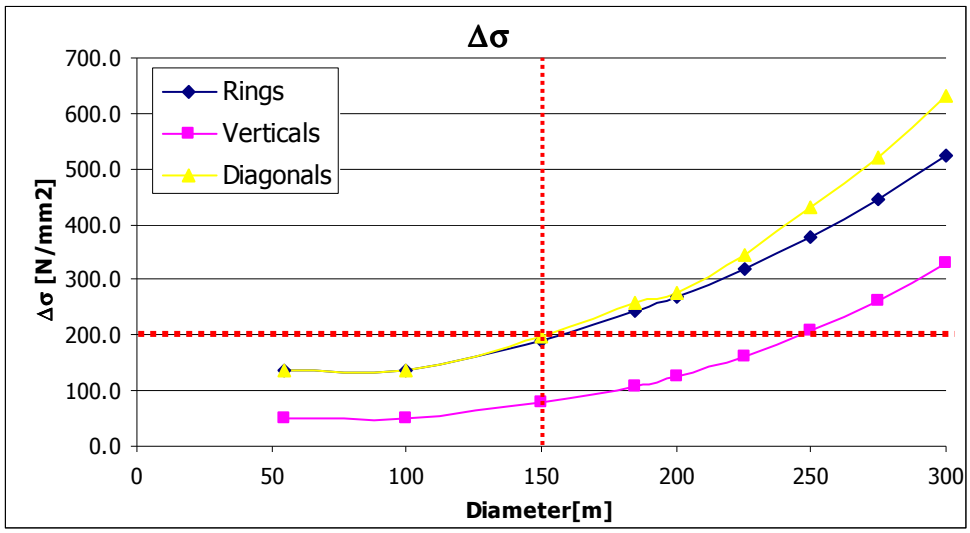

Figure 12.3: Stress range with wind load

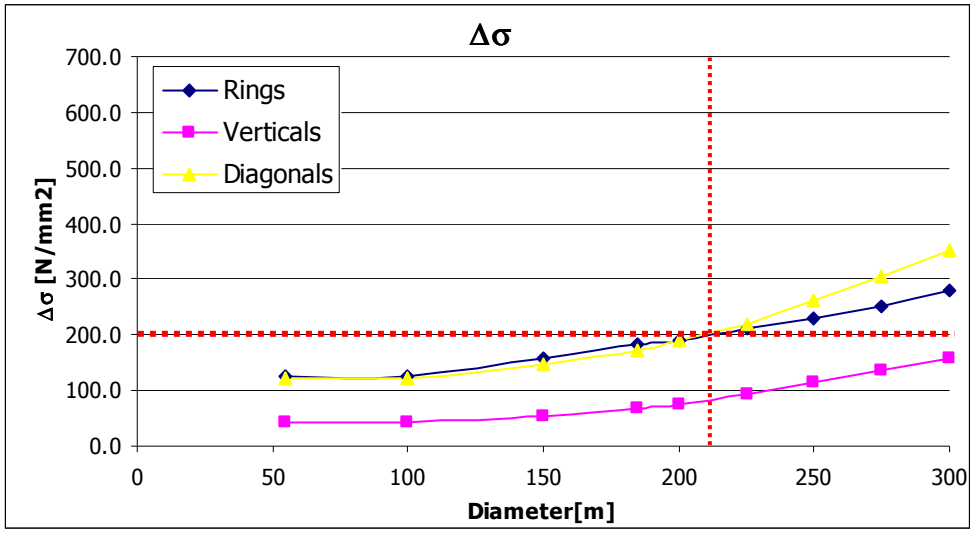

Figure 12.4: Stress range without wind load

Some remarks do have to be made regarding this maximum possible diameter. The sections used are still the same sections as used in the first part of this Master thesis. It was chosen to keep using these sections as the design wasn't feasible and it was thought that the highest priority was on getting a feasible design. The sections which are used are already big sections these already have to be fabricated out of plates. To not affect the transparency of the Great Dubai wheel too much it is chosen that the used sections are the maximum allowable sections in size.

12.4. Conclusion

The maximum possible diameter of the Great Dubai Wheel inside the boundaries and restrictions given in this report is about 210m. This means that the Great Dubai Wheel if build with the height of 210m would be the biggest Ferris wheel in the world, and would be the only Ferris wheel without spokes in the world today.

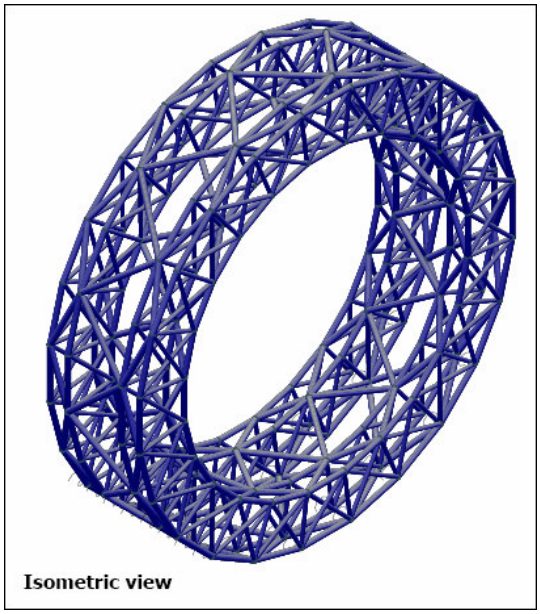

Figure 12.5: Isometric view of 3D-model 210m

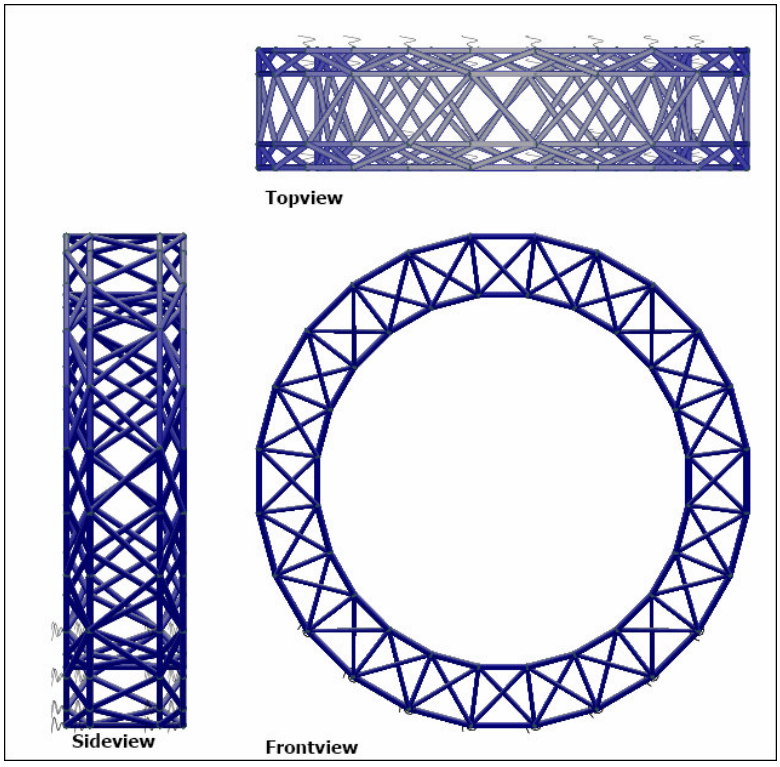

Figure 12.6: Top front and side view of 3D-model 210m

13. Conclusions and recommendations

In this Master thesis the question of what the maximum possible diameter of the Great Dubai Wheel is, is investigated. The findings of this research are stated in this chapter as conclusions, and because for the final design more research is needed also recommendations for further research are given.

13.1. Conclusions

The conclusions can be categorized in two parts; the first part contains the conclusions regarding the structure of the Great Dubai Wheel. And the second part will contain the conclusions of the approach of the Master thesis itself.

13.1.1. Conclusions structure of the Great Dubai Wheel

The proposed design of Royal Haskoning Architects and, which won the contest was proven not feasible in chapter 10. The main problem was the non-efficient material usage in the structure. The challenge in the Great Dubai Wheel is that the structure is rotating and that there is no possibility to use less material on the top as on the bottom, as every point in the structure will be in some time in one rotation be on the bottom and at the top. Several possible solutions are investigated and some of these solutions proved to be very attractive for lowering the stresses and stress ranges in the Great Dubai Wheel.

- The adding of an extra ring to the structure is investigated. The wind load is evenly distributed over two rings instead as over one ring in the original design. This reduces the stresses and stress ranges by about 30%.
- Changing the truss geometry from a modified Warren truss to a cross truss reduces the stresses considerably. Stress reductions of about 25% are achieved and the stress range is also reduced considerably.
- The adding of braces is investigated, the investigation proves that it is beneficial to apply braces, but the stress reductions are not that big compared to the cross truss and the extra ring, reductions of about 10% occur.
- The proposed solutions are combined and the conclusion is that the combination of the adding of the extra ring and the cross truss is the most favourable solution for the Great Dubai Wheel. The stresses are reduced by 50% - 60% and the stress ranges are reduced by 40% - 60%.

With the combination of the adding of the extra ring and the cross truss the Great Dubai Wheel becomes a feasible design. However the design is still in a preliminary phase and is seen as a feasible concept for the final design of the Great Dubai Wheel to which further research is needed.

13.1.2. Conclusions approach of the Master thesis

In this Master thesis parametric design is used as a useful tool. Implementing parametric design into this Master thesis made it possible to quickly learn what the effect of the possible solutions mentioned in the previous paragraph are.

The sections used in the Great Dubai Wheel are kept the same during the entire Mater thesis. This made it possible to measure the improvements gained by the possible solutions on a stress level, this proved to be an effective way to do the comparison between the different models discussed in chapter 11. But this also means that for the final design the optimization of the sections still has to be done.

Making the ring stationary as mentioned as a possible solution in chapter 3, is not considered in this Master thesis. It was felt that this was an essential structural demand of the Great Dubai Wheel which made it special. The entire rotating structure makes sure that the Great Dubai Wheel is a building to everyone's imagination. This choice of not making the Great Dubai Wheel stationary made this Master thesis into a challenging research on one of the worlds structurally most interesting buildings.

13.1.3. Recommendations

As seen in chapter 12 a feasible design is present. But it is still in preliminary stages. Also in the design some possible unwanted choices regarding the transparency of the Great Dubai Wheel are made. It is therefore necessary to check if the design is still in demand, does Dubai still want to realise this design or not. Perhaps a normal Ferris wheel is preferred. If the design is still in demand this Master thesis can be the basis for the final design. But many questions regarding the Great Dubai Wheel still exist. Therefore, for the future more research is needed to come to the final design. These questions arise in many different categories from financial to structural. In this chapter only the questions with a structural nature will be mentioned.

Dynamics

In this Master thesis the dynamic behaviour is not intensively looked at. But because of the fully rotating structure, and the complex wind loading (the wind will blow between the steel members creating vortexes) more research is needed. Also in this Master thesis earthquakes are not taken into account, the behaviour of the Great Dubai Wheel to a earthquake should be further investigated.

Wind loading

Already mentioned, the complex wind loading should be researched more. The Great Dubai Wheel has a complex shape which is also rotating. It is proven in this report and by the analyses done that the maximum wind loading can be taken by the structure. But the dynamic wind loading is not taken into account. A full study in which the wind spectrum is concerned should be done. This is also important for the fatigue behaviour of the structure. At the end of chapter 12 it is said that the wind load is in a totally different spectrum as a full rotation. So it can not be added to the load case fatigue but should be handled as a totally separate fatigue case. And it could well be that the fatigue behaviour due to the wind is governing for the total fatigue behaviour. This means that further research to the wind loading of the Great Dubai Wheel should be performed.

Supporting structure

The supporting structure has not been looked at in this Master thesis, and however a feasible design for the Great Dubai Wheel is present. There are question on how to support this rotating wheel. More research is needed to know what the options are and if perhaps it is possible to not only support the Great Dubai Wheel axially but also in a lateral way.

Hinges

In this Master thesis some research has been done on member releases and if it is beneficial. It proved to be less beneficial as was expected. But still some reduction of stresses was achieved. It was chosen not to implement the member releases in chapter 12 because of questions regarding detailing of those releases. More research is needed on how this detailing should be done. And if it is a economical solution to apply hinges instead of rigid joints.

Parametric design

The introduction of parametric design in this Master thesis made it possible to quickly get insight of how certain parameters affect the total design. It should therefore be mentioned that a parametric design approach can be a very useful tool, especially in the early stages of a design to quickly find the governing parameters, and to be able to quickly modify the design to the customer's need.

Prestressing

The possibilities of prestressing the Great Dubai Wheel are not researched in this Master thesis. It is possible that with the introduction of prestressing in the Great Dubai Wheel the used material will be used in a more effective way. It should therefore be further investigated what the possibilities of prestressing the Great Dubai Wheel are.

Joints

The final design of this Master thesis is a frame with complex joints. In this Master thesis the joints are fully cast steel joints. It is not researched if this is the best option for the joints. Therefore the joints should be researched further. Certainly because the simplest joint in the structure is a KT-joint and the more complex joints are multi planar KT-joints, the limitations and possibilities of these joints should be determined. This can be done in experiments as well as a numerical analysis. For the joints is in appendix C stated what requirements the joints have to fulfil.

References

[1] Wardenier, J., Kurobane, Y, Packer, J.A., Dutta, D. and Yeomans, N.: Design guide or circular hollow sections (CHS) joints under predominantly static loading. CIDECT, Germany, 1991. ISBN 3-88585-975-0.

[2] Zhao, X.L., Herion, S., Packer, J.A., Puthli, R.S., Sedlaeck, G., Wardenier, J., Weynand, k. Wingerde, A.M. van. and Yeomans, N.F.: Design guide for circular and rectangular hollow sections welded joints under fatigue loading (8). CIDECT, Germany, 2001. ISBN 3-8249-0565-5.

[3] NEN 6702: TGB 1990 Loadings and deformations, Technische grondslagen voor bouwconstructies, NEN, Netherlands, 1993.

[4] Dutta, D., Würker, K.G.: Handbuch Hohlprofile in stahlkonstruktionen, Verlag TÜV Rheinland GmbH, Köln, Germany, 1988. ISBN 3-88585-528-3.

[5] Wardenier. J.: Hollow sections in structural applications. Bouwen met Staal, Netherlands, 2002. ISBN 90-72830-39-3;

[6] Romeijn. A.: Fatigue dictaat deel I, CT51216, TU-DELFT. Netherlands, 2006.

[7] Efthymiou. M.: Development of SCF formulae and generalised influence functions for use in fatigue analysis, Shell B.V. 1988.

[8] http://en.wikipedia.org/wiki/Ferris_wheel

[9] http://www.wienerriesenrad.com/index.php

[10] Berenbak, J.: Hollands glorie in hartje Londen, Bouwen met Staal 154, Krimpen aan de IJssel, Netherlands, 2000.

[11] Berenbak, J.: Lanser, A.: Ontwerpen en bouwen tegelijk, Bouwen met Staal 154, Krimpen aan de IJssel, Netherlands, 2000.

[12] Berenbak, J.: Hoogendijk, N.G.D.: Balanceren met 1500 ton staal, Bouwen met Staal 154, Krimpen aan de IJssel, Netherlands, 2000.

[13] Bolleboom, S.: Great Dubai Wheel "De constructieve haalbaarheid van 's werelds eerste spaakloze reuzenrad", Rijswijk, Netherlands, 2008.

[14] OASYS-LTD: User manual GSA 8.3, London, England, 2008.

[15] http://www.royalhaskoningarchitecten.com

List of figures

List of tables